

Large N analysis of the Higgs mass triviality bound

URS M. HELLER^a, HERBERT NEUBERGER^b,
PAVLOS VRANAS^a

^a *Supercomputer Computations Research Institute
The Florida State University
Tallahassee, FL 32306*

^b *Department of Physics and Astronomy
Rutgers University
Piscataway, NJ 08855-0849*

ABSTRACT: We calculate the triviality bound on the Higgs mass in scalar field theory models whose global symmetry group $SU(2)_L \times SU(2)_{\text{custodial}} \approx O(4)$ has been replaced by $O(N)$ and N has been taken to infinity. Limits on observable cutoff effects at four percent in several regularized models with tunable couplings in the bare action yield triviality bounds displaying a large degree of universality. Extrapolating from $N = \infty$ to $N = 4$ we conservatively estimate that a Higgs particle with mass up to 0.750 TeV and width up to 0.290 TeV is realizable without large cutoff effects, indicating that strong scalar self interactions in the standard model are not ruled out.

1. INTRODUCTION.

This paper examines the regularization scheme dependence of the triviality bound on the Higgs mass in a $O(N)$ symmetric scalar field theory to leading order in $1/N$. Our purpose in doing this is two-fold: we wish to investigate the issue by explicit, analytical calculations and we need the results both directly and indirectly to complement numerical work at $N = 4$. The results are needed directly for estimating cutoff effects on physical observables that are not accessible by Monte Carlo and indirectly for guiding our search in the space of lattice actions to the region where heavier Higgs particles are possible.

A preliminary account of some of our results has been presented in [1,2,3]. Our general reasons for suspecting that the present numbers for the bound are too low in the context of the minimal standard model have been explained before [1,4,5] and will not be repeated here.

The basic logic of our approach has also been explained before [6,5,7] but, in order to make this paper more or less self contained, we shall briefly review the main points. We are working with a scalar field theory at a finite cutoff. The field has N components ($N = 4$ for the minimal standard model) and the action is $O(N)$ symmetric. We are interested in the broken phase in which the symmetry is spontaneously broken and wish to pick cutoff schemes that preserve as many of the continuum space-time symmetries as possible. Our cutoff scheme must also exclude unitarity violations at the energies and momenta of interest which are small relative to the cutoff.

The physical scale is set by F_π , the “pion decay constant”, and we are interested in M_H the “Higgs mass”. Because of triviality the ultraviolet cutoff cannot be removed and therefore cutoff effects are unavoidable. We require those cutoff effects that are observable to be bounded by a few percent in relative magnitude. This imposes a limit on the ratio M_H/F_π . Generically, the leading cutoff effects are of order inverse cutoff squared. It is possible in some models to arrange that the leading cutoff effects be of order inverse cutoff to the fourth power instead. We regard such “finely tuned” models as overly contrived. The cutoff effects of the low energy effective theory are ultimately determined by the underlying full theory and we believe it is highly unlikely that such a “finely tuned” model would be produced without any particular reason. We wish to find a region in the space of actions where, without excessive “fine tuning”,* M_H/F_π gets to be as large as possible.

Since the cutoff effects are assumed to be small and “fine tuning” has been excluded we conclude that we can use the RG to count the dimensions of the space of actions we ought to look at. We have one relevant operator of dimension 2, two operators of dimension 4 and four operators of dimension 6. We do not need to consider higher dimension operators

* Except the one possibly needed to make F_π small relative to the cutoff in the first place.

because their effects are subleading and we have excluded the fine tuning of the leading effects to zero. Since we are interested only in physical effects, namely in cutoff effects in the S-matrix, we have to eliminate the redundant operators induced by field redefinitions. For dimensions up to six there are three such operators. Thus, we end up with a $7-3=4$ dimensional space. One dimension corresponds to the relevant direction and sets the scale, another to the marginally irrelevant parameter and the two remaining parameters span all the possible leading order observable cutoff effects. It is preferable to think only about dimensionless physical observables with the natural physical quantity obtained by multiplication by the appropriate power of F_π . All momenta are also measured in units of F_π and so is M_H ; the marginally relevant direction can be thought of as parametrized by $g = 3M_H^2/F_\pi^2$.

Intuitively, we would expect to increase g by approaching the nonlinear limit where the field $\vec{\phi}$ has fixed length. Hence, for mass bound studies one can restrict one's attention to nonlinear models. This is known to be true with naïve lattice actions and we have checked it for some other actions at $N = \infty$. Hence we shall concentrate on nonlinear actions. At the most naïve level one can think of a nonlinear action as obtained from a linear one by taking the bare four point coupling to infinity and adjusting the other couplings so that the model has a limit. From this point of view one of the four free parameters has been eliminated; in other words, the effort to maximize g is assumed to guarantee the elimination of one of the four parameters, leaving us with only three. The nonlinear actions can also be viewed as chiral effective actions in the sense defined by Weinberg [8]. The low momentum behavior of any broken theory (even with a cutoff if the latter is sufficiently symmetric) can be parametrized by such an effective action and, to first nontrivial order, one needs three parameters. This is exactly the number we came up with after reducing by one the original dimensionality. Therefore we know that the three parameter set of nonlinear actions we intend to focus on is reasonably general, since it can at least reproduce all “pion” scatterings to first subleading order in the external momenta. To be sure, we still expect the cutoff effects to depend on **two** parameters as before the restriction to nonlinear actions, because such a constraint should not reduce the number of contributing operators in the vicinity of the Gaussian fixed point.

Our further approximation will be to take N to infinity. We shall see that this effectively reduces the number of parameters from three to two and, moreover, at $N = \infty$ the cutoff effects we shall be interested in can now be parametrized by a single parameter.* The situation becomes as simple as it could get: we have one parameter that sets the scale (“coarseness” of grid in the lattice case) and another that represents the entire freedom that is available at first subleading order in the expansion of the S-matrix in inverse

* Even a bare action that has only a single free parameter, will, in principle, have observable cutoff effects that are parameterizable by two coefficients, associated with the leading “irrelevant” operators after elimination of “redundants”.

powers of the cutoff. For fixed value of the second parameter one can imagine that some extremization of g has already been carried out by taking the bare four point coupling to infinity. This simplification at infinite N makes it easy to relate very different cutoff schemes and leads to a reasonably “universal” bound on g . These facts, derived below, provide a basis confirming the general validity of the $N = \infty$ results[†] obtained previously by Einhorn [9,10].

We shall work with a class of Pauli–Villars regularizations parametrized in addition to the continuous parameters discussed above by an integer $n \geq 3$, and with lattice regularizations on hypercubic and F_4 lattices. When the range of the additional couplings is suitably restricted (but not “finely tuned”) all these regularizations give very consistent estimates for the $N = \infty$ bound. We present our results properly scaled to $N = 4$ and obtain, with $F_\pi = 0.246 \text{ TeV}$, $M_H \leq 0.820 \text{ TeV}$ with rather stringent bounds on the cutoff effects; changing the latter by a factor of 10 may affect the bound by about 0.050 TeV in the obvious direction. We can try to guess what correction on the bound might be due to N being four rather than infinity by looking at the available numerical data at $N = 4$. This leads us to expect for $N = 4$ a bound somewhere between 0.750 TeV and 0.800 TeV . While the relatively recent previous estimates were not much lower[#] (0.600 TeV to 0.650 TeV) the effect on the width, Γ_H , is more significant: Γ_H/M_H may reach 0.4 when the bound is close to saturation and this implies that strong scalar self–interactions without strong observable cutoff effects are possible.

Since the previous bounds were obtained from a very restricted class of actions, chosen just because they were simpler to analyze for technical reasons, it was somewhat premature to put forward the 0.550 TeV to 0.650 TeV range as **the** lattice triviality bounds with lattice spacings between $1/(5M_H)$ and $1/(2M_H)$ and imply direct relevance to experiment [13]. To be sure, we do not contest the validity of the numbers within the particular regularization that they were obtained in, and, in retrospect, they were not very far off even in the general context. Our analysis shows that we are nowhere near a ratio $M_H/F_\pi \sim 6$ that would be expected in a QCD like theory and our Higgs is quite “elementary”. We have no explanation for why the range $3 \leq M_H/F_\pi \leq 5$ seems to be so difficult to attain with “an elementary” Higgs; this looks like a stronger numerical reflection of triviality than one might have originally suspected.

Throughout the paper we shall use a notation with capital letters, F_π , M_H and Γ_H , to denote the physical quantities, measured in TeV , and with lower case letters, f_π , m_H and γ_H , to denote those quantities in units of the cutoff, Λ , or a^{-1} for lattice regularizations.

[†] With some small, inessential corrections.

[#] Very early estimates [11,12] were actually around 0.800 TeV but this was accidental; these authors also used the simplest possible lattice action for which we have nowadays better results.

In the large N limit the renormalized vacuum expectation value (pion decay constant), f_π , diverges as \sqrt{N} but m_H and γ_H stay finite. We therefore rescale f_π and F_π by \sqrt{N} to make them also finite at $N \rightarrow \infty$. From now on and until sections 7 and 8 f_π and F_π refer to the rescaled values. Of course, when we use the large N results for $N = 4$, we undo this rescaling; when we present our large N results in physical units we take the rescaled F_π as $0.246/\sqrt{4} \text{ TeV} = 0.123 \text{ TeV}$.

The outline of the paper is as follows: In the next section we shall briefly analyze linear models with particular higher dimensional operators to see explicitly that in order to estimate the bound we have to look only at the nonlinear limit. We proceed to define the class of nonlinear models we shall consider in the rest of the paper. In section 3 we work out the large N phase diagram of the models in the Pauli–Villars class. Section 4 deals with the cutoff effects in the Pauli–Villars class of models, first in a simplified manner and then in detail. Sections 5 and 6 repeat the analysis for the lattice models. In section 7 we present the results of our large N study of cutoff effects for the Higgs width to mass ratio and for Goldstone pion scattering and the implications on the Higgs mass bound. Also, a comparison between large N and available numerical results at $N = 4$ is carried out. This allows us to make inferences from the results obtained in this paper to the $N = 4$ case of actions that have not yet been studied numerically. Our conclusions are presented in section 8. Three appendices have been added to present some technical details and expand on side issues.

2. LINEAR VERSUS NONLINEAR ACTION.

In this section we briefly discuss the linear case. We shall see why we were led to consider only nonlinear actions in the sequel. Also, by comparing the formulae derived later on for the nonlinear case to the ones in this section, one can see explicitly that the nonlinearity of the bare action has no observable effect in the critical regime as expected by general RG arguments. More precisely, by making physical measurements in the critical regime and at low enough momenta one cannot say whether the bare theory was linear or not. It is because of this that simulations employing a nonlinear action have something to say about the standard model as we know it.

We shall use the following notations: The partition function is \mathcal{Z} , the metric is Euclidean and the action is denoted by S . \mathcal{Z} is given by

$$\mathcal{Z} = \int \exp(-S) \ , \tag{2.1}$$

where the fields have been suppressed in the action and integration measure. For spatial

$(x, y \dots)$ and momentum $(p, q, k \dots)$ integration we use

$$\int_x \equiv \int d^4x , \quad \int_p \equiv \int \frac{d^4p}{(2\pi)^4} , \quad (2.2)$$

and as usual

$$(\partial_\mu f)^2 \equiv \sum_\mu (\partial_\mu f)^2 . \quad (2.3)$$

Λ denotes the cutoff. We shall suppress arguments whenever possible.

2.1. The general linear action and the saddle point equations.

According to the discussion in the introduction the most natural set of actions we should be studying is given by

$$S = \int_{x_0} \left[\frac{1}{2} \vec{\phi}_0 K_0 (-\partial_0^2) \vec{\phi}_0 + \frac{\mu_0^2}{2} \vec{\phi}_0^2 + \frac{\lambda}{4N} (\vec{\phi}_0^2)^2 + \frac{\eta_{1,0}}{2N} \vec{\phi}_0^2 (\partial_\mu \vec{\phi}_0)^2 + \frac{\eta_{2,0}}{2N} (\partial_\mu (\vec{\phi}_0^2))^2 + \frac{\eta_{3,0}}{6N^2} (\vec{\phi}_0^2)^3 \right] . \quad (2.1.1)$$

The subscript ‘‘0’’ denotes dimensionful parameters. The kinetic term is regulated in a yet unspecified manner, but it is assumed that all subsequent potential ultraviolet divergences are cut off at about Λ . Thus we write

$$K_0(-\partial_0^2) = \Lambda^2 K(-\partial_0^2/\Lambda^2) . \quad (2.1.2)$$

(2.1.2) contains seven free parameters (two of them are implicit in $K_0(-\partial_0^2)$), one for each operator of dimension ≤ 6 . Later we shall choose to fix some of these parameters to simplify our analysis.

We scale Λ out of the problem by defining

$$x = \Lambda x_0 , \quad \vec{\phi}_0 = \Lambda \vec{\phi} , \quad \mu_0^2 = \Lambda^2 \mu^2 , \quad \eta_{1,0} = \frac{\eta_1}{\Lambda^2} , \quad \eta_{2,0} = \frac{\eta_2}{\Lambda^2} , \quad \eta_{3,0} = \frac{\eta_3}{\Lambda^2} \quad (2.1.3)$$

and all our variables become dimensionless

$$S = \int_x \left[\frac{1}{2} \vec{\phi} K(-\partial^2) \vec{\phi} + \frac{\mu^2}{2} (\vec{\phi}^2)^2 + \frac{\lambda}{4N} (\vec{\phi}^2)^2 + \frac{\eta_1}{2N} \vec{\phi}^2 (\partial_\mu \vec{\phi})^2 + \frac{\eta_2}{2N} (\partial_\mu (\vec{\phi}^2))^2 + \frac{\eta_3}{6N^2} (\vec{\phi}^2)^3 \right] . \quad (2.1.4)$$

Introducing into the functional integral

$$\prod_x \int_{-\infty}^{\infty} d\sigma(x) \frac{N}{4\pi} \int_{-i\infty}^{i\infty} d\omega(x) \exp \left\{ \frac{N}{2} \omega(x) \left[\sigma(x) - \frac{\vec{\phi}^2(x)}{N} \right] \right\} = 1 , \quad (2.1.5)$$

we obtain a new action with more fields

$$S_1 = \frac{1}{2} \int_x \vec{\phi} [K - \eta_1 \partial_\mu \sigma \partial_\mu + \omega] \vec{\phi} + \frac{N}{2} \int_x [\eta_2 (\partial_\mu \sigma)^2 + \mu^2 \sigma + \frac{\lambda}{2} \sigma^2 + \frac{\eta_3}{3} \sigma^3 - \sigma \omega] . \quad (2.1.6)$$

The zero mode of $\vec{\phi}$ needs special treatment requiring that we separate it out explicitly

$$\vec{\phi}(x) = \sqrt{N} \vec{v} + \hat{v} H(x) + \vec{\pi}(x) , \quad \hat{v} = \frac{\vec{v}}{v} , \quad |\vec{v}| = v , \quad \hat{v} \cdot \vec{\pi} = 0 , \quad \int_x H(x) = \int_x \pi^j(x) = 0 . \quad (2.1.7)$$

We integrate out the H and $\vec{\pi}$ fields and, with $\hat{K} = K - \eta_1 \partial_\mu \sigma \partial_\mu + \omega$, restricted to operate in the space of non-constant functions, we obtain

$$S_2 = \frac{N}{2} \text{Tr} \log \hat{K} - \frac{N}{2} v^2 \int \omega' \hat{K}^{-1} \omega' + \frac{N}{2} v^2 \int_x \omega + \frac{N}{2} \int_x [\eta_2 (\partial_\mu \sigma)^2 + \mu^2 \sigma + \frac{\lambda}{2} \sigma^2 + \frac{\eta_3}{3} \sigma^3 - \sigma \omega] . \quad (2.1.8)$$

Here ω' is the non-constant part of ω

$$\partial_\mu (\omega - \omega') = 0 , \quad \int_x \omega' = 0 . \quad (2.1.9)$$

ω' rather than ω comes in because $\int_x \omega H = \int_x \omega' H$ as a result of the zero mode, \vec{v} being separated out. In the functional integral one is still left with a piece $\int_0^\infty v^{N-1} dv$ because v hasn't been integrated over. In the infinite volume limit, and assuming translational invariance, this piece can be ignored.* Taking N to infinity we obtain the general saddle point equations

$$\begin{aligned} \int_p \frac{1}{K(p^2) + \eta_1 \sigma_s p^2 + \omega_s} + v^2 &= \sigma_s \\ \eta_1 \int_p \frac{p^2}{K(p^2) + \eta_1 \sigma_s p^2 + \omega_s} + \mu^2 + \lambda \sigma_s + \eta_3 \sigma_s^2 &= \omega_s . \end{aligned} \quad (2.1.10)$$

We notice that η_2 has disappeared from the saddle point equations because we assumed translational invariance of the saddle.

If we keep v as a free variable and plug in the solutions of the saddle point equations into S_2 we obtain the effective potential. Here, however, we just wish to fix v at the vacuum expectation value of $\vec{\phi}$. In the broken phase one then has $\omega_s = 0$. For $\omega_s > 0$ v will vanish.

* The large N analysis can be easily extended to finite volumes where the probability distribution of v can be calculated showing explicitly how the infinite volume limit is approached.

We are looking for the candidate transition surface. It is only “candidate” because it might be cut by other transition surfaces rendering some portions of it metastable. However, any true second order transition point we are interested in must be on this surface. The condition for criticality fixes $\mu^2 = \mu_c^2(\eta_1, \eta_3, \lambda)$. μ_c^2 is implicitly defined by

$$\begin{aligned} \int_p \frac{1}{K(p^2) + \eta_1 \sigma_s p^2} &= \sigma_s \\ \eta_1 \int_p \frac{p^2}{K(p^2) + \eta_1 \sigma_s p^2} + \mu_c^2 + \lambda \sigma_s + \eta_3 \sigma_s^2 &= 0 \quad . \end{aligned} \quad (2.1.11)$$

For the time being we ignore questions regarding global stability. We take $\delta\mu^2 \equiv \mu^2 - \mu_c^2$ to be negative and small relative to unity. This should place us in the broken phase close to the transition.

2.2. Small fluctuations around the saddle point in the broken phase.

We now wish to compute the propagators. We take \hat{v} to point in direction 1 in the internal space. Hence $\pi^1 = 0$; we use latin letters to label the $N - 1$ nonvanishing components and view the “pion” field as made out of them only. The $N = \infty$ propagator is immediately read off, in Fourier space, as

$$\langle \pi^a \pi^b \rangle = \frac{\delta^{ab}}{K(p^2) + \eta_1 \sigma_s p^2} \equiv \frac{\delta^{ab}}{\Delta_s(p^2)} \quad . \quad (2.2.1)$$

To get the Higgs field propagator we integrate out the π^a fields

$$\begin{aligned} S_3 = \frac{N-1}{2} \text{Tr} \log \hat{K} + \frac{1}{2} \int_x H \hat{K} H + \frac{N}{2} v^2 \int_x \omega + \sqrt{N} v \int_x \omega H + \\ \frac{N}{2} \int_x [\eta_2 (\partial_\mu \sigma)^2 + \mu^2 \sigma + \frac{\lambda}{2} \sigma^2 + \frac{\eta_3}{3} \sigma^3 - \sigma \omega] \quad . \end{aligned} \quad (2.2.2)$$

At large N we expand around the saddle point with $\delta\sigma = \sigma - \sigma_s$, $\delta\omega = \omega$ and $\delta H = H$. We get, neglecting order $1/N$ corrections,

$$\begin{aligned} S_3^{(2)} = \frac{N}{2} \int_p [\frac{1}{2} \delta\sigma B_{\sigma\sigma} \delta\sigma + \frac{1}{2} \delta\omega B_{\omega\omega} \delta\omega + \delta\sigma B_{\sigma\omega} \delta\omega] + \frac{1}{2} \int_p \delta H \Delta_s \delta H + \sqrt{N} v \int_p \delta\omega \delta H + \\ \frac{N}{2} \int_x [\eta_2 (\partial_\mu \delta\sigma)^2 + \frac{\lambda}{2} (\delta\sigma)^2 + \eta_3 \sigma_s (\delta\sigma)^2 - \delta\sigma \delta\omega] \end{aligned} \quad (2.2.3)$$

where

$$\begin{aligned}
B_{\sigma\sigma}(p^2) &= -\eta_1^2 \int_q \frac{(\frac{1}{4}p^2 - q^2)^2}{\Delta_s(\frac{1}{2}p - q)\Delta_s(\frac{1}{2}p + q)} \\
B_{\omega\omega}(p^2) &= -\int_q \frac{1}{\Delta_s(\frac{1}{2}p - q)\Delta_s(\frac{1}{2}p + q)} \\
B_{\omega\sigma}(p^2) &= -\eta_1 \int_q \frac{\frac{1}{4}p^2 - q^2}{\Delta_s(\frac{1}{2}p - q)\Delta_s(\frac{1}{2}p + q)} .
\end{aligned} \tag{2.2.4}$$

To find the propagator of H one has to invert a 3×3 matrix whose entries can be read off from (2.2.3, 2.2.4). Note that η_2 reappeared and the Higgs mass will depend on it.

2.3. Restriction to $\eta_1 = \eta_3 = 0$.

The problem simplifies considerably when we set $\eta_1 = \eta_3 = 0$ because η_2 doesn't appear in the saddle point equations and affects only the Higgs mass. Note that using field redefinitions and keeping terms up to order inverse cutoff square η_1 and η_3 can be eliminated from the action (2.1.4). Intuitively η_2 looks like a parameter that may have a significant effect because in (2.1.4) it gives some extra “stiffness” to the modulus of $\vec{\phi}$. We wish to see whether keeping $\eta_2 > 0$ can lead to a situation where the Higgs mass is no longer monotonically increasing with λ (since σ is a real field [see (2.1.5)] η_2 must now be non-negative to keep the action bounded from below). We shall see that any reasonable limitation on the cutoff effects in $\pi\pi$ scattering prohibits this from happening. Hence, as far as the triviality bound is concerned, we end up being driven to $\lambda = \infty$ and the dependence on η_2 ultimately drops out from the Higgs mass too. We shall assume later on that turning on the other η couplings would have had similar consequences, and that the triviality bound would be independent of them too.

Our action in dimensionless variable is now given by

$$S = \int_x \left[\frac{1}{2} \vec{\phi} K (-\partial^2) \vec{\phi} + \frac{\mu^2}{2} \vec{\phi}^2 + \frac{\lambda}{4N} (\vec{\phi}^2)^2 + \frac{\eta_2}{2N} (\partial_\mu (\vec{\phi}^2))^2 \right] . \tag{2.3.1}$$

The saddle point equations become

$$v^2 + \int_p \frac{1}{K(p^2) + \omega_s} = \sigma_s , \quad \mu^2 + \lambda \sigma_s = \omega_s . \tag{2.3.2}$$

One can show that there are no competing saddles here and hence, once $\eta_1 = \eta_3 = 0$, questions about global stability do not arise.

The critical line is given by

$$\mu_c^2 = -\lambda \int_p \frac{1}{K(p^2)} \tag{2.3.3}$$

and the broken phase is where

$$\delta\mu^2 = \mu^2 - \mu_c^2 < 0 \quad . \quad (2.3.4)$$

There, $\omega_s = 0$ and the vacuum expectation value v is given by

$$v^2 = \frac{-\delta\mu^2}{\lambda} \quad . \quad (2.3.5)$$

Denoting the fields δH , $\delta\omega$ and $\delta\sigma$ by ψ_1 , ψ_2 and ψ_3 respectively, we obtain the following propagators in Fourier space

$$\langle \psi_A \psi_B \rangle = (M^{-1})_{AB} \quad (2.3.6)$$

where

$$M = \begin{pmatrix} K(p^2) & \sqrt{-\frac{N}{\lambda}\delta\mu^2} & 0 \\ \sqrt{-\frac{N}{\lambda}\delta\mu^2} & -\frac{N}{2}I(p^2) & -\frac{N}{2} \\ 0 & -\frac{N}{2} & \frac{N}{2}(\lambda + 2\eta_2 p^2) \end{pmatrix} \quad (2.3.7)$$

and

$$I(p^2) = \int_q \frac{1}{K(\frac{1}{2}p - q)K(\frac{1}{2}p + q)} \quad . \quad (2.3.8)$$

Instead of looking at the Higgs propagator we look at $\pi \pi$ scattering. The invariant amplitude \mathcal{M} for the process $\pi^a(1) + \pi^b(2) \rightarrow \pi^c(3) + \pi^d(4)$ is

$$\begin{aligned} out \langle cd | \mathcal{M} | ab \rangle_{in} &= A(s, t, u) \delta_{ab} \delta_{cd} + A(t, s, u) \delta_{ac} \delta_{bd} + A(u, t, s) \delta_{ad} \delta_{bc} \\ s &= (p_1 + p_2)^2, \quad t = (p_1 - p_2)^2, \quad u = (p_1 - p_4)^2, \quad p_j^2 = 0 \end{aligned} \quad (2.3.9)$$

in standard Minkowski space notation. At $N = \infty$, $A(s, t, u)$ depends only on s and, in our restricted model, is proportional to the $\delta\omega$ propagator at $p^2 = -s$. Hence, by looking at the $\delta\omega$ propagator we can get both the Higgs mass and estimate the cutoff effects in $\pi \pi$ scattering and on the width to mass ratio for the Higgs. From (2.3.6, 2.3.7) we obtain

$$\langle \delta\omega \delta\omega \rangle = -\frac{2}{N} \frac{K(p^2)}{2v^2 + K(p^2)[I(p^2) + \frac{1}{\lambda + 2\eta_2 p^2}]} \quad . \quad (2.3.10)$$

We now make our choice for $K(p^2)$:

$$K(p^2) = p^2 + (p^2)^2 + \epsilon(p^2)^3 \quad . \quad (2.3.11)$$

By setting the coefficient of the $(p^2)^2$ term to one we have restricted another parameter, leaving us with 3 free parameters. With a rescaling of the cutoff and the fields* one can

* The rescaling of the fields, by itself, would lead to unphysical cutoff effects only, but the rescaling of the cutoff does induce a physically observable change in the action.

easily adapt the analysis to the case where the coefficient of the $(p^2)^2$ term is different from one, as long as it stays positive. We don't expect small changes in this coefficient to affect our final conclusion in any way, but have not checked explicitly whether our conclusion still holds when the changes are allowed to become large.

To make μ_c^2 finite we need $\epsilon > 0$. We introduce an ϵ dependence in μ^2 such that in the limit $\epsilon \rightarrow 0^+$ μ^2 diverges and $\delta\mu^2$ stays finite. Everywhere else only $\delta\mu^2$ appears and ϵ can be set to zero.[†] Thus, in the definition of $I(p^2)$ we take

$$\frac{1}{K(p^2)} = \frac{1}{p^2} - \frac{1}{p^2 + 1} \quad (2.3.12)$$

which gives us

$$I(p^2) = \frac{1}{8\pi^2} \left[-\frac{1}{2} \log(p^2) + \left(1 + \frac{1}{p^2}\right) \log(1 + p^2) - \sqrt{1 + \frac{4}{p^2}} \operatorname{arcsinh} \left(\sqrt{\frac{p^2}{4}} \right) \right] . \quad (2.3.13)$$

It is easy to check that the local stability requirement $I(p^2) > 0$ of the saddle holds for all Euclidean momenta; it is known [14] that if one extrapolates the leading asymptotic expression for $I(p^2)$ valid for small momenta to large ones, the stability requirement appears to be violated; this gives rise to the ‘‘tachyon’’ problem in the renormalized expressions and signals that for high momenta one cannot remove the cutoff dependence from the theory.

When we analytically continue to the physical regime for $\pi\pi$ scattering we replace p^2 by $-w - i0^+$ with positive w . We obtain

$$I(-w - i0^+) = \frac{i}{16\pi} - \frac{1}{8\pi^2} \left[\frac{1}{2} \log(w) + \left(\frac{1}{w} - 1\right) \log(1 - w) + \sqrt{\frac{4}{w} - 1} \arcsin \left(\sqrt{\frac{w}{4}} \right) \right] . \quad (2.3.14)$$

2.4. Higgs mass in the restricted model.

As a measure of the Higgs mass we choose the more accessible quantity, m_R^2 , defined as the smallest positive root of $\operatorname{Re}[\langle \delta\omega\delta\omega \rangle^{-1}(w)]$. It makes physical sense to only allow center of mass energies for which ghosts cannot be produced. On the other hand, the range of center of mass energies must be allowed to surpass m_R by a factor of 2–4. A pair of

[†] Note that when the coefficient of the $(p^2)^2$ term is negative ϵ cannot be taken to zero; nearest neighbor lattice actions have a negative coefficient for $(p^2)^2$ and therefore lattice actions ought to be analyzed separately. An example of such an analysis is presented in Appendix C.

ghosts can be created with $w \geq 4$. We therefore restrict m_R by $m_R \leq 0.5$. Later on we shall sharpen this requirement somewhat.

It is clear that a zero will develop in $\langle \delta\omega\delta\omega \rangle$ for $w = \lambda/\xi$, where we introduced $2\eta_2 = \xi > 0$ (see eq. (2.3.10)). This is a cutoff effect of large relative magnitude that has to be forbidden at least for energies as low as $w \leq 1$ and maybe up to $w = 4$. The unwanted zero is pushed to sufficiently high energies if we impose the requirement $\lambda/\xi > 1$ or maybe even $\lambda/\xi > 4$. We shall be able to derive our main conclusion even with the milder restriction $\lambda/\xi > 1$ and therefore we shall stick to it from now on.

Defining $x = m_R^2$ and $G = m_R^2/(2v^2)$ we have to solve the equation

$$\frac{8\pi^2}{G} = (1-x) \left[\frac{8\pi^2}{\lambda - \xi x} - \phi(x) \right] \equiv \frac{\phi'(x)}{x} \quad (2.4.1)$$

with

$$\begin{aligned} \phi(x) &= \frac{1}{2} \log(x) + \frac{1-x}{x} \log(1-x) + \sqrt{\frac{4}{x} - 1} \arcsin \left(\sqrt{\frac{x}{4}} \right) \\ &\approx \frac{1}{2} \log x + \frac{5}{12}x + \frac{19}{120}x^2 + \frac{23}{280}x^3 + \frac{251}{5040}x^4 + \dots \end{aligned} \quad (2.4.2)$$

Note the absence of a constant term in (2.4.2). When x is very small compared to unity we get

$$\frac{8\pi^2}{G} \approx \frac{8\pi^2}{\lambda} - \frac{1}{2} \log x \quad , \quad (2.4.3)$$

and clearly the maximal G is obtained at $\lambda = \infty$. This conclusion has been obtained in the perturbative regime and applies only when G is quite small even at its largest value. We want to show that the conclusion holds irrespectively of the magnitude of G .

Observe that $\phi'(x)$ will have a maximum, $0 < \bar{x}(\lambda, \xi) < 1$ and a solution x exists for a given v^2 only if v^2 satisfies $\phi'(\bar{x}) \geq 16\pi^2 v^2$. We are interested in the smallest positive root of (2.4.1); it satisfies $x < \bar{x}$. A short analysis shows that $\bar{x}(\lambda, \xi) \geq \bar{x}(\infty, 0) \approx 0.18$ and that $\phi'(x)/x$ decreases monotonically for $x \in (0, C)$. C is some number that can be shown to be larger than $\bar{x}(\infty, 0)$.

The cutoff effects can be chosen to be characterized by m_R . We now decide to limit the cutoff effects by the bound $m_R < \sqrt{p}$. We pick some positive p satisfying $p \leq \bar{x}(\infty, 0) \approx 0.18$. We shall see later on that this restriction on p is not at all severe (we already argued above for a $p \leq 0.25$). The smaller p is chosen to be, the more stringently the cutoff effects are limited.

One can view v^2 , λ , and ξ as free positive parameters restricted only by $\lambda/\xi > 1$. Indeed, any desired value for v^2 can be attained by tuning μ^2 in (2.3.5). We now look for the largest possible coupling G that satisfies (2.4.1) with some $x \leq p$. More explicitly, we are looking for the set $\{v^2, \lambda, \xi\}$ for which the equation $16\pi^2 v^2 = \phi'(x)$ (see eq. (2.4.1))

gives an x that leads to the largest G possible while x is not permitted to exceed p . Suppose we have found this set and its associated x and G . The monotonic decrease of $\phi'(x)/x$ and eq. (2.4.1) imply

$$\frac{8\pi^2}{G} \geq \frac{\phi'(p)}{p} \geq -(1-p)\phi(p) \quad . \quad (2.4.4)$$

For the largest G possible both inequalities in eq. (2.4.4) ought to become equalities. Note that ϕ does not depend on λ and ξ . The first inequality becomes an equality simply by setting $x = p$, which shows explicitly that indeed the coupling is maximized when the cutoff effects are as large as they are allowed to get. This shows that, as expected, in order to make the coupling as large as possible one has to allow the cutoff effects to grow up to the bound one has declared from the beginning; in other words, the cutoff effects as measured by the mass to cutoff ratio and the coupling, defined by the mass to v ratio, are monotonically related. The second inequality in eq. (2.4.4) can be made into an equality only when $\lambda \rightarrow \infty$; ξ is not restricted as long as it is assumed to always obey $0 \leq \xi \leq \lambda$. With any finite $\lambda \geq \xi \geq 0$ the coupling G would have been smaller for any x , including the “best” value, namely $x = p$. Therefore the Higgs mass bound is obtained in the limit $\lambda \rightarrow \infty$ and does not depend on ξ and hence the coupling η_2 .

One can compute the true pole location and one gets, for example, with $M_R/\Lambda = \sqrt{x} = \sqrt{p} = 0.397 M_H/\Lambda = 0.188$ and $\Gamma_H/\Lambda = 0.198$ showing that our restriction on p did allow for sufficiently wide (and hence heavy) Higgs particles. Note that M_H/Λ and m_R are very different numbers for such large couplings; still, in the whole range they are monotonically related so our main conclusion is unaffected.

2.5. Nonlinear actions.

In the introduction we counted the number of parameters our space of actions should depend on. In this section we saw that just having the right number of parameters is not sufficient; for example, with $\eta_1 = \eta_3 = 0$, varying η_2 in the physical range had no effect on the bound, which is obtained in the limit $\lambda \rightarrow \infty$. We also considered a linear model on an F_4 lattice having the equivalent of the couplings η_2 and η_3 and found again that the Higgs mass bound is obtained in the limit $\lambda \rightarrow \infty$. This analysis is sketched in Appendix C, since it relies heavily on methods developed in subsequent sections. We believe that the same conclusion would be found if η_1 , η_2 and η_3 were allowed to vary simultaneously. When $\lambda \rightarrow \infty$ with a properly adjusted $\mu^2 \rightarrow -\infty$ we get a nonlinear action and the $\eta_{1,2,3}$ either drop out or can be absorbed in K . In the nonlinear limit, power counting reduces to derivative counting. The leading cutoff effects are now parametrized by “dimension” four operators (the leading nonlinear term is of “dimension” two), and we therefore need

to add four-derivative terms to the non-linear action. There are three such terms, but one is redundant and can be eliminated by a suitable field redefinition.

We now have to address the question whether this time there will be some dependence on the couplings when they vary in reasonable intervals. By “reasonable” we mean intervals of order unity for the dimensionless couplings; we expect all sorts of effects to limit the range in which these couplings can vary but it is almost certain that when everything is taken into account the allowed intervals will be of order unity. We now argue that indeed, with a nonlinear action, sizable variations can be induced in physical observables by variations of order one in the couplings.

For this purpose it is useful to view the nonlinear action as a chiral effective Lagrangian rather than a cutoff version of the usual renormalizable scalar field theory. Let us do some numerology: From previous work we know that for the bound we have $M_H/(2F_\pi) \sim 2.5^*$ and Λ , the maximal allowed “momentum”, is about $2\pi M_H$. Thus $\Lambda/(4\pi(2F_\pi)) \sim 1.25$ and loop effects will be of relative order one for observables depending on external momenta smaller than Λ [15].[†] Since loop effects are more or less of the same order as tree level effects, we can reasonably expect that order one variations in the bare couplings will have measurable effects. In short, unlike in the linear case, investigating the dependence of the bound on the additional terms won’t be a waste of time.

All our actions have a derivative expansion of the form

$$S_c = \int_x \left[\frac{1}{2} \vec{\phi} (-\partial^2 + 2b_0(-\partial^2)^2) \vec{\phi} - \frac{b_1}{2N} (\partial_\mu \vec{\phi} \cdot \partial_\mu \vec{\phi})^2 - \frac{b_2}{2N} (\partial_\mu \vec{\phi} \cdot \partial_\nu \vec{\phi} - \frac{1}{4} \delta_{\mu,\nu} \partial_\sigma \vec{\phi} \cdot \partial_\sigma \vec{\phi})^2 \right] \quad (2.5.1)$$

where $\vec{\phi}^2 = N\beta$. The parameter b_0 can be absorbed in b_1 and b_2 by a field redefinition

$$\vec{\phi} \rightarrow \frac{\vec{\phi} - b_0 \partial^2 \vec{\phi}}{\sqrt{\vec{\phi}^2 + b_0^2 (\partial^2 \vec{\phi})^2 - 2b_0 \vec{\phi} \partial^2 \vec{\phi}}} \sqrt{N\beta} \quad . \quad (2.5.2)$$

Out of the four parameters β , b_0 , b_1 and b_2 only three combinations affect the leading and subleading terms in the expansion of pion scattering amplitudes in the external momenta. With Pauli–Villars cutoff we shall simply set $b_0 = 0$, but on the lattice it is usually more convenient to stick with the particular value for b_0 that comes from the expansion of the lattice kinetic energy term at small momenta. This has to be taken into account when a bare action regulated by Pauli–Villars propagators is compared to one regulated by a lattice. At infinite N the b_2 term won’t contribute to the saddle point equations because

* Recall that we are working with a rescaled F_π .

† There are arguments that would lead us to consider, in our normalization, $\Lambda/(4\pi(\sqrt{2}F_\pi)) \approx 1.76$ instead [16].

the $O(N)$ invariant bilinear that appears in it cannot acquire a vacuum expectation value as long as Lorentz invariance is preserved. More analysis will show that this term doesn't contribute to the leading cutoff effects on $\pi\pi$ scattering and the Higgs width. Hence, up to questions of global stability b_2 can be ignored and simply set to zero. This fact will be used as an argument to simplify the kind of lattice actions we are going to consider explicitly.

The class of actions regulated by Pauli–Villars terms we choose to investigate is, in dimensionless units, given by

$$S = \int_x \left[\frac{1}{2} \vec{\phi} [-\partial^2 + (-\partial^2)^{n+1}] \vec{\phi} - \frac{1}{2Ng_1} (\partial_\mu \vec{\phi} \cdot \partial_\mu \vec{\phi})^2 - \frac{1}{2Ng_2} (\partial_\mu \vec{\phi} \cdot \partial_\nu \vec{\phi} - \frac{1}{4} \delta_{\mu,\nu} \partial_\sigma \vec{\phi} \cdot \partial_\sigma \vec{\phi})^2 \right] \quad (2.5.3)$$

where $\vec{\phi}^2 = N\beta$ and $n \geq 3$ is an integer. When $n \rightarrow \infty$ we approach a sharp momentum cutoff. For such a cutoff the parameter counting presented in the introduction doesn't work because even at first subleading order in the inverse cutoff nonlocal higher dimensional operators make their appearance. We are interested in large n values, however, because there one expects a greater similarity to the lattice, in the sense that arbitrarily high momentum excitations are almost totally suppressed.

We shall also study actions regularized on the lattice because only the latter can be solved nonperturbatively by Monte Carlo. We shall consider the F_4 lattice and the hypercubic lattice. On a hypercubic lattice the operator counting is slightly wrong because of the existence of a Lorentz breaking dimension six operator which has no counterpart in any conceivable extension of the minimal standard model. This has no effect on the particular observables that we will consider at $N = \infty$, but would lead to measurable effects at order inverse cutoff square in other observables. Such a problem does not arise for the F_4 lattice.

The most concise action on the F_4 lattice that reduces, up to higher order terms, in the continuum limit to the form (2.5.1) is

$$S = -2N\beta_0 \sum_{\langle x, x' \rangle} \vec{\Phi}(x) \cdot \vec{\Phi}(x') - N\beta_1 \sum_{\langle x, x' \rangle} [\vec{\Phi}(x) \cdot \vec{\Phi}(x')]^2 - N \frac{\beta_2}{8} \sum_x \sum_{\substack{\langle l, l' \rangle \\ l \cap x \neq \emptyset, l' \cap x \neq \emptyset, l \cap l' \neq \emptyset, x, x', x'' \text{ all n.n.}}} \left[\left(\vec{\Phi}(x) \cdot \vec{\Phi}(x') \right) \left(\vec{\Phi}(x) \cdot \vec{\Phi}(x'') \right) \right] \quad (2.5.4)$$

where x, x', x'' denote sites and $\langle x, x' \rangle, l, l'$ links. Here the field is constrained by $\vec{\Phi}^2(x) = 1$. Geometrically, the first two terms couple two fields connected by a nearest neighbor bond and the last term couples three fields that live at the corners of an equilateral triangle whose sides are nearest neighbor bonds. The existence of elementary triangular

“plaquettes” is a special feature of the F_4 lattice and provides here for the desirable feature that (2.5.4) couples only nearest neighbors.

This feature is desired for Monte Carlo simulations because these do not yield direct measurements of physical cutoff effects and one usually estimates the latter by looking at the range of interactions in the ultraviolet expressed in terms of the measured estimates for the Higgs mass. This range is simply the lattice spacing when the action couples only nearest neighbors. It is independent of the values of the couplings in the action. If the action contained both nearest neighbor and next nearest neighbor couplings it would be less clear what to view as the range and it would be quite reasonable to assume that the range does depend this time on the couplings in the action. In the pure nearest neighbor case we still don’t know, from Monte Carlo alone, how large the observable cutoff effects really are, but we can expect with reasonable confidence that variations of the bare couplings affect the cutoff effects only through variations in the Higgs mass as measured in lattice units. However, when there is a mixture of nearest neighbor and next nearest neighbor terms in the action one may suspect that what one calls the “lattice unit” changes when the couplings are varied.

To take the continuum limit we rescale the field $\vec{\phi} = \sqrt{6N(\beta_0 + \beta_1 + \beta_2)}\vec{\Phi}$ (we only consider the region $\beta_0 + \beta_1 + \beta_2 > 0$). The combination $\frac{1}{36} \frac{\beta_1}{(\beta_0 + \beta_1 + \beta_2)^2}$ is then analogous to b_2 and the combination $\frac{1}{48} \frac{\beta_1 + \beta_2}{(\beta_0 + \beta_1 + \beta_2)^2}$ analogous to b_1 . The first term in (2.5.4) gives the usual kinetic term, $g(p)$, on the F_4 lattice,

$$g(p) = \frac{1}{6} \sum_{\mu \neq \nu} [2 - \cos(p_\mu + p_\nu) - \cos(p_\mu - p_\nu)] = p^2 - \frac{1}{12}(p^2)^2 + O(p^6) \quad . \quad (2.5.5)$$

The p^4 part corresponds to a negative b_0 in (2.5.1) which, with the field redefinition (2.5.2), generates a positive contribution to b_1 . Thus the naïve nonlinear nearest neighbor F_4 lattice action corresponds effectively to a continuum action with a positive b_1 -type term.

For hypercubic lattices the inclusion of next nearest neighbor couplings is unavoidable if one wishes to obtain (2.5.1) in the long wavelength limit. The argument against next nearest neighbor terms holds only within the limitations of Monte Carlo methods and is therefore relevant to the physical case of $N = 4$. However, at $N = \infty$ “mixed” actions are as useful as “pure” ones because we have at our disposal means to directly evaluate the observable cutoff effects. Therefore we shall also consider “mixed” lattice actions.

As a matter of fact the large N analysis of the model (2.5.4) is quite complicated while certain “mixed” models are easier. The reason is that at large N one has to introduce auxiliary fields to decouple the terms in the action that are quartic in the fields. One would need an auxiliary field for each of the “positive” bonds emanating from a site (12 on an F_4 lattice) and additional auxiliaries for enforcing the nonlinear constraint. This large

number of coupled fields makes an analytical treatment cumbersome on the F_4 lattice. In Pauli-Villars regularization one also has quite a few auxiliary fields but most can be easily decoupled exploiting Euclidean $O(4)$ invariance. On a lattice the symmetry is only a discrete subgroup of $O(4)$, and while this might be sufficient, we chose to avoid carrying out this exercise. The Pauli-Villars analysis will teach us that all the extra auxiliaries are irrelevant to the order in inverse cutoff that we are interested in. But to this order, the F_4 lattice is essentially $O(4)$ invariant so the same conclusion should hold on it too. Therefore it seems somewhat a waste of effort to struggle to fully solve (to infinite order in the inverse cutoff) the pure nearest neighbor action. Moreover, this “exact solution” only goes as far as giving us expressions involving some lattice momentum integrals, and, in practice, one still has to evaluate the latter by numerical means making it again necessary to approximate by ignoring terms that have no effect to leading order in the inverse cutoff. To be sure, in Monte Carlo simulations, at $N = 4$, we are advocating the use of the “triangle” action (2.5.4).

We have argued earlier that for Pauli-Villars regularization the b_2 term plays no role to the order in the inverse cutoff considered. We assume that this would also happen on the lattice and set β_1 to 0. We have also explained that we would like to avoid having to deal with the β_2 term in (2.5.4). To preserve the freedom of varying the strength of the important couplings in the long wavelength limit we need to replace this term by another one that has a similar effect at long wavelength but which can be easily “decoupled” preferably employing one auxiliary field only. We choose an action that does this:

$$S = -2N\beta_0 \sum_{\langle x,x' \rangle} \vec{\Phi}(x) \cdot \vec{\Phi}(x') - N \frac{\beta_2}{16\gamma} \sum_x \left[\sum_{\substack{l \cap x \neq \emptyset \\ l = \langle x,x' \rangle}} \vec{\Phi}(x) \cdot \vec{\Phi}(x') \right]^2. \quad (2.5.6)$$

The parameter γ has been introduced because the same formula will work for the hypercubic lattice also; for the F_4 lattice $\gamma = 3$, but for the hypercubic lattice $\gamma = 1$. Geometrically, the new term corresponds to a coupling between any four fields that live at the ends of two bonds that have a site in common. Before, on the F_4 lattice, we only had such coupling if the two bonds spanned an angle of sixty degrees at the common site. Now larger angles are included and fields living on sites separated by more than a single lattice spacing are coupled.

On a hypercubic lattice it is impossible to write down an action like (2.5.4) involving only nearest neighbor terms. The second term in (2.5.4), when considered on a hypercubic lattice, becomes in the continuum limit proportional to $\sum_\mu (\partial_\mu \vec{\Phi} \cdot \partial_\mu \vec{\Phi})^2$ and thus breaks Lorentz invariance. We therefore have an additional reason to ignore it as we did before for the F_4 lattice. The action (2.5.6) considered on a hypercubic lattice reduces, after rescaling $\vec{\phi} = \sqrt{2N(\beta_0 + \beta_2)} \vec{\Phi}$, almost to the form (2.5.1) with $b_2 = 0$ and $\frac{1}{32} \frac{\beta_2}{(\beta_0 + \beta_2)^2}$

analogous to b_1 . The difference is that instead of the b_0 term in (2.5.1) we now have a Lorentz invariance breaking term $\vec{\phi} \sum_{\mu} \partial_{\mu}^4 \vec{\phi}$. In view of this we have no strong reason for considering this particular form of the action, except that it includes, with β_2 set to 0, the case most thoroughly investigated to date for $N = 4$.

In naïve nonlinear models on the hypercubic lattice the Lorentz invariance breaking term can be avoided by using a ‘‘Symanzik improved’’ action. For $N = 4$ the exact elimination of Lorentz invariance breaking terms at order inverse cutoff square is not an attractive proposition because it would necessitate an impracticable amount of ‘‘fine tuning’’. At infinite N this problem is less severe and we can do quite well with just generalizing the (tree level) Symanzik improved action to also contain a b_1 like term with four fields and four derivatives. We are thus led to also consider the action

$$S_{SI} = -2N\beta_0 \sum_{x,\mu} \left(\frac{4}{3} \vec{\Phi}(x) \cdot \vec{\Phi}(x+\mu) - \frac{1}{12} \vec{\Phi}(x) \cdot \vec{\Phi}(x+2\mu) \right) - N \frac{\beta_2}{20} \sum_x \left[\sum_{\pm\mu} \left(\frac{4}{3} \vec{\Phi}(x) \cdot \vec{\Phi}(x+\mu) - \frac{1}{12} \vec{\Phi}(x) \cdot \vec{\Phi}(x+2\mu) \right) \right]^2 . \quad (2.5.7)$$

As will be seen later on, this choice of the transcription of the four-derivative term exactly eliminates Lorentz breaking terms in the full pion propagator at order inverse cutoff square.

3. PHASE DIAGRAM FOR THE PAULI–VILLARS MODELS.

Similarly to the linear case we introduce auxiliary fields in (2.5.3) to make the dependence on $\vec{\phi}$ bilinear. We obtain a new action

$$S_1 = \int_x \left[\frac{1}{2} \vec{\phi} K \vec{\phi} + \frac{1}{2} \lambda (\partial_{\mu} \vec{\phi})^2 + \frac{1}{2} \rho (\vec{\phi}^2 - N\beta) + \frac{1}{2} \omega_{\mu\nu} [\partial_{\mu} \vec{\phi} \partial_{\nu} \vec{\phi} - \frac{1}{4} \delta_{\mu\nu} (\partial_{\sigma} \vec{\phi})^2] \right] + \frac{1}{8} \int_x [g_1 N \lambda^2 + g_2 N \omega_{\mu\nu} \omega_{\mu\nu}] \quad (3.1)$$

where $\omega_{\mu\mu} = 0$ (summation over repeated indices is implied) and $\omega_{\mu\nu} = \omega_{\nu\mu}$ and hence the $\delta_{\mu\nu}$ terms above can be replaced by zero. In more condensed notation we have

$$S_1 = \frac{1}{2} \int_x \vec{\phi} \hat{K} \vec{\phi} - \frac{N}{2} \int_x [\beta \rho - \frac{1}{4} g_1 \lambda^2 - \frac{1}{4} g_2 \omega_{\mu\nu} \omega_{\mu\nu}] \quad (3.2)$$

with

$$\hat{K} = K - \partial_{\mu} \lambda \partial_{\mu} + \rho - \partial_{\mu} \omega_{\mu\nu} \partial_{\nu} . \quad (3.3)$$

We separate the zero mode of $\vec{\phi}$ as in the linear case in (2.1.7) and integrate out $\vec{\pi}$ and H . We obtain

$$S_2 = \frac{N}{2} \left[\text{Tr} \log \hat{K} + v^2 \int_x \rho - v^2 \int \rho' \hat{K}^{-1} \rho' - \int_x (\beta \rho - \frac{1}{4} g_1 \lambda^2 - \frac{1}{4} g_2 \omega_{\mu\nu} \omega_{\mu\nu}) \right] \quad (3.4)$$

with

$$\partial_\mu (\rho - \rho') = 0, \quad \int_x \rho' = 0. \quad (3.5)$$

3.1. Saddle point equations and dominating saddles.

The saddle point equations are

$$\begin{aligned} \int_p \frac{1}{K(p^2) + \lambda_s p^2 + \rho_s} + v^2 &= \beta \\ \int_p \frac{p^2}{K(p^2) + \lambda_s p^2 + \rho_s} &= -\frac{1}{2} g_1 \lambda_s. \end{aligned} \quad (3.1.1)$$

As promised, the saddle point equations do not depend on g_2 . Sometimes they may admit several solutions. In these cases we need to find the dominating one. Among the possible solutions some may have broken symmetry and some unbroken symmetry all at the same couplings. In such regions of the phase diagram the order–disorder transition can become discontinuous. The analytic continuation of the continuous transition into these domains yields metastable critical regimes that have to be eliminated from our search for the Higgs mass bound. Therefore, a complete analysis of the competing saddles is necessary. We shall ignore possible dominating “end point” contributions because we are pretty sure that they will not affect our conclusions regarding the accessible critical regime. As will be clear later on, the possibility of first order transitions cutting into the critical regime is realized and has physical content teaching us something about the dynamics that is both relevant and illuminating for the mass bound issue.

From (3.4) it is clear that we wish to find the solution (λ_s, ρ_s) that minimizes the following function of λ and ρ :

$$\psi(\lambda, \rho) = \int_p \log \frac{p^2(1 + p^{2n}) + \lambda p^2 + \rho}{p^{2(n+1)}} + v^2 \rho - \beta \rho + \frac{1}{4} g_1 \lambda^2. \quad (3.1.2)$$

The function is completely defined when one adds that $v^2 > 0$ implies $\rho = 0$ and $\rho > 0$ implies $v^2 = 0$. Both ρ and v^2 are nonnegative.

To simplify the analysis we introduce some rescaled variables

$$u = (1 + \lambda)(16\pi^2 \beta)^{\frac{n}{n-1}}, \quad t = \rho(1 + \lambda)^{-\frac{n+1}{n}}. \quad (3.1.3)$$

It is also useful to factor out a positive constant from ψ and consider from now on only the minimization of $\hat{\psi}$, defined by

$$\hat{\psi}(u, t) = u^{\frac{2}{n}} \int_0^\infty \xi d\xi \log \frac{t + \xi + \xi^{n+1}}{\xi^{n+1}} + \frac{v^2}{\beta} t u^{\frac{n+1}{n}} - t u^{\frac{n+1}{n}} + \frac{1}{2} g^* (u - u^*)^2 \quad (3.1.4)$$

where

$$g_1 = 32\pi^2 \beta^2 g^* , \quad u^* = (16\pi^2 \beta)^{\frac{n}{n-1}} . \quad (3.1.5)$$

It is easy to check that the saddle point equations are reproduced by setting the derivatives of $\hat{\psi}$ with respect to u and t to zero. This of course had to be true.

We now split the candidate saddles into two classes according to whether the symmetry is broken at the saddle or not. In the symmetric phase $v^2 = 0$ and the equation $\partial\hat{\psi}/\partial t = 0$ can be used to define a function $t(u)$ for $0 \leq u \leq u_0$ by

$$\int_0^\infty \frac{\xi d\xi}{\xi^{n+1} + \xi + t(u)} = u^{\frac{n-1}{n}} , \quad u_0 = \left(\int_0^\infty \frac{d\xi}{1 + \xi^n} \right)^{\frac{n}{n-1}} = \left(\frac{\pi}{n \sin(\frac{\pi}{n})} \right)^{\frac{n}{n-1}} . \quad (3.1.6)$$

$t(u)$ varies between zero and positive infinity when u goes from u_0 to 0.

Let u_s and t_s be the coordinates of a saddle point in the symmetric phase. Starting from

$$\hat{\psi}(u_s, t_s) = \int_{u_0}^{u_s} \frac{\partial\hat{\psi}}{\partial u}(u, t(u)) + \hat{\psi}(u_0, 0) \quad (3.1.7)$$

we derive

$$\hat{\psi}(u_s, t_s) = \int_{u_0}^{u_s} [G(u) + g^*(u - u^*)] + \hat{\psi}(u_0, 0) \quad (3.1.8)$$

where

$$G(u) = u^{\frac{2-n}{n}} \int_0^\infty \frac{\xi^2 d\xi}{\xi^{n+1} + \xi + t(u)} . \quad (3.1.9)$$

G is defined in the interval $(0, u_0)$ and is monotonically decreasing there.

In the broken phase the equation

$$\left(\frac{\partial\hat{\psi}}{\partial t} \right)_{t=0} = 0 \quad (3.1.10)$$

together with the requirement $v^2 \geq 0$ yields the restriction $u_s \geq u_0$. The function $\hat{\psi}$ at the saddle can be written as

$$\hat{\psi}(u_s, 0) = \frac{n}{2} u^{\frac{2}{n}} \int_0^\infty \frac{\xi d\xi}{1 + \xi^n} + \frac{1}{2} g^* (u - u^*)^2 . \quad (3.1.11)$$

If we extend the range of the function G from $u \in (0, u_0)$ to the segment $u \in [u_0, \infty)$ with

$$G(u) = u^{\frac{2-n}{n}} \int_0^\infty \frac{\xi d\xi}{1 + \xi^n} = u^{\frac{2-n}{n}} \frac{\pi}{n \sin(\frac{2\pi}{n})} \quad \text{for } u > u_0 \quad (3.1.12)$$

we can rewrite (3.1.11) as

$$\hat{\psi}(u_s, 0) = \int_{u_0}^{u_s} [G(u) + g^*(u - u^*)] + \hat{\psi}(u_0, 0) \quad . \quad (3.1.13)$$

The advantage of these manipulations is that equations (3.1.8) and (3.1.13) have identical forms and can be geometrically interpreted.

$G(u)$ is somewhat complicated but independent of the continuously varying couplings – hence it can be computed once n is given. The dependence on the couplings comes in through the parameterization of the straight line $-g^*(u - u^*)$; different couplings correspond to different intercepts and slopes of the straight line. All candidate saddles are found at intersections between the straight line and the “universal” function G . The quantity to be minimized is the signed area bounded by G , the straight line, the line $u = u_0$ and by the particular intersection point under investigation. When the straight line $-g^*(u - u^*)$ intersects G three times and the two areas between the consecutive intersection points are of equal magnitude we are at a symmetry breaking transition point of first order. When the straight line intersects G only once at the point $(u_0, G(u_0))$ the transition is second order if the straight line is steeper than the line representing the tricritical case. The tricritical case corresponds to a straight line that goes through $(u_0, G(u_0))$ and, in addition, is tangent to G there. These cases are illustrated in Fig. (3.1) for $n = 3$. When the straight line does not intersect G there is no translationally invariant saddle and we are in a frustrated phase.

In equations the conditions for criticality are as follows: The tricritical point has parameters given by

$$g_{t.c.}^* = \frac{n-2}{2\pi} \tan\left(\frac{\pi}{n}\right) \quad , \quad u_{t.c.}^* = 2\frac{n-1}{n-2}u_0 \quad (3.1.14)$$

and the second order line is described by

$$u^* = u_0 \left(1 + \frac{n}{n-2} \frac{g_{t.c.}^*}{g^*} \right) \quad , \quad \frac{g_{t.c.}^*}{g^*} < 1 \quad . \quad (3.1.15)$$

3.2. Physical properties of the phase diagram.

The details of the complete phase diagram are not essential; the schematic structure is presented in Fig. (3.2). The “frustrated region” corresponds to regions where translational invariance breaks spontaneously and regular saddle points are either not competitive or do not exist.

It is important to understand the source of the tricritical point: As already mentioned, the action can also be viewed as an effective chiral Lagrangian with couplings of order one.

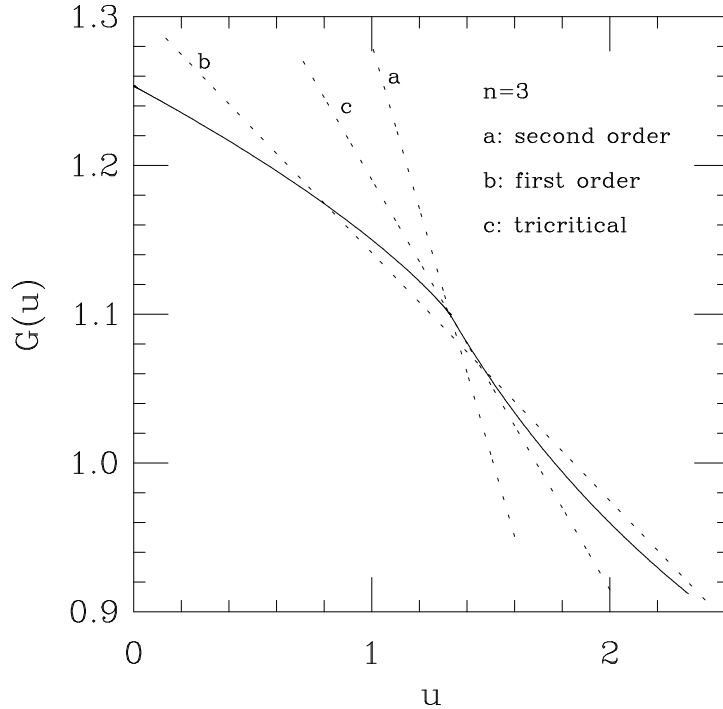


Figure 3.1 The solid line is the function $G(u)$ for $n = 3$ and the straight dotted lines represent $-g^*(u - u^*)$ for three typical transition points. All candidate saddles are found at intersections between the straight line and the function G ; the coupling constants in the action only affect g^* and u^* .

The single stable particles are the pions. Two pions will attract if they are in a relative zero angular momentum and total isospin singlet state. This is easy to understand: If two field configurations corresponding to an approximately localized pion are placed one on top of the other and the isospin indices match appropriately, the net state will be closer to the vacuum than a state where the pions are far apart. The index matching will be right when the total isospin is zero. Hence, soft pions attract in the $I = 0, J = 0$ state, a well known fact. One can change the interaction between the pions only at subleading order in their momenta, p^4 (even the logarithmic part $p^4 \log p^2$ is fixed by current algebra), and this is the main physical effect produced by varying the couplings (of course the value of F_π/Λ is also changed by the variation of the couplings, but this is an “unphysical” effect). If one introduces extra attraction, it is possible that two pions of some nonvanishing momentum each (in units of the cutoff), can bind to a zero mass state which will be stable and condense. We believe that this is what is happening at the tricritical point and we shall

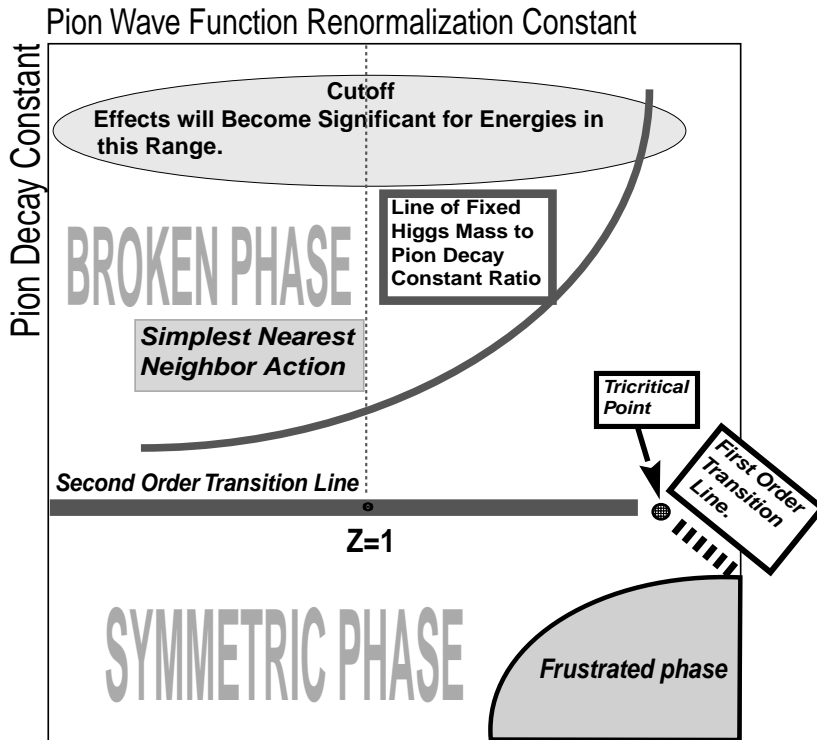


Figure 3.2 Generic phase diagram containing the qualitative features common to all models investigated.

present some evidence later on. As far as the Higgs mass bound goes, we want to make the resonance replacing the above bound state as heavy as possible. This will be achieved if we introduce as much repulsion as possible between the pions, thus delaying the formation of the resonance to higher momenta of the “constituent” pions. We shall see that this reasoning is born out by explicit calculations.

To complete our investigation of the region of the phase diagram we are interested in, we must also ascertain the local stability of our saddle points (global stability was checked in section (3.1) but we ignored until now the question of local stability). To do this part

of the analysis we need to compute the small fluctuations around the saddle points. Since we are interested only in a particular region, our computations will be restricted to that part of the phase diagram. We should also remember that some of the field variables are auxiliaries. The integration contour for auxiliary fields that are unphysical can be deformed in the stable directions, so stability isn't really an issue there. However, we are not allowed to deform the integration contours for the “physical” fields, because if we did that we would easily lose the approximate unitarity we have at low energies. Among the auxiliaries only ρ is “unphysical” as its role was just to impose the fixed length constraint; however, $\omega_{\mu\nu}$ and λ are simply related to bilinears of field gradients and should stay real fields. In short, we must make sure that the pion, Higgs, ω and λ propagators come out to be positive in Euclidean momentum space.

3.3. Pion propagator and ghosts.

From now on we shall always assume that the couplings are chosen in such a way that we are somewhere in the broken phase close to the second order transition.

We again separate out the zero mode from the field $\vec{\phi}$ and parametrize the remainder by H and $\vec{\pi}$ (see (2.1.7)). Expanding around the saddle we introduce the shifted fields

$$\delta\lambda = \lambda - \lambda_s, \quad \delta H = H, \quad \delta\vec{\pi} = \vec{\pi}, \quad \delta\omega_{\mu\nu} = \omega_{\mu\nu}, \quad \delta\rho = \rho. \quad (3.3.1)$$

From (3.3) we read off the pion propagator in Fourier space

$$\langle \delta\pi^a \delta\pi^b \rangle = \frac{\delta^{ab}}{K(p^2) + \lambda_s p^2} = \frac{\delta^{ab}}{(1 + \lambda_s)p^2 + (p^2)^{n+1}}. \quad (3.3.2)$$

There are ghosts in this propagator (poles with residues that are not real positive numbers). Their presence reflects the fact that Lorentz invariant Pauli–Villars regularization is achieved at the expense of exact unitarity in Minkowski space. The ghost poles are located on a circle in the complex p^2 plane

$$|p_{ghost}^2| = (1 + \lambda_s)^{\frac{1}{n}}. \quad (3.3.3)$$

The condition $\lambda_s \geq -1$ is always satisfied. When the energies in a process approach $(1 + \lambda_s)^{\frac{1}{2n}} \Lambda \equiv \Lambda_s$ one expects violent cutoff effects to set in. Thus, the “physical” cutoff scale is coupling dependent and different from the “bare” cutoff Λ . In retrospect we see that it makes more sense to measure our dimensionful quantities not in terms of Λ as we did until now but rather in terms of Λ_s . When we do the lattice analysis we shall see that violations of Euclidean rotational invariance occur in the pion propagator at a distance of the order of the lattice spacing and that there is no dependence on the couplings. In our

case the correct analogue of the inverse lattice spacing is Λ_s , not Λ , and rescaling by Λ_s here is analogous to the standard practice of setting the lattice spacing equal to unity in lattice work.

We rescale all our fields (including the auxiliaries) and couplings, but keep the old notation,

$$\begin{aligned}
\partial_\mu, p &\rightarrow \partial_\mu, p \times (1 + \lambda_s)^{\frac{1}{2n}} \\
\partial_p, x &\rightarrow \partial_p, x \times (1 + \lambda_s)^{-\frac{1}{2n}} \\
\vec{\phi}, H, \vec{\pi} &\rightarrow \vec{\phi}, H, \vec{\pi} \times (1 + \lambda_s)^{\frac{1}{2n}} \\
\lambda &\rightarrow \lambda \\
\rho &\rightarrow \rho \times (1 + \lambda_s)^{\frac{1}{n}} \\
\omega &\rightarrow \omega \\
v &\rightarrow v \times (1 + \lambda_s)^{\frac{1}{2n}} \\
g_{1,2} &\rightarrow g_{1,2} \times (1 + \lambda_s)^{\frac{2}{n}} .
\end{aligned} \tag{3.3.4}$$

The original constraint $\vec{\phi}^2 = N\beta$ now becomes $\vec{\phi}^2 = (1 + \lambda_s)^{-\frac{1}{n}} N\beta$ and the pion propagator becomes

$$\langle \delta\pi^a \delta\pi^b \rangle = \frac{\delta^{ab}}{(1 + \lambda_s)[p^2 + (p^2)^{n+1}]} = \frac{\delta^{ab}}{(1 + \lambda_s)K(p^2)} . \tag{3.3.5}$$

With standard conventions we define the pion wave function renormalization constant Z_π by

$$Z_\pi = \frac{1}{1 + \lambda_s} . \tag{3.3.6}$$

This constant is fixed by the couplings through the saddle point equations. From our analysis of the phase diagram we deduce that the range in which Z_π is allowed to vary is

$$0 \leq Z_\pi \leq \frac{2(n-1)}{n-2} . \tag{3.3.7}$$

Z_π depends only on g_1 and it is useful to invert the relationship viewing Z_π as the external control parameter restricted only by (3.3.7)

$$\frac{1}{g_1} = \frac{1}{2 \int_k \frac{k^2}{K(k)}} \left(\frac{1}{Z_\pi} - \frac{1}{Z_\pi^2} \right) . \tag{3.3.8}$$

(3.3.8) is a rewriting of the second saddle point equation and fixes λ_s . The other saddle point equation fixes v . We know that ultimately we shall be more interested in the quantity v^2/Z_π because it is equal to the pion decay constant. So we choose to write the first saddle point equation in the form

$$\frac{v^2}{Z_\pi} = \beta Z_\pi^{\frac{1-n}{n}} - \int_k \frac{1}{K(k^2)} . \tag{3.3.9}$$

3.4. Small fluctuations in the broken phase.

After integrating out the pions from the action (3.2) and taking into account the rescalings (3.3.4), we expand around the saddle point. To quadratic order in the small fluctuations we obtain

$$\begin{aligned}
S_2^{(2)} &= \frac{1}{2Z_\pi} \int_k \delta H K \delta H + \sqrt{N}v \int_k \delta \rho \delta H + \frac{N}{8} \int_k (g_1 \delta \lambda^2 + g_2 \delta \omega_{\mu\nu}^2) + \\
&\frac{N-1}{2} Z_\pi^2 \int_k \left[\frac{1}{2} \delta \lambda B^{\lambda\lambda} \delta \lambda + \delta \lambda B_{\mu\nu}^{\omega\lambda} \delta \omega_{\mu\nu} + \frac{1}{2} \delta \omega_{\mu\nu} B_{\mu\nu, \mu'\nu'}^{\omega\omega} \delta \omega_{\mu'\nu'} \right] + \\
&\frac{N-1}{2} Z_\pi^2 \int_k \left[\frac{1}{2} \delta \rho B^{\rho\rho} \delta \rho + \delta \rho B^{\rho\lambda} \delta \lambda + \delta \rho B_{\mu\nu}^{\omega\rho} \delta \omega_{\mu\nu} \right]
\end{aligned} \tag{3.4.1}$$

where

$$\begin{aligned}
B^{\rho\rho}(p^2) &= - \int_k \frac{1}{K(\frac{1}{2}p+k)K(\frac{1}{2}p-k)} \\
B^{\lambda\lambda}(p^2) &= - \int_k \frac{(\frac{1}{4}p^2 - k^2)^2}{K(\frac{1}{2}p+k)K(\frac{1}{2}p-k)} \\
B^{\rho\lambda}(p^2) &= \int_k \frac{\frac{1}{4}p^2 - k^2}{K(\frac{1}{2}p+k)K(\frac{1}{2}p-k)} \\
B_{\mu\nu}^{\omega\rho}(p^2) &= \int_k \frac{\frac{1}{4}p_\mu p_\nu - k_\mu k_\nu - \frac{1}{4}\delta_{\mu\nu}(\frac{1}{4}p^2 - k^2)}{K(\frac{1}{2}p+k)K(\frac{1}{2}p-k)} \\
B_{\mu\nu}^{\omega\lambda}(p^2) &= - \int_k \frac{[\frac{1}{4}p_\mu p_\nu - k_\mu k_\nu - \frac{1}{4}\delta_{\mu\nu}(\frac{1}{4}p^2 - k^2)](\frac{1}{4}p^2 - k^2)}{K(\frac{1}{2}p+k)K(\frac{1}{2}p-k)} \\
B_{\mu\nu, \mu'\nu'}^{\omega\omega}(p^2) &= \\
&- \int_k \frac{[\frac{1}{4}p_\mu p_\nu - k_\mu k_\nu - \frac{1}{4}\delta_{\mu\nu}(\frac{1}{4}p^2 - k^2)][\frac{1}{4}p_{\mu'} p_{\nu'} - k_{\mu'} k_{\nu'} - \frac{1}{4}\delta_{\mu'\nu'}(\frac{1}{4}p^2 - k^2)]}{K(\frac{1}{2}p+k)K(\frac{1}{2}p-k)} .
\end{aligned} \tag{3.4.2}$$

To compute the various propagators we would have to invert a 12×12 matrix. To simplify this task we exploit rotational invariance to block diagonalize the matrix. We decompose the field $\delta \omega_{\mu\nu}$ in a spin-zero, spin-one and spin-two field. To do this we introduce Euclidean polarization vectors $W_\mu^j(p)$, where $j = 1, 2, 3$,

$$W_\mu^j(p) W_\mu^k(p) = \delta^{jk} , \quad p_\mu W_\mu^j(p) = 0 . \tag{3.4.3}$$

We now define new ω fields

$$\begin{aligned}
\delta \omega_{\mu\nu}(p) &= \\
W_\mu^j(p) W_\nu^k(p) \delta \omega_{jk}(p) &+ \frac{1}{2|p|} [p_\mu W_\nu^j(p) + p_\nu W_\mu^j(p)] \delta \omega_j(p) + \frac{1}{p^2} [p_\mu p_\nu - \frac{1}{4} \delta_{\mu\nu} p^2] \delta \omega(p) .
\end{aligned} \tag{3.4.4}$$

The spin–two field $\delta\omega_{jk}$ is symmetric and traceless. Because of Lorentz invariance the 12×12 matrix must now split up into three blocks: a 4×4 block involving the scalar fields δH , $\delta\lambda$, $\delta\rho$ and $\delta\omega$, a diagonal 3×3 block for the vector field $\delta\omega_j$ and a diagonal 5×5 block for the tensor field $\delta\omega_{jk}$. This decomposition is exact in Pauli–Villars regularization because of the preservation of rotational invariance; on a lattice this decoupling would not be exact, but, as long as one is ultimately going to expand in the inverse cutoff only to leading and subleading order, a similar simplification should occur for F_4 lattice actions that don't break the lattice symmetries. In terms of the new $\delta\omega$ fields the quadratic action becomes, ignoring order $1/N$ corrections,

$$\begin{aligned}
S_2^{(2)} &= \frac{1}{2Z_\pi} \int_k \delta H K \delta H + \sqrt{N}v \int_k \delta\rho \delta H + \frac{N}{2} Z_\pi^2 \\
&\int_k \left[\delta\lambda \left(\frac{1}{2} B^{\lambda\lambda} + \frac{1}{4Z_\pi^2} g_1 \right) \delta\lambda + \delta\lambda B^{\omega\lambda} \delta\omega + \frac{1}{2} \delta\rho B^{\rho\rho} \delta\rho + \delta\rho B^{\rho\lambda} \delta\lambda + \delta\rho B^{\omega\rho} \delta\omega \right] + \frac{N}{2} Z_\pi^2 \\
&\int_k \left[\delta\omega \left(\frac{1}{2} B^{\omega\omega} + \frac{3}{16Z_\pi^2} g_2 \right) \delta\omega + \delta\omega_j \left(\frac{1}{2} B_V^{\omega\omega} + \frac{1}{8Z_\pi^2} g_2 \right) \delta\omega_j + \delta\omega_{jk} \left(\frac{1}{2} B_T^{\omega\omega} + \frac{1}{4Z_\pi^2} g_2 \right) \delta\omega_{jk} \right] .
\end{aligned} \tag{3.4.5}$$

The B “bubbles” in (3.4.5) are projections of the B bubbles in (3.4.2) via (3.4.4). Their explicit forms can be read off equation (3.4.8) below. Introducing the four component fields ψ_A , representing δH , $\delta\rho$, $\delta\lambda$ and $\delta\omega$ for $A = 1, 2, 3, 4$, respectively, we rewrite eq. (3.4.5) as

$$S_2^{(2)} = \frac{1}{2} \int_k \psi_A M_{AB} \psi_B + \frac{1}{2} \int_k [M_V \sum_j (\delta\omega_j)^2 + M_T \sum_{jk} (\delta\omega_{jk})^2] . \tag{3.4.6}$$

The variables M are functions of the couplings and momentum square; they can all be expressed in terms of six elementary “bubble” integrals $I_{n,m}(p^2)$, $m + n \leq 2$:

$$I_{n,m}(p^2) = \int_k \frac{(k^2)^n (p \cdot k)^{2m}}{(p^2)^m K(\frac{1}{2}p + k) K(\frac{1}{2}p - k)} . \tag{3.4.7}$$

M_{AB} is symmetric with non-vanishing entries

$$\begin{aligned}
M_{11} &= \frac{K}{Z_\pi} \\
M_{12} &= \sqrt{N}v \\
M_{22} &= -\frac{1}{2}NZ_\pi^2 I_{0,0} \\
M_{23} &= \frac{1}{2}NZ_\pi^2 \left(\frac{p^2}{4}I_{0,0} - I_{1,0} \right) \\
M_{24} &= \frac{1}{2}NZ_\pi^2 \left(\frac{3p^2}{16}I_{0,0} - I_{0,1} + \frac{1}{4}I_{1,0} \right) \\
M_{33} &= \frac{1}{2}NZ_\pi^2 \left(\frac{g_1}{2Z_\pi^2} - \frac{(p^2)^2}{16}I_{0,0} + \frac{p^2}{2}I_{1,0} - I_{2,0} \right) \\
M_{34} &= \frac{1}{2}NZ_\pi^2 \left(-\frac{3(p^2)^2}{64}I_{0,0} + \frac{p^2}{4}I_{0,1} + \frac{p^2}{8}I_{1,0} - I_{1,1} + \frac{1}{4}I_{2,0} \right) \\
M_{44} &= \frac{1}{2}NZ_\pi^2 \left(\frac{3g_2}{8Z_\pi^2} - \frac{9(p^2)^2}{256}I_{0,0} + \frac{3p^2}{8}I_{0,1} - I_{0,2} - \frac{3p^2}{32}I_{1,0} + \frac{1}{2}I_{1,1} - \frac{1}{16}I_{2,0} \right) \\
M_V &= \frac{1}{2}NZ_\pi^2 \left(\frac{g_2}{4Z_\pi^2} + \frac{1}{3}I_{0,2} - \frac{1}{3}I_{1,1} \right) \\
M_T &= \frac{1}{2}NZ_\pi^2 \left(\frac{g_2}{2Z_\pi^2} - \frac{2}{15}I_{0,2} + \frac{4}{15}I_{1,1} - \frac{2}{15}I_{2,0} \right) .
\end{aligned} \tag{3.4.8}$$

3.5. Spontaneous breakdown of space–time invariances and local stability.

We are finally in position to check local stability for the vector and tensor fields. The corresponding matrix entries M_T and M_V first vanish at zero momentum when g_2 decreases to a critical value g_{2c} given by

$$g_{2c} = \frac{Z_\pi^2}{6} \int_k \frac{(k^2)^2}{K^2(k)} . \tag{3.5.1}$$

At $g_2 = g_{2c}$ also the entry M_{44} vanishes at zero momentum. In all our subsequent calculations we shall assume g_2 to be safely larger than this critical value so that even for negative (but small in absolute magnitude relative to unity) values of p^2 these entries are of order unity and positive. Physically, we wish to keep the masses of the vector and the tensor of the order of the cutoff. Note that both fields are isoscalars.

On a lattice a related phenomenon would be that a non-translational invariant saddle takes over. In Pauli–Villars regularization when translations get broken so do rotations

and we obtain both a massless vector and a massless tensor. On a lattice rotations aren't a continuous symmetry and we would not expect a "tensor" like particle to also become massless.

Thus, although g_2 doesn't appear in the phase diagram there is some bound on it too. Once this bound is satisfied we have no evidence for any other source of local instability and we believe that the 4×4 matrix M will be positive definite for all Euclidean momenta. We have not tested this fully, but from the behavior at low momenta, which we did test (see below), it seems very safe to assume that no local instability is hiding at high momenta and that all critical regions that we shall henceforth be interested in are indeed accessible.

3.6. Spontaneous breakdown of scale invariance at the tricritical point.

The limitation on Z_π in (3.3.7) is turned by eq. (3.3.8) into a limitation on g_1

$$-\infty < \frac{1}{g_1} < \frac{2\pi n^2(n-2) \sin \frac{2\pi}{n}}{(n-1)^2} . \quad (3.6.1)$$

The tricritical point is at $g_1 = g_{1,t.c.}$ where

$$g_{1,t.c.} = \frac{(n-1)^2}{2\pi n^2(n-2) \sin \frac{2\pi}{n}} . \quad (3.6.2)$$

Note that the rescalings (3.3.4) have changed the definition of g_1 so that (3.6.2) differs from the combined effect of (3.1.5), (3.1.6) and (3.1.14) by a factor of $Z_\pi^{\frac{2}{n}}$.

When g_1 approaches $g_{1,t.c.}$ it is easy to check that the matrix element M_{33} from (3.4.8) vanishes at $p^2 = 0$. This implies that $\det M(p^2 = 0) = 0$, because, at $p^2 = 0$ also M_{11} and M_{34} vanish and then the first and third row of M are proportional to each other. The zero eigenvector is a particular linear combination of δH and $\delta \lambda$. The field λ is related by the equations of motion to $(\partial_\mu \vec{\phi})^2$; this is obvious from eq. (3.1). A pole at zero momentum in $\delta \lambda$ is therefore likely to be interpretable as a dilaton. Therefore, at $g_1 = g_{1,c}$ the Higgs particle becomes massless and also plays the role of a dilaton. This behavior is similar to the one discovered by Bardeen, Moshe and Bander in three dimensions with a bare action that was renormalizable [17].

4. HIGGS MASS BOUND AND CUTOFF EFFECTS WITH PAULI-VILLARS REGULARIZATION.

We are now ready to address the main problem: How large can one make the ratio m_H/f_π while keeping cutoff effects small? We shall carry out our analysis in two stages.

At the first stage an approximate but simple calculation will tell us what to expect. At the second stage we shall perform a complete analysis.

First we need to make an observation that will simplify matters for both stages: The Higgs mass will be obtained from the matrix M_{AB} of (3.4.8). We are only interested in small values of f_π (*i.e.*, F_π in units of Λ_s) and for such values the Higgs resonance will appear at small complex value of p^2 (also in units of Λ_s) because the physical coupling, even if large, is a finite number. Therefore, it is consistent to expand the entries $M_{AB}(p^2)$ in powers and logarithms of p^2 . In ordinary, renormalized continuum field theory (*i.e.* when calculating only universal quantities), we would stop the expansion at leading order. Here we shall be going to one order higher. The observation we wish to make is that to first subleading order the scalar $\delta\omega$ decouples and the Higgs mass and width can be obtained from the 3×3 upper left corner of the 4×4 scalar block of M . We shall denote this submatrix by M^r .

In addition, $\delta\omega$ contributes to $\pi \pi$ scattering, given by the exchange of the scalar auxiliary fields, only at orders that we shall be neglecting. Almost all the information needed for calculating $\pi \pi$ scattering to first subleading order in the inverse cutoff is contained in M^r . Fluctuations in the approximately decoupled low momentum components of $\delta\omega$ are under control because, as we have seen, local stability requirements for the vector and tensor low momentum excitations stabilize also the scalar $\delta\omega$. Thus, finally, the dependence on the precise value of g_2 also disappears from all the processes we shall be interested in.

Once we decided to go only to first subleading order we have to focus on M^r and from (3.4.7) and (3.4.8) we see that we only need 3 out of the 6 “bubble” integrals in (3.4.7), namely $I_{n,0}$ for $n \leq 2$. For arbitrary n it would be very inconvenient to try to work out closed forms for the complete integrals as we did in the linear case. Moreover, unlike in the linear case, we have already dropped some higher order terms when we reduced our problem to M^r so we should be consistent and keep only the leading and subleading terms in the external momentum for the three bubbles that we need. Some of the technical details of the relevant computations are sketched in Appendix A. The results are

$$\begin{aligned}
I_{0,0}(p^2) &= \frac{1}{16\pi^2} \left[-\log p^2 + 1 - \frac{1}{n} - \left(1 - \frac{1}{n^2}\right) \frac{\pi}{12 \sin \frac{\pi}{n}} p^2 \right] + \dots \\
I_{1,0}(p^2) &= \frac{1}{16\pi^2} \left[\left(1 - \frac{1}{n}\right) \frac{\pi}{n \sin \frac{\pi}{n}} + \frac{1}{4} p^2 \log p^2 + \frac{3 - 6n - n^2}{12n} p^2 \right] + \dots \\
I_{2,0}(p^2) &= \frac{1}{16\pi^2} \left[\frac{(n-2)\pi}{n^2 \sin \frac{2\pi}{n}} - \frac{(n-1)(n+4)\pi}{12n^2 \sin \frac{\pi}{n}} p^2 \right] + \dots .
\end{aligned} \tag{4.1}$$

Note that the limit $n \rightarrow \infty$ can be taken on the leading terms but not on the subleading ones. This reflects the fact that with a sharp momentum cutoff the first correction is

suppressed by $|p|$ and not by p^2 which means that non-local operators come into play. Also, there is a slight error in the equation for the simplest bubble, $I_{0,0}$, in [9,10]: at infinite n we get to leading order in p^2 , $I_{0,0}(p^2) = \frac{1}{16\pi^2}[-\log p^2 + 1]$, while in [9,10] $I_{0,0}(p^2) = \frac{1}{16\pi^2}[-\log p^2 + 2]$ is used. This has no significant effect on the physical numbers obtained in these papers. As a matter of fact, many workers adopt a convention where the “physical” cutoff Λ_L (the “Landau pole”) is defined as the point where the asymptotic expansion of $I_{0,0}$, $I_{as} = \frac{1}{16\pi^2}[-\log p^2 + c]$ obviously breaks down, namely, $I_{as}(\Lambda_L^2) = 0$. With such a convention, the particular value of the constant c does not need to be known, and all dependence on the cutoff scheme disappears. This convention is of course quite arbitrary but not totally unreasonable; it does explain to a certain extent the effective “universality” of the triviality bound.

4.1. Approximate calculation.

It is much easier to do calculations for weak couplings. Ultimately we wish to find out how strong the physical coupling can become without distorting the theory too much. This is achieved by limiting the cutoff effects. If we make this limitation extremely stringent the cutoff is very high and because of triviality we are forced to weak physical couplings where it is easy to calculate. Even for very stringent limitations on the cutoff effects there will be a dependence on the bare couplings and in some region of the space of bare couplings the physical coupling will be allowed to be larger (while still very small in absolute magnitude) than in other regions. It is very reasonable to assume that there is some smoothness in the dependence on the higher dimensional operators that is induced by the variation in the bare couplings and, therefore, the region we shall be interested in is the one where we expect the largest possible coupling even when the cutoff effects are less stringently limited. In particular, we already know that in practice the physical coupling cannot be made large in a sense that would invalidate perturbation theory completely. The major result to date is that even for relatively small physical couplings the cutoff effects become sizable disallowing further increases. Therefore, our decision to first work where the physical coupling is small is not expected to lead us astray.

When the physical coupling is small the width of the Higgs particle is small too and, to simplify the formulae, we shall ignore width effects and concentrate on the quantity m_R defined by

$$\text{Re}[\det M^r(p^2)]_{p^2=-m_R^2} = 0 \quad . \quad (4.1.1)$$

m_R is related to, but not equal to, m_H . It can become quite different from m_H even for moderate physical couplings but the relationship between the two is monotonic and, for the purpose of identifying the right region in the action space, m_R is perfectly adequate. Similar considerations were presented in our study of the linear models.

In our approximate analysis all the subleading effects are small but still hard to calculate. Since they are small, they do not affect the numerical value of the leading order answer.* We could do without calculating them explicitly if we had an independent means to tell when a given case will have larger cutoff effects than another case. The easiest is to use the pion propagator, because it has a simple explicit form to all orders in the inverse cutoff (see eq. (3.3.5)). In units of Λ_s we know that ghosts will appear for energies of order one and this is independent of the bare couplings. Therefore, making m_R in units of Λ_s as small as possible while keeping the ratio m_R/f_π constant will diminish the cutoff effects and identify the right region in the space of bare actions where a larger triviality bound ought to be found. To be sure, our approximation isn't quite consistent logically because the cutoff effects on the pion propagator are suppressed by more than one power of p^2 and hence do not reflect the dimension six operators. We still think that our approximation is useful because, if one does not "fine tune" in the sense explained before, once the cutoff effects induced by the dimension 6 operators become sizable (of the order of 10 percent) all the higher dimensional operators also quickly become important. Therefore, the pion propagator does sense the point where cutoff effects turn on in an overwhelming way. Our argument is also helped by the fact that our more complete analysis confirms the findings we shall present here. We should point out that most lattice work was essentially equivalent to viewing the inverse lattice spacing as $\sim \Lambda_s/\pi$. This point of view is not logically superior to the one we adopt in this section but nevertheless produces quite reasonable results when compared to the outcome of a more sophisticated analysis.

By general arguments we know that

$$m_R^2 \approx C^2(Z_\pi) \exp[-96\pi^2/g_R] \quad (4.1.2)$$

where

$$g_R = 3 \frac{m_R^2}{f_\pi^2}, \quad f_\pi^2 = \frac{v^2}{Z_\pi}, \quad (4.1.3)$$

and we have already used the fact that any desired value of f_π can be obtained for any Z_π by tuning β . Therefore the constant C depends only on Z_π (which has been traded for g_1 in (3.3.8)). All that is left to compute is this constant and for this we only need the leading terms in eq. (4.1). We plug in the needed results from (4.1) in (3.4.8) and then in (4.1.1) ending up with

$$C(Z_\pi) = \exp \left[\frac{n-1}{2n} \left(1 + \frac{\pi}{n \tan(\pi/n)} \zeta(Z_\pi) \right) \right] \quad (4.1.4)$$

$$\zeta(Z_\pi) = \frac{Z_\pi - 1}{1 - Z_\pi(n-2)/(2(n-1))} .$$

* A quantitative feeling may be obtained from the analogous situation in the linear case: see the expansion in eq. (2.4.2).

Since, as explained above, we want to find the range of Z_π where, for a fixed ratio m_R/f_π , m_R is minimal, we need to minimize C . We must remember that Z_π is restricted by (3.3.7). The fact that Z_π has to be positive is no surprise and we now see that, at the other end of the interval, where $Z_\pi = 2(n-1)/(n-2)$, C diverges showing that the critical region shrinks to zero there. This is where the tricritical point is located and our analysis confirms our physical arguments that indicated that the bound would be largest when one stays as far as possible from the tricritical point.

As far as the numerical validity of the approximation is concerned we can get some feeling by looking at the higher order (neglected here) terms in (4.1) or at the expansion in (2.4.2) for an analogous problem. An accurate evaluation will be given later on in subsection (4.6). The numerical values one gets from (4.1.2) are, for example, good to one percent if m_R corresponds to a physical Higgs mass no larger than 0.800 TeV , $Z_\pi \leq 1$ and $n \leq 100$. For larger values of n the accuracy deteriorates somewhat.

4.2. Some numbers.

To get a feeling for the numbers involved let us take $N = 4$ and ask what change in C will induce a noticeable change in $\frac{m_R}{2f_\pi}$ away from the value $\frac{m_R}{2f_\pi} = \frac{\pi}{2^{1/3}} \approx 2.5$ corresponding more or less to the present bound. Maintaining the cutoff effects at a fixed magnitude with $\delta(m_R) = 0$ we get

$$-\delta \log C = \frac{8\pi^2}{\left(\frac{m_R}{2f_\pi}\right)^3} \delta\left(\frac{m_R}{2f_\pi}\right) = \frac{16}{\pi} \delta\left(\frac{m_R}{2f_\pi}\right) \approx 5 \delta\left(\frac{m_R}{2f_\pi}\right) = 20\delta M_R [\text{in TeV}] . \quad (4.2.1)$$

To increase M_R by 0.100 TeV we need to decrease C by a factor of $e^2 \approx 7.4$. Between $Z_\pi = 0$ and $Z_\pi = 1$ little variation is induced, but when Z_π approaches $2\frac{n-1}{n-2}$, $\frac{m_R}{f_\pi}$ will decrease sharply. In summary, for almost all large enough n 's the region $0 \leq Z_\pi \leq 1$ seems to give reasonable estimates for the bound. In terms of g_1 this region corresponds to $g_1 \leq 0$, showing that the parameterization of the space of actions we chose is a reasonable one and lending support to our physical understanding of the mechanism affecting the bound.

When $Z_\pi = 1$ $\frac{1}{g_1} = 0$ by (3.3.8) and the model is the simplest nonlinear model possible. While this is not the most optimal place to look for the bound, it is reasonably close to it. Therefore, even the simplest model, and even setting $n = \infty$, as we discussed above, will give us reasonable and quite high estimates for the bound. On the lattice the situation is not exactly the same, however, and this is the main reason for present estimates being quite significantly lower. A lattice action of the naïve type has generically, in the notation of eq. (2.5.1), a nonvanishing negative parameter b_0 in the derivative expansion.

To approximately translate this into a Pauli–Villars regularization one must redefine the fields according to (2.5.2) and this induces an effective g_1 coupling (and some g_2 coupling also, but this has no effect) with a positive sign. Hence naïve lattice actions are somewhat outside the region where reasonable estimates for the bound can be obtained and, because of this, the lattice bound is expected to increase. We shall see that the increase is not negligible, but not very dramatic either.

4.3. Computing leading cutoff effects in $1/N$.

We have reached the point that we wish to do a complete calculation. In this subsection we explain in detail the calculation conceptually.

The physical scale is set by the unitless f_π . Therefore, we consider f_π as an exact function of the bare parameters. By definition there are no “cutoff effects” in f_π . Similarly we define another “exact” quantity, the coupling $g = 3m_H^2/f_\pi^2$. m_H is the exact real part of the pole of the amplitude for $I = 0, J = 0$ $\pi-\pi$ scattering when continued to the second sheet below the physical cut. m_H is a function of the bare couplings with no “cutoff effects” by definition.

Consider now some new physical quantity. We make it dimensionless by extracting the appropriate power of f_π and denote it by P . P may depend on momenta q_i which we measure also in units of f_π : $q_i = r_i f_\pi$. Let the bare action depend on n bare parameters. We imagine changing variables to f_π, g and $n - 2$ remaining parameters p and consider P as a function of them: $P = P(r_1, r_2, \dots; f_\pi, g; p)$. The change of variables holds in some neighborhood of a particular point in the broken phase that we wish to investigate. We keep p fixed and carry out a double expansion of P in f_π^2 and g without paying attention to whether the change of variables is one to one also in the region where this expansion is sensible. Note that the dependence on f_π is both explicit and implicit via the momenta.

If we expand P in g at fixed r_i, f_π and p renormalizability and universality tell us that to any finite order in g the limit $f_\pi \rightarrow 0$ exists and is independent of p . The summation of all orders in g of the $f_\pi = 0$ terms is ambiguous in the full theory because the series is badly behaved. However, in our case we expand P in $1/N$ after the appropriate rescaling and redefinition of g . To leading order in $1/N$ P has a nontrivial limit as $f_\pi \rightarrow 0$ even without expanding in g . It is unlikely that this continues to be the case at subleading orders in $1/N$ because one cannot replace the leading order (in $1/N$) propagators in higher order (in $1/N$) terms by their leading asymptotic expressions in f_π as this will induce divergences in the momentum integration at the positions of the “Landau poles”. But at leading order we are lucky and this simplifies our task considerably.

The above may look like a contradiction to triviality, because we just argued that at

leading order in $1/N$ we can obtain a nontrivial continuum limit. The catch is that the change of variables from the bare parameters to f_π , g and p excludes precisely the region where the continuum limit is taken. There are no values of the bare parameters that are physically acceptable and can maintain a nonvanishing coupling g while f_π is taken to zero.* However, we can carry out our change of variables away from the critical line in the broken phase and work out the expansion by analytically continuing (even without noticing) into the inaccessible region.† In this way we can, at least at leading order in $1/N$, disentangle the issue of triviality from the issue of summability of the renormalized perturbation theory.

Once we have the $f_\pi \rightarrow 0$ limit, $P_{N=\infty}(r_1, r_2, \dots; 0, g)$, we can expand in the inverse cutoff

$$P_{N=\infty}(r_1, r_2, \dots; f_\pi^2, g; p) - P_{N=\infty}(r_1, r_2, \dots; 0, g) = \Delta P_{N=\infty}(r_1, r_2, \dots; f_\pi^2, g; p) + O(f_\pi^4 \log^\Upsilon f_\pi) \quad (4.3.1)$$

where Υ is some finite number. We define the leading cutoff effect by

$$\delta_P(r_1, r_2, \dots; f_\pi^2, g; p) = \frac{\Delta P_{N=\infty}(r_1, r_2, \dots; f_\pi^2, g; p)}{P_{N=\infty}(r_1, r_2, \dots; 0, g)} . \quad (4.3.2)$$

In practice we always work on a one dimensional line connecting the given point in the broken phase where we wish to calculate the cutoff effects to some point on the critical line. We change variables in our parameter space (and this change is globally well defined in a large region that includes the critical manifold) from the original n parameters to $n - 1$ parameters \bar{p} and one parameter ξ . ξ can be traded in a one to one fashion for g . Varying \bar{p} and g we span the whole region we are interested in. We organize our work by fixing \bar{p} and varying g along the line. Our purpose is to find the region in \bar{p} where g can be maximized under the restriction that the cutoff effects on some physical observable(s) do not exceed a given amount. Along the line f_π is monotonically dependent on g and the cutoff effect is measured by $\bar{\delta}$ where

$$\bar{\delta}_P(r_1, r_2, \dots; g; \bar{p}) \equiv \delta_P(r_1, r_2, \dots; f_\pi^2(g), g; p) . \quad (4.3.3)$$

In practice, we cannot compute the function g exactly in terms of the bare parameters and cannot carry out the change of variables explicitly. But, we can compute $\bar{\delta}$ exactly,

* This can be seen as follows: For small g and fixed Z_π , m_H satisfies an equation that is similar to (4.1.2) and for all acceptable Z_π one has $C(Z_\pi) \geq C_{min} > 0$. Replacing m_H on the left hand side of the equation by f_π and g we see that if g is fixed f_π is bounded from below away from zero.

† There are claims that if this is really done with care one will discover ambiguities and these are a direct reflection of the singularity structure of P in the Borel variable conjugate to g [18].

because errors of order $f_\pi^4 \log^\Upsilon f_\pi$ or higher in g have no effect and it is practical to compute $f_\pi(g)$ neglecting order $f_\pi^4 \log^\Upsilon f_\pi$ contributions. In plots we shall always show $\bar{\delta}$ as a function of $M_H \equiv \sqrt{g/3} \times 0.123 \text{ TeV}$ in order to be able to immediately read off the Higgs mass bound in TeV .

There is a fundamental difference between our way of calculating cutoff effects here and the one employed previously in the triviality context. Here, the single approximation in computing $\bar{\delta}$ is the expansion in $1/N$. In other computations, at $N = 4$, one uses the loop expansion. In terms of the bare coupling, the loop expansion is a finite rearrangement of the perturbative expansion. An answer correct to l loops will be also correct to order l in the bare coupling. This is still true when the series is reexpressed in terms of an appropriately defined renormalized coupling, g . The series for $\bar{\delta}$ in g has the following general structure:

$$\bar{\delta} = g^\Upsilon f_\pi^2 \sum_{n=0}^{\infty} g^n \sum_{l=0}^n \mathcal{P}_{n,l}(\log f_\pi^2) \quad (4.3.4)$$

where $\mathcal{P}_{n,l}$ is a polynomial of degree l , l is the number of loops, and Υ is some number. Along a line in the space of bare actions that touches the critical surface at its end we have $f_\pi \sim \exp[-48\pi^2/g]$ (at $N = \infty$) and one needs to go to an infinite number of loops to get $\bar{\delta}$ to a reasonable accuracy, even when g is small. Therefore, estimates of cutoff effects obtained by truncating the loop expansion are not under good control. In Appendix B we give an explicit example of this problem.

4.4. Leading corrections to the width to mass ratio.

The Higgs resonance is a complex root of $\det M^r(p^2) = 0$ on the second sheet

$$\det M^r\left(-\left(m_H - \frac{i}{2}\gamma_H\right)^2\right) = 0 \quad . \quad (4.4.1)$$

What is meant by “second sheet” is that the branch of the logarithm is chosen so that, for $0 \leq \gamma_H/m_H \ll 1$,

$$\log\left(-\left(m_H - \frac{i}{2}\gamma_H\right)^2\right) \approx \log(m_H^2) - i\frac{\gamma_H}{m_H} - i\pi \quad . \quad (4.4.2)$$

In practice it will turn out that we have to restrict our attention to the region where the width does not exceed the mass by much.

With rescaled bubble integrals

$$B_j(p^2) = 16\pi^2 I_{j,0}(p^2) \quad , \quad (4.4.3)$$

the explicit form of eq. (4.4.1), for $p^2 = -(m_H - \frac{i}{2}\gamma_H)^2$ is

$$\frac{32\pi^2 f_\pi^2}{K(p^2)} = -B_0(p^2) - \frac{[\frac{1}{4}p^2 B_0(p^2) - B_1(p^2)]^2}{\frac{n}{(n-2)(Z_\pi-1)}B_2(0) - \frac{1}{16}p^4 B_0(p^2) + \frac{1}{2}p^2 B_1(p^2) - B_2(p^2)} . \quad (4.4.4)$$

Our problem is to solve this complex equation for the real unknowns m_H and γ_H as a function of f_π^2 , to first subleading order (logarithms are counted as order one) for small f_π^2 . We no longer assume weak coupling, so the ratio m_H/f_π is taken to be of order one too (up to logarithms).

We are working along lines of constant Z_π which plays the role of the set of parameters \bar{p} in section (4.3). It is useful to introduce a convenient parameterization of the line which is chosen so that the equation simplifies. On the line we have three real unknowns, all small relative to unity: f_π , m_H and γ_H . (4.4.4) gives us two relations among the unknowns and the remaining free parameter describes the line. We choose the free parameter to be an angle θ defined by

$$(m_H - \frac{i}{2}\gamma_H)^2 = \mu^2 \exp[-i\theta] \quad (4.4.5)$$

where μ^2 is real and positive. We shall be interested only in that portion of the line where the mapping between θ and the coupling

$$g = 3 \frac{m_H^2}{f_\pi^2} \quad (4.4.6)$$

is one to one (in practice this limits the magnitude of g but cutoff effects become large before this limit is reached). This portion of the line includes the critical point at one of its ends.

The two real equations (4.4.4) have to be solved now for μ^2 and g in terms of θ . We shall obtain the solution by first solving to leading order and then perturbing around it with the subleading terms. The leading order solution is

$$\begin{aligned} \mu_0 &= C(Z_\pi) \exp \left[-\frac{\theta_0 + \pi}{2 \tan(\theta_0)} \right] \\ g_0 &= \frac{96\pi^2 \cos^2(\frac{\theta_0}{2}) \sin(\theta_0)}{(\theta_0 + \pi)} . \end{aligned} \quad (4.4.7)$$

It is easy to check that, as $\theta_0 \rightarrow 0$ we get for m_H the same equation we wrote down for m_R in (4.1.2). Note that $g_0(\theta_0)$ is bounded in the interval of interest, $0 \leq \theta_0 \leq \pi$.

The physical quantity, $P(; 0, g) = \frac{\gamma_H}{m_H}$, we are interested in is dimensionless, and has no external momenta (we suppress the subscript $N = \infty$ that we used in section (4.3)). To leading order in the cutoff we have

$$P(; 0, g_0) = 2 \tan(\frac{\theta_0}{2}) \quad (4.4.8)$$

where θ_0 is given in terms of g_0 by the inverse of the second equation in (4.4.7).

To calculate to next order we treat all three variables θ , g and μ^2 on equal footing. These variables are defined by (4.4.5) and (4.4.6). At leading order we had $\theta = \theta_0$, $\mu = \mu_0$ and $g = g_0$ given by (4.4.7) with θ_0 as a free parameter, a coordinate along the constant Z_π line. If we treat all three parameters on an equal footing we ought to also allow for the subleading terms to change the coordinate along the line. We set

$$\begin{aligned}\mu^2 &= \mu_0^2 + \delta_\mu \\ \theta &= \theta_0 + \delta_\theta \\ g &= g_0 + \delta_g \ .\end{aligned}\tag{4.4.9}$$

The equations (4.4.4), when expanded to subleading order give us two relations among the three δ 's above. The needed third relation comes from noting that the quantity $P(; f_\pi^2, g; Z_\pi)$ in (4.3.1) is evaluated at the same g as the quantity $P(; 0, g)$ there. Therefore we have

$$\delta_g = 0 \ .\tag{4.4.10}$$

Carrying out the algebra we obtain

$$\bar{\delta}_{\frac{\Gamma_H}{M_H}}(g_0; Z_\pi) = \frac{D(Z_\pi, n)\mu_0^2}{1 + (\pi + \theta_0) \left[\tan\left(\frac{\theta_0}{2}\right) - \cot(\theta_0) \right]}\tag{4.4.11}$$

where, on the right hand side, θ_0 and μ_0 are functions of g_0 defined in (4.4.7). g_0 is a free parameter and the subscript 0 has no particular meaning any more. The function $D(Z_\pi, n)$ is given by

$$D(Z_\pi, n) = \frac{\pi(n^2 - 1)}{12n^2 \sin \frac{\pi}{n}} + \frac{(n + 3) \cos \frac{\pi}{n}}{6} \zeta(Z_\pi, n) + \frac{\pi(n - 1)(n - 2) \cos^2 \frac{\pi}{n}}{12n^2 \sin \frac{\pi}{n}} \zeta^2(Z_\pi, n) \ .\tag{4.4.12}$$

The function $\zeta(Z_\pi, n)$ was defined in (4.1.4), only now we have written out explicitly its dependence on n .

The overall structure of eq. (4.4.11) is very simple. The correction has factorized into a function that carries all the dependence on the coupling g and is universal times a function that carries all the information about the cutoff, through the dependence on Z_π and n , namely $C^2(Z_\pi, n)D(Z_\pi, n)$. It is amusing to note that the dependence on Z_π always comes in through the combination that appears in the definition of ζ .

This factorization is more powerful than what one would have expected on the basis of the Symanzik improvement formulae, as they are usually presented, in several respects. First, we seem to have only a single operator insertion because if we had a linear superposition of several operator insertions nothing special should be evident when one looks at a

single momentum independent observable as we are. Second, the coefficient of the operator is independent of the renormalized coupling. Third, the logarithms in the subleading terms have been summed in closed form. To be sure, we are looking at a physical operator, not an arbitrary correlation function, so the operator counting should be different. Also, we are working at $N = \infty$ where additional simplifications should occur. Our result could be explained if it were true that, at $N = \infty$, all cutoff effects in on-shell dimensionless physical quantities (that are functions of dimensionless momenta) are given by an effective renormalized action,

$$S_{eff} = S_R + c \exp[-96\pi^2/g]\mathcal{O} \quad , \quad (4.4.13)$$

where \mathcal{O} is a renormalized operator, c is a g independent free parameter containing all the non-universal information and S_R is describing the usual universal part of physical observables with the unit of energy set by $f_\pi = 1$. In terms of general RG reasoning this representation of the S_{eff} is not unreasonable if one accepts that at $N = \infty$ the number of available independent operators decreases. We shall see that this would also explain our results for the π - π scattering amplitude.

$D(Z_\pi, n)$ is a quadratic polynomial in the variable ζ and has two negative roots. It turns out that one of the roots can be realized in the allowed range of Z_π . For $n = 3$ the root is at $Z_\pi \approx 0.52$ while when $n \rightarrow \infty$ the root is realized by $Z_\pi \approx \frac{6}{\sqrt{n}}$. We see that for all n the roots are for Z_π between 1 and 0. If we set Z_π to be at the appropriate root for the value of n chosen we have achieved “improvement” in the sense of Symanzik in that the leading cutoff correction has been made to vanish. This would be the type of fine tuning that we excluded because, as far as we know, it is unreasonable to expect the more complete theory in which the minimal standard model is embedded (assuming that this is the situation in nature) to conspire to achieve such a more refined decoupling. We are entitled however to use a reasonable range, say $0 \leq Z_\pi \leq 0.5$ and $n \leq 100$ to estimate the bound.

We find that for $M_H \leq 0.820 \text{ TeV}$ the cutoff effect on the width to mass ratio is less than half a percent, as will be shown in Fig. 7.3d. At such a high mass at infinite N the system is strongly interacting.

4.5. Leading corrections to π - π scattering

We now repeat the analysis of the previous section for π - π scattering. We are considering the process $\pi^a(1) + \pi^b(2) \rightarrow \pi^c(3) + \pi^d(4)$ where a, b, c, d are isospin indices and (1-4) denote momenta. We work in the center of mass frame and wish to compute the invariant amplitude $A(s, t, u)$ defined in (2.3.9) to first non-vanishing order in $\frac{1}{N}$.

To leading order in $1/N$ and up to and including subleading order in the inverse cutoff, $A(s, t, u)$ is dominated by the exchange of scalar–isoscalar fields and therefore is just a function of s , $A(s)$. The differential cross–section with identical isospin indices for the in–coming pions, in the center of mass frame, is isotropic and given by

$$\left(\frac{d\sigma}{d\Omega}\right)_{CM} = \frac{N}{64\pi^2 s} |A(s)|^2 \quad (4.5.1)$$

where s is the square of the center of mass energy, henceforth denoted by W , and we are working to leading order in $1/N$.

In fact, keeping only the leading order in $1/N$ alone, at any finite cutoff, is enough to exclude the contribution of exchanges of the spin–one field, $\delta\omega_j$, by Bose symmetry. However, the exchange of the spin–two field, $\delta\omega_{jk}$, does come in, only at one order higher in the inverse cutoff than the order we are calculating to. In the case of a linear action we had a similar simplification. An immediate consequence of this is that we shall see no higher spin resonance in our computations (a ρ –like particle for example). To see an even spin resonance it might be sufficient to just keep all orders in the cutoff, but to see an odd spin resonance one must go to a higher order in $1/N$.

To evaluate $A(s)$ and see where the observations in the previous paragraph come from, we need to write down the pion interactions. We go back to equation (3.2) and introduce the pion fields and the Higgs field by eq. (2.1.7):

$$S_1 = \frac{1}{2} \int_x [\vec{\pi} \hat{K} \vec{\pi} + H \hat{K} H] - \frac{N}{2} v^2 \int_x \rho - \sqrt{N} v \int_x \rho H - \frac{N}{2} \int_x [\beta \rho - \frac{1}{4} g_1 \lambda^2 - \frac{1}{4} g_2 \omega_{\mu\nu} \omega_{\mu\nu}] \quad (4.5.2)$$

Here \hat{K} is defined in (3.3) as $\hat{K} = K - \partial_\mu \lambda \partial_\mu + \rho - \partial_\mu \omega_{\mu\nu} \partial_\nu$. We expand around the saddle point, carry out the rescalings (3.3.4), but do not integrate out δH and $\delta \vec{\pi}$ yet. There are three types of vertices involving pions, all involve two pion fields with isospin indices contracted and a third field, which is $\delta\rho$, $\delta\lambda$ and $\delta\omega_{\mu\nu}$, respectively. At leading order in $1/N$, $A(s)$ is dominated by diagrams containing two vertices of the above type and the full propagators (to leading order in $1/N$) of the ψ fields ((3.4.6)) and of $\delta\omega_{jk}$ ((3.4.4)).

The expansion in the inverse cutoff is an expansion in f_π^2 where, up to logarithms, m_H^2 and all momenta p_j^2 are of order unity in f_π^2 . We are still assuming that g_2 is safely larger than g_{2c} ((3.5.1)) and therefore the spin–two field has a “mass” of order unity. We also know that ultimately we shall continue analytically to Minkowski space with on–shell external pions, $p_j^2 = 0$. Under these conditions we first carry out an order of magnitude estimation of the vertices and propagators that can be read off (4.5.2). For this purpose it is better not to think in terms of the full propagator, but use multiple insertions of the two point vertices in (4.5.2), which amounts to the same thing. It is then easy to see that the only kind of diagrams that contribute to leading order have the external pions

connected to two $\pi\pi\delta\rho$ vertices. The internal line has multiple insertions of $\delta\rho\delta H$ vertices and of the various $\pi\pi$ bubbles. When we decide to also keep the first subleading terms we have to add diagrams where two of the external pions are still coupled by a $\pi\pi\rho$ vertex but the other two external pions couple to a $\pi\pi\lambda$ vertex. The internal lines in these new diagrams have essentially the same structure as before. The conclusion is that, in terms of full propagators, we have, with Euclidean $q = p_1 + p_2$, but keeping only terms that will contribute to the on-shell amplitude,

$$A(q^2) \propto [\langle \delta\rho\delta\rho \rangle (q^2) - q^2 \langle \delta\rho\delta\lambda \rangle (q^2)] . \quad (4.5.3)$$

The full propagator $\langle \delta\rho\delta\rho \rangle (q^2)$ is needed to leading and subleading order, while the full propagator $\langle \delta\rho\delta\lambda \rangle (q^2)$ is needed only to leading order. These propagators are obtained from the inverse of the matrix M (3.4.6, 3.4.7, 3.4.8). Some more order of magnitude estimates show that the 4×4 matrix M can be replaced, to the order we are interested in, by the 3×3 matrix M^r defined at the beginning of section 4.

In the notation of section (4.3), the dimensionless quantity we are interested in here is chosen to be

$$P(r; f_\pi^2, g; Z_\pi) = |A(p^2 \rightarrow -r^2(f_\pi^2 + i0^+))|^2 \quad (4.5.4)$$

where $r = W/F_\pi$. One expects a bump in P when $W = M_H$ and the width Γ_H is small. It therefore makes more sense to replace r by another dimensionless number, R , so that in R the bump would be independent of g when the width of the Higgs is small. We therefore define

$$R = \frac{W^2}{4M_H^2} \equiv \frac{3r^2}{4g} \quad (4.5.5)$$

and will express the center of mass energy dependence via R . When computing the cutoff effect we are required to keep r and g fixed and this is equivalent to keeping R and g fixed.

Using (4.4.7) we obtain, for the leading order,

$$P(R; 0, g_0) = |A_0(R, g_0)|^2$$

$$NA_0(R, g_0) = \frac{4Rg_0}{3 \left[1 + 4R \left[-\cos^2\left(\frac{\theta_0}{2}\right) \cos(\theta_0) + \frac{\cos^2\left(\frac{\theta_0}{2}\right) \sin(\theta_0)}{\theta_0 + \pi} (\log(4R \cos^2\left(\frac{\theta_0}{2}\right)) - i\pi) \right] \right]} . \quad (4.5.6)$$

Including the subleading order, we obtain

$$P(R; f_\pi^2, g_0; Z_\pi) = P(R; 0, g_0) \left| 1 + \frac{NA_0(R, g_0) \mu_0^2 D(Z_\pi, n)}{32\pi^2} \right.$$

$$\left. \left[4R \cos^2\left(\frac{\theta_0}{2}\right) - \cos(\theta_0) - \sin(\theta_0) \frac{(\pi + \theta_0)(1 + \cot(\theta_0) \tan(\frac{\theta_0}{2})) - \tan(\frac{\theta_0}{2})}{1 + (\pi + \theta_0)(\tan(\frac{\theta_0}{2}) - \cot(\theta_0))} \right] \right|^2 . \quad (4.5.7)$$

The variable g_0 is free and expressible in terms of θ_0 by the second equation in (4.4.7). The function $D(Z_\pi, n)$ is given in (4.4.12). From (4.5.7) we obtain the cutoff correction

$$\bar{\delta}_{|A|^2} = \frac{\mu_0^2 D(Z_\pi, n)}{16\pi^2} \operatorname{Re}[N A_0(R, g_0)] \left[4R \cos^2\left(\frac{\theta_0}{2}\right) - \cos(\theta_0) - \sin(\theta_0) \frac{(\pi + \theta_0)(1 + \cot(\theta_0) \tan(\frac{\theta_0}{2})) - \tan(\frac{\theta_0}{2})}{1 + (\pi + \theta_0)(\tan(\frac{\theta_0}{2}) - \cot(\theta_0))} \right]. \quad (4.5.8)$$

Its structure is similar to the one seen in the calculation of the width to mass ratio. Note that again the dependence on Z_π and n factorizes and that it comes in through the same coefficient as in (4.4.11). Here this is even more non-trivial because it holds for all center of mass energies measured by R . This result provides additional evidence for (4.4.13) showing that for the cross-section we would be needing the same c as for the width to mass ratio. All the dependence on g_0 and on R is coming from the operator \mathcal{O} and the action S_R . Another check for eq. (4.4.13) will be provided by our lattice work where we shall see that the same dependence on g_0 and on R enters, the whole difference being expressible by a different parameter c . In the present case, a particular observation we can already make is that, had we decided to “improve” the width to mass ratio by fine tuning Z_π so that $D(Z_\pi, n) = 0$, we would also have automatically “improved” the scattering cross-section.

Some feeling for the numbers involved can be obtained from Fig. 7.4d, showing $\bar{\delta}_{|A|^2}$ as a function of the Higgs mass in TeV for several choices of R and at several values of Z_π .

With $n \leq 100$ and $0 \leq Z_\pi \leq 0.5$, the cutoff effect on the square of the invariant amplitude is less than 3 percent for center of mass energies less than four times the Higgs mass, as long as the Higgs mass does not exceed $0.820 TeV$. So one can have a strongly interacting Higgs particle, at infinite N , with relatively minor cutoff effects.

4.6. Leading corrections to m_R .

As promised in subsection (4.1) we present here the leading correction to equation (4.1.2) there. We write

$$m_R^2 = m_{R0}^2 (1 + \delta_{m_{R0}} m_{R0}^2) . \quad (4.6.1)$$

Here m_{R0}^2 is a function of g_{R0} of the same form as in (4.1.2). By essentially the same methods as before, only this time the coupling we keep constant is g_{R0} (as defined in (4.1.3)), we derive a formula for $\delta_{m_{R0}}$. It reads

$$\delta_{m_{R0}} = D(Z_\pi, n) + \frac{96\pi^2 \cos(\frac{\pi}{n}) \zeta(Z_\pi, n)}{g_{R0}} . \quad (4.6.2)$$

In addition to completing the calculations in section (4.1) this formula shows us that an unphysical quantity will not necessarily have its cutoff dependent corrections proportional to the function $D(Z_\pi, n)$ only. The quantity m_R is unphysical because its definition in equation (4.1.1) involved $\text{Re}[\det M^r(p^2)]$. This matrix M^r has a rather complicated relation to the correlation functions, and it is obvious that the zero of the real part of its determinant is not an “on-shell” quantity. Even if we used fine tuning to “improve” all the physical observables by setting $D(Z_\pi, n)$ to zero the correction to m_R would still be nonvanishing at leading order in the inverse cutoff. However, without “fine tuning”, the correction to m_R is quite similar numerically to the corrections to the physical observables. Therefore, it made practical sense to discuss m_R first, exploiting its relative simplicity, in order to get an indication for where in the space of actions the mass bound is likely to be larger.

5. PHASE DIAGRAM FOR THE LATTICE MODELS.

We are going to investigate the lattice models defined in (2.5.6) for the F_4 and hypercubic lattices and in (2.5.7) for the hypercubic Symanzik improved case. We shall introduce a common notation for all three cases with the parameters and symbols having a slightly different meaning in each case as explained below.

Using the constraint $\vec{\Phi}^2 = 1$ we rewrite the lattice actions, up to additive constants, as

$$S = \eta N(\beta_0 + \beta_2) \frac{1}{2} \int_{x,y} \vec{\Phi}(x) g_{x,y} \vec{\Phi}(y) - N \beta_2 \frac{\eta^2}{8\epsilon} \int_x \left[\int_y \vec{\Phi}(x) g_{x,y} \vec{\Phi}(y) \right]^2 . \quad (5.1)$$

$g_{x,y}$ is the kinetic term with Fourier transform $g(p) = p^2 + \dots$ with the higher order terms explicitly given below for each case. To obtain the continuum normalization the fields have to be rescaled as $\vec{\phi} = \sqrt{\eta N(\beta_0 + \beta_2)} \vec{\Phi}$. We therefore restrict ourselves to the region $\beta_0 + \beta_2 > 0$.

It is convenient to use a lattice type dependent Kronecker delta function, $\tilde{\delta}_{x,y} = b\delta_{x,y}$, where the parameter b is the volume of the Brillouin zone on the particular lattice. On F_4 $b = 1/2$ while on the hypercubic lattice $b = 1$.

In the F_4 case η , ϵ , \int_x and g are given by

$$\eta = 6 , \quad \epsilon = 12 , \quad \int_x = 2 \sum_x , \quad \int_p = \int_{B^*} \frac{d^4 p}{(2\pi)^2} \\ g_{x,y} = 4\tilde{\delta}_{x,y} - \frac{1}{6} \sum_{\substack{l \cap x \neq \emptyset \\ l = \langle x, x' \rangle}} \tilde{\delta}_{y, x'} . \quad (5.2)$$

$g(p)$ was already given explicitly in (2.5.5) and B^* is the Brillouin zone of F_4 [6].

For the hypercubic lattice we are considering two cases:

The first hypercubic case (HC) is without improvement and has

$$\begin{aligned} \eta = 2, \quad \epsilon = 8, \quad \int_x &= \sum_x, \quad \int_p = \int_{-\pi}^{\pi} \frac{d^4 p}{(2\pi)^2} \\ g_{x,y} &= 8\tilde{\delta}_{x,y} - \sum_{\pm\mu} \tilde{\delta}_{y,x+\mu} \\ g(p) &= 2 \sum_{\mu} (1 - \cos(p_{\mu})) = p^2 - \frac{1}{12} \sum_{\mu} p_{\mu}^4 + O(p^6) . \end{aligned} \quad (5.3)$$

The second hypercubic case (SI) has Symanzik improvement, and the definitions are

$$\begin{aligned} \eta = 2, \quad \epsilon = 10, \quad \int_x &= \sum_x, \quad \int_p = \int_{-\pi}^{\pi} \frac{d^4 p}{(2\pi)^2} \\ g_{x,y} &= 10\tilde{\delta}_{x,y} - \sum_{\pm\mu} \left[\frac{4}{3}\tilde{\delta}_{y,x+\mu} - \frac{1}{12}\tilde{\delta}_{y,x+2\mu} \right] \\ g(p) &= \sum_{\mu} \left[\frac{4}{3}(1 - \cos(p_{\mu})) - \frac{1}{12}(1 - \cos(2p_{\mu})) \right] = p^2 - O(p^6) . \end{aligned} \quad (5.4)$$

With the above conventions we can treat all three cases simultaneously. We first introduce auxiliary fields in (5.1) to make the dependence on $\vec{\Phi}$ bilinear and relax the fixed length constraint.

$$\begin{aligned} S_1 &= \eta N(\beta_0 + \beta_2) \frac{1}{2} \int_{x,y} \vec{\Phi}(x) g_{x,y} \vec{\Phi}(y) + \eta N \frac{1}{2} \int_x \lambda(x) \left[\int_y \vec{\Phi}(x) g_{x,y} \vec{\Phi}(y) \right] + \\ &\quad \frac{1}{2} N \int_x \rho(x) (\vec{\Phi}^2(x) - 1) + \frac{1}{2} N \frac{\epsilon}{\beta_2} \int_x \lambda^2(x) \\ &= \frac{N}{2} \int_{x,y} \vec{\Phi} \hat{K} \vec{\Phi} + \frac{N}{2} \int_x \left[\frac{\epsilon}{\beta_2} \lambda^2 - \rho \right] \end{aligned} \quad (5.5)$$

with

$$\hat{K}_{x,y} = \eta \left(\beta_0 + \beta_2 + \frac{1}{2}(\lambda(x) + \lambda(y)) \right) g_{x,y} + \rho(x) \tilde{\delta}_{x,y} . \quad (5.6)$$

We separate out the zero mode by

$$\vec{\Phi}(x) = \vec{v} + \frac{1}{\sqrt{N}} \hat{v} H(x) + \frac{1}{\sqrt{N}} \vec{\pi}(x), \quad \hat{v} = \frac{\vec{v}}{v}, \quad |\vec{v}| = v, \quad \hat{v} \cdot \vec{\pi} = 0, \quad \int_x H(x) = \int_x \pi^j(x) = 0, \quad (5.7)$$

and integrate out $\vec{\pi}$ and H . Then we obtain

$$S_2 = \frac{N}{2} \left[\text{Tr} \log \hat{K} + v^2 \int_x \rho - v^2 \int (\rho' + \frac{\eta}{2} \lambda' g) \hat{K}^{-1} (\rho' + \frac{\eta}{2} g \lambda') + \int_x \left(\frac{\epsilon}{\beta_2} \lambda^2 - \rho \right) \right] \quad (5.8)$$

where λ' and ρ' are, as usual, the non-constant parts of λ and ρ and \hat{K} now denotes the operator from (5.6) restricted to the space of functions whose lattice average vanishes.

5.1. Saddle point equations and dominating saddles.

The saddle point equations are

$$\begin{aligned} 1 - v^2 &= \frac{1}{\eta(\beta_0 + \beta_2 + \lambda_s)} \int_p \frac{1}{g(p) + \hat{\rho}_s} = \frac{J_1(\hat{\rho}_s)}{\eta(\beta_0 + \beta_2 + \lambda_s)} \\ -\frac{2\epsilon}{\beta_2} \lambda_s &= \frac{1}{(\beta_0 + \beta_2 + \lambda_s)} \int_p \frac{g(p)}{g(p) + \hat{\rho}_s} = \frac{1}{(\beta_0 + \beta_2 + \lambda_s)} (b - \hat{\rho}_s J_1(\hat{\rho}_s)) \quad . \end{aligned} \quad (5.1.1)$$

In this equation we have defined

$$\rho = \eta(\beta_0 + \beta_2 + \lambda) \hat{\rho} \quad . \quad (5.1.2)$$

Also, J_1 is the lattice integral introduced by [19] for the hypercubic and by [6] for the F_4 lattice. The definition for SI is the same in our notation. By definition, one has $\int_p 1 = b$.

The symmetric phase is characterized by $v^2 = 0$, $\hat{\rho}_s > 0$ and the broken phase by $v^2 > 0$, $\hat{\rho}_s = 0$. A candidate critical point has $v^2 = \hat{\rho}_s = 0$. As for the Pauli–Villars models the saddle point equations may admit several competing solutions. We shall find the dominating saddle by the method used in section (3.1) for the Pauli–Villars models. Our presentation will be much more sketchy here.

Defining

$$u = \eta(\beta_0 + \beta_2 + \lambda) \quad , \quad \beta^* = \frac{2\epsilon}{\eta^2 \beta_2} \quad , \quad u^* = \eta(\beta_0 + \beta_2) \quad , \quad (5.1.3)$$

we have to minimize the function

$$\hat{\Psi}(u, \hat{\rho}) = \int_p \log[g(p) + \hat{\rho}] + b \log u + (v^2 - 1)u\hat{\rho} + \frac{1}{2}\beta^*(u - u^*)^2 \quad . \quad (5.1.4)$$

In the symmetric phase, with $v^2 = 0$, the equation $\partial\hat{\Psi}/\partial\hat{\rho} = 0$ can be used to define a function $\hat{\rho}(u)$ for $0 \leq u \leq u_0$

$$J_1(\hat{\rho}(u)) = u \quad , \quad u_0 = J_1(0) = r_0 \quad , \quad (5.1.5)$$

with the lattice constant r_0 given by

$$r_0 = 0.13823047 \quad \text{for } F_4 \quad , \quad r_0 = 0.15493339 \quad \text{for HC} \quad \text{and} \quad r_0 = 0.12919024 \quad \text{for SI} \quad . \quad (5.1.6)$$

The values for the HC and F_4 cases can be found in [19,6], while the value for the SI case was computed by similar methods. We then derive

$$\begin{aligned}\hat{\Psi}(u_s, \hat{\rho}_s) &= \int_{u_0}^{u_s} [G(u) + \beta^*(u - u^*)] + \hat{\Psi}(u_0, 0), \\ G(u) &= \frac{b}{u} - J_1^{-1}(u) \quad \text{for } 0 \leq u \leq u_0 .\end{aligned}\tag{5.1.7}$$

In the broken phase $(\partial\hat{\Psi}/\partial\hat{\rho})_{\hat{\rho}=0} = 0$ together with $v^2 \geq 0$ yields the restriction $u_s \geq u_0$. Then, extending the range of the function G from $u \in (0, u_0)$ to the segment $u \in [u_0, \infty)$ by $G(u) = b/u$, we can write the function $\hat{\Psi}$ at the saddle as

$$\hat{\Psi}(u_s, 0) = \int_{u_0}^{u_s} [G(u) + \beta^*(u - u^*)] + \hat{\Psi}(u_0, 0) .\tag{5.1.8}$$

Again we have identical forms in both phases and can introduce a geometrical interpretation like in the Pauli–Villars case. We find a tricritical point at

$$\beta_{t.c.}^* = \frac{b}{u_0^2} = \frac{b}{r_0^2}, \quad u_{t.c.}^* = 2u_0 = 2r_0 .\tag{5.1.9}$$

In terms of the original couplings this corresponds to

$$\beta_{2,t.c.} = \frac{2\epsilon r_0^2}{b\eta^2}, \quad \beta_{0,t.c.} = \frac{2r_0}{\eta} - \beta_{2,t.c.} .\tag{5.1.10}$$

The second order critical line is described by

$$u^* = \left(\frac{\beta_{t.c.}^*}{\beta^*} + 1 \right) u_0, \quad \frac{\beta_{t.c.}^*}{\beta^*} < 1 ,\tag{5.1.11}$$

which translates into

$$\beta_{0,c} = \left(\frac{\beta_2}{\beta_{2,t.c.}} + 1 \right) \frac{r_0}{\eta} - \beta_2, \quad \beta_2 < \beta_{2,t.c.} .\tag{5.1.12}$$

The restriction $(\beta_0 + \beta_2) > 0$ leads on the critical line to the requirement

$$\beta_2 > -\beta_{2,t.c.} = -\frac{2\epsilon r_0^2}{b\eta^2} .\tag{5.1.13}$$

To ascertain the local stability of our saddle points we need to investigate the small fluctuations around the saddle points. This will be done in the next section.

5.2. Small fluctuations in the broken phase.

Separating out the zero mode from the field $\vec{\Phi}$ as in (5.7) we want to expand the action (5.5) around the saddle point. For this we introduce the shifted fields, recalling that $\rho_s = 0$ in the broken phase,

$$\delta\lambda = \lambda - \lambda_s, \quad \delta H = H, \quad \delta\vec{\pi} = \vec{\pi}, \quad \delta\rho = \rho. \quad (5.2.1)$$

We can easily read of the pion propagator in Fourier space

$$\langle \delta\pi^a \delta\pi^b \rangle = \frac{\delta^{a,b}}{\eta(\beta_0 + \beta_2 + \lambda_s)g(p)}. \quad (5.2.2)$$

From this we find the pion wave function renormalization constant

$$Z_\pi = \frac{1}{\eta(\beta_0 + \beta_2 + \lambda_s)}. \quad (5.2.3)$$

We see that the renormalized pion propagator is independent of the couplings and hence so are its cutoff corrections. We also see that in the SI case the inverse pion propagator has no order p^4 contribution and thus is Symanzik improved.

Using Z_π given above and $v^2 = Z_\pi f_\pi^2$ we obtain from the first saddle point equation in (5.1.1) ($\hat{\rho}_s = 0$ in the broken phase)

$$Z_\pi = \frac{1}{r_0 + f_\pi^2}. \quad (5.2.4)$$

Then, also using the second saddle point equation, we find

$$\beta_0 = \frac{1}{\eta Z_\pi} + \left(\frac{b\eta Z_\pi}{2\epsilon} - 1 \right) \beta_2 = \frac{r_0 + f_\pi^2}{\eta} + \left(\frac{b\eta}{2\epsilon(r_0 + f_\pi^2)} - 1 \right) \beta_2. \quad (5.2.5)$$

Therefore, at fixed β_2 , we can trade the coupling β_0 for f_π^2 .

Integrating out the pions from the action (5.5), with the zero mode separated out, we obtain, up to quadratic order in the fluctuations,

$$S_2^{(2)} = \frac{1}{2} \int_p \psi_A M_{AB} \psi_B. \quad (5.2.6)$$

Here the three component fields ψ_A represent δH , $\delta\rho$ and $\delta\lambda$ for $A = 1, 2, 3$ respectively. The non-vanishing entries of the symmetric matrix $M_{AB}(p)$ are, neglecting $1/N$ correc-

tions,

$$\begin{aligned}
M_{11} &= \frac{g(p)}{Z_\pi} \\
M_{12} &= \sqrt{N}v \\
M_{13} &= \frac{1}{2}\sqrt{N}v\eta g(p) \\
M_{22} &= -\frac{1}{2}NZ_\pi^2 \int_k \frac{1}{g(k+\frac{1}{2}p)g(k-\frac{1}{2}p)} \equiv -\frac{1}{2}NZ_\pi^2 I(p) \\
M_{23} &= -\frac{1}{2}NZ_\pi^2 \eta \int_k \frac{\frac{1}{2}[g(k+\frac{1}{2}p)+g(k-\frac{1}{2}p)]}{g(k+\frac{1}{2}p)g(k-\frac{1}{2}p)} = -\frac{1}{2}NZ_\pi^2 \eta r_0 \\
M_{33} &= -\frac{1}{2}NZ_\pi^2 \eta^2 \int_k \frac{\frac{1}{4}[g(k+\frac{1}{2}p)+g(k-\frac{1}{2}p)]^2}{g(k+\frac{1}{2}p)g(k-\frac{1}{2}p)} + \frac{N\epsilon}{\beta_2} \equiv -\frac{1}{2}NZ_\pi^2 \eta^2 \left(Q(p) - \frac{2\epsilon}{Z_\pi^2 \eta^2 \beta_2} \right) .
\end{aligned} \tag{5.2.7}$$

We need two ‘bubble’ integrals, $I(p)$ and $Q(p)$. $I(p)$ has already been computed in an expansion in the momentum p in [19] for the HC lattice and in [6] for F_4 . The computation for SI, employing the same method, is straightforward. One finds for F_4 and SI

$$I(p) = -\frac{1}{16\pi^2} \log p^2 + c_1 - c_2 p^2 + O(p^4 \log p^2) \tag{5.2.8}$$

with the constants c_i

$$\begin{aligned}
c_1 &= 0.0466316 , & c_2 &= -5.4968 \cdot 10^{-4} & \text{for } F_4 \\
c_1 &= 0.0283716 , & c_2 &= -3.5981 \cdot 10^{-4} & \text{for SI} .
\end{aligned} \tag{5.2.9}$$

For HC the result is

$$I(p) = -\frac{1}{16\pi^2} \log p^2 + c_1 - c_{2,1} p^2 - c_{2,2} \sum_\mu p_\mu^4 / p^2 + O(p^4 \log p^2) \tag{5.2.10}$$

with

$$c_1 = 0.0366783 , \quad c_{2,1} = -7.524 \cdot 10^{-5} , \quad c_{2,2} = -2.6386 \cdot 10^{-4} . \tag{5.2.11}$$

Again, at order $1/\Lambda^2$, the HC lattice has a Lorentz invariance breaking term. However we shall need $I(p)$ only for ‘time’ like, and thus on-axis, momenta. Then the HC result reduces to the form (5.2.8) with $c_2 = c_{2,1} + c_{2,2} = -3.3910 \cdot 10^{-4}$. We see here explicitly how the specific choices of observables that we made effectively hide the Lorentz breaking effects of the HC case.

An expansion in p for the integral $Q(p)$ is easily computed with the result

$$Q(p) = b + \gamma p^2 + O(p^4) \tag{5.2.12}$$

with

$$\gamma = 0.00661524 \text{ for } F_4, \quad \gamma = 0.01496670 \text{ for HC} \quad \text{and} \quad \gamma = 0.01736345 \text{ for SI} . \quad (5.2.13)$$

We are now in the position to discuss the local stability of our saddle points. It is easy to see that on the critical line, *i.e.*, for $Z_\pi = r_0^{-1}$ ((5.2.4)), M_{33} vanishes at $p = 0$ when β_2 approaches $\beta_{2,t.c.}$ from below. At $p = 0$ M_{11} and M_{13} also vanish and hence at the tricritical point $\det M = 0$. Thus, as in the Pauli–Villars models, the Higgs particle becomes massless at the tricritical point and also plays the role of a dilaton. For $\beta_2 < \beta_{2,t.c.}$ we find, at least in the neighborhood of the critical line, that $\det M$ stays positive for Euclidean momenta. Thus the saddle points in the critical regime that we are interested in are locally stable.

6. HIGGS MASS BOUND AND CUTOFF EFFECTS WITH LATTICE REGULARIZATIONS.

As in the Pauli–Villars case we will first do an approximate calculation to see the basic trends. Next we follow up with an accurate evaluation including the computation of the leading cutoff correction to the width to mass ratio and to $\pi - \pi$ scattering.

6.1. Approximate calculation.

We will first study the quantity m_R , defined by

$$\text{Re}[\det M(p)]_{p=(im_R, \vec{0})} = 0 . \quad (6.1.1)$$

From (5.2.7) we obtain

$$\det M(p) = \frac{1}{4} N^2 Z_\pi^3 \eta^2 \left[\left(Q(p) - \frac{2\epsilon}{Z_\pi^2 \eta^2 \beta_2} \right) \left(g(p) I(p) + 2f_\pi^2 \right) - g(p) r_0^2 - 2r_0 f_\pi^2 g(p) + \frac{1}{2} f_\pi^2 g(p)^2 I(p) \right] . \quad (6.1.2)$$

We use $Z_\pi^{-1} = r_0 + f_\pi^2$ and solve (6.1.1) for m_R^2 , $f_\pi^2 \ll 1$, counting logs to be of order 1. To leading order we find, as expected, the form (4.1.2, 4.1.3) with the proportionality constant C now depending on β_2

$$C(\beta_2) = \exp \left\{ 8\pi^2 c_1 - \frac{8\pi^2 r_0^2}{b - \frac{2\epsilon r_0^2}{\eta^2 \beta_2}} \right\} . \quad (6.1.3)$$

We see that C diverges, as for the Pauli–Villars models, when the tricritical point is approached. Again we want to be as far away from this point as possible.

When we decrease β_2 , $C(\beta_2)$ and hence m_R (in lattice units) becomes smaller at constant g_R (which means that the mass is kept fixed in physical units although m_R varies). Then the cutoff effects become smaller and g_R can be allowed to increase. Thus we expect to obtain the largest mass bound at the smallest acceptable β_2 , (5.1.13). The ratio of the C 's for the standard non-linear action and for this extreme case is found to be

$$\frac{C(0)}{C(-\beta_{2,t.c.})} = \exp \left\{ \frac{4\pi^2 r_0^2}{b} \right\} . \quad (6.1.4)$$

This evaluates to 4.521, 2.580 and 1.933 for F_4 , HC and SI respectively. According to the rough estimates of section (4.2) we would expect the change of β_2 from 0 to $-\beta_{2,t.c.}$ to induce increases of about 0.075 TeV , 0.047 TeV , 0.033 TeV in the Higgs mass bound for the three cases. In the next section we shall see that these rough estimates for the increase of the Higgs mass are accurate within a factor of two.

As in section (4.6) for the Pauli–Villars case we can compute the leading correction to m_R given by (4.1.2) and (6.1.3). In the notation of (4.6.2) we find

$$\delta_{m_{R0}} = 16\pi^2 \left(c_2 - \frac{\gamma r_0^2 \eta^4 \beta_2^2}{(b\eta^2 \beta_2 - 2\epsilon r_0^2)^2} \right) + \frac{96\pi^2}{g_{R0}} \left(\zeta - \frac{br_0 \eta^4 \beta_2^2}{(b\eta^2 \beta_2 - 2\epsilon r_0^2)^2} \right) \quad (6.1.5)$$

where ζ is defined through $g(p) = p^2 - \zeta p^4 + O(p^6)$ for on-axis momenta p . From equations (5.2, 5.3, 5.4) we find $\zeta = 1/12$ for F_4 and HC and $\zeta = 0$ for SI. This correction is less than 15% in the region of interest.

We can make the lattice result look even more like the Pauli–Villars one by going to continuum normalization. We denote the corresponding pion wavefunction renormalization constant by \tilde{Z}_π , $\tilde{Z}_\pi = \eta(\beta_0 + \beta_2)Z_\pi$. Then, using eq. (5.2.4) and (5.2.5) we obtain

$$\begin{aligned} \eta(\beta_0 + \beta_2) &= \tilde{Z}_\pi(r_0 + f_\pi^2) \\ \frac{b}{2\epsilon} \frac{\beta_2}{(\beta_0 + \beta_2)^2} &= \frac{\tilde{Z}_\pi - 1}{\tilde{Z}_\pi^2} . \end{aligned} \quad (6.1.6)$$

Therefore we can now trade the couplings β_0 and β_2 for f_π^2 and \tilde{Z}_π . The critical line is now given by $f_\pi^2 = 0$ and $0 \leq \tilde{Z}_\pi \leq 2$. The upper limit corresponds to the tricritical point. $\tilde{Z}_\pi = 1$ denotes the standard non-linear lattice action, without the term with four derivatives and four fields.

In this normalization the term $Q(p) - \frac{2\epsilon}{Z_\pi^2 \eta^2 \beta_2}$ in $\det M$ of eq. (6.1.2) has to be replaced by $b \frac{(\tilde{Z}_\pi - 2)}{(\tilde{Z}_\pi - 1)} + Q(p) - b$. The proportionality constant in eq (4.1.2) now depends on \tilde{Z}_π and

becomes

$$C(\tilde{Z}_\pi) = \exp \left\{ 8\pi^2 c_1 - \frac{8\pi^2 r_0^2}{b} \frac{\tilde{Z}_\pi - 1}{\tilde{Z}_\pi - 2} \right\} \quad (6.1.7)$$

to be compared to eq. (4.1.4) for the Pauli–Villars models.

However, keeping \tilde{Z}_π fixed, while varying f_π^2 does not correspond to keeping β_2 fixed. In a numerical simulation of the lattice models one cannot easily follow a line of fixed \tilde{Z}_π . It is much more natural to carry out simulations at a fixed value of β_2 , approach the critical point along this line and subsequently vary β_2 . Therefore we will return in what follows to the usual lattice normalization.

6.2. Leading correction to the width to mass ratio.

Again, the computation in this section closely follows that of the Pauli–Villars model, section (4.4). The Higgs resonance is a complex root on the second sheet of $\det M(p) = 0$ for $p = (i(m_H - \frac{i}{2}\gamma_H), \vec{0})$. $\det M$ is given in (6.1.2) where we again insert $Z_\pi^{-1} = r_0 + f_\pi^2$. The leading order solution, with notation (4.4.5) and (4.4.6) is

$$\begin{aligned} \mu_0 &= C(\beta_2) \exp \left[-\frac{\theta_0 + \pi}{2 \tan(\theta_0)} \right] \\ g_0 &= \frac{96\pi^2 \cos^2(\frac{\theta_0}{2}) \sin(\theta_0)}{\theta_0 + \pi} \end{aligned} \quad (6.2.1)$$

with $C(\beta_2)$ given in eq. (6.1.3).

To compute the subleading terms we expand again as in (4.4.9) and set $\delta_g = 0$ (see (4.4.10) and the explanation leading to it). Straightforward algebra then leads to

$$\bar{\delta}_{\frac{\Gamma_H}{M_H}}(g_0; \beta_2) = \frac{16\pi^2 \left(c_2 - \frac{\gamma r_0^2 \eta^4 \beta_2^2}{(b\eta^2 \beta_2 - 2\epsilon r_0^2)^2} \right) \mu_0^2}{1 + (\pi + \theta_0) \left[\tan\left(\frac{\theta_0}{2}\right) - \cot(\theta_0) \right]} . \quad (6.2.2)$$

As for the Pauli–Villars case, the cutoff correction factorizes into a universal g dependent part and a part carrying all the information about the cutoff through the dependence on β_2 . The latter is given here by $16\pi^2 [c_2 - \frac{\gamma r_0^2 \eta^4 \beta_2^2}{(b\eta^2 \beta_2 - 2\epsilon r_0^2)^2}] C^2(\beta_2)$. The universal factor is identical to the one obtained in the Pauli–Villars case, eq. (4.4.11).

On the lattice we are also interested in comparing directly to numerical data obtained at $N = 4$. For this comparison we need some “unphysical” quantity, like m_H . We therefore write down the explicit formula to first subleading order in the cutoff

$$m_H^2 = m_{H0}^2 (1 + \delta_{m_{H0}} \mu_0^2 + O(\mu_0^4)) \quad (6.2.3)$$

and obtain

$$\begin{aligned}
m_{H0} &= \mu_0 \cos\left(\frac{\theta_0}{2}\right) \\
\delta m_{H0} &= 16\pi^2 \left(c_2 - \frac{\gamma r_0^2 \eta^4 \beta_2^2}{(b\eta^2 \beta_2 - 2\epsilon r_0^2)^2} \right) \\
&\quad \left[\cos\theta_0 + \sin(\theta_0) \frac{(\pi + \theta_0)(1 + \cot(\theta_0) \tan(\frac{\theta_0}{2})) - \tan(\frac{\theta_0}{2})}{1 + (\pi + \theta_0)(\tan(\frac{\theta_0}{2}) - \cot(\theta_0))} \right] \\
&\quad + \frac{\pi + \theta_0}{\sin\theta_0} \left[\zeta - \frac{br_0 \eta^4 \beta_2^2}{(b\eta^2 \beta_2 - 2\epsilon r_0^2)^2} \right] .
\end{aligned} \tag{6.2.4}$$

6.3. Leading correction to $\pi - \pi$ scattering.

Scattering on the lattice was discussed in [19] for the HC lattice and generalized in [6] to the F_4 lattice. It is easy to see that at first non-vanishing order in $1/N$ the invariant amplitude $A(\hat{s}, \hat{t}, \hat{u})$, where \hat{s} , \hat{t} and \hat{u} are the lattice versions of the Mandelstam variables s , t and u , [6] describing $\pi - \pi$ scattering in the center of mass frame, is only a function of the lattice center of mass energy squared \hat{s} . For our purposes we do not need the full expressions for the variables with hats and it suffices to know that $\hat{s} = W^2 + O(W^6)$ where W is the center of mass energy. The differential cross-section with equal isospin indices on the incoming pions is given by

$$\left(\frac{d\sigma}{d\Omega} \right)_{CM} = \frac{N}{64\pi^2 W^2} |A(\hat{s})|^2 . \tag{6.3.1}$$

The kinematic prefactor has no cutoff corrections of order $1/\Lambda^2$. For the F_4 and SI models this is true for incoming and outgoing momenta in any direction, while for the HC model, due to the Lorentz invariance breaking at order $1/\Lambda^2$, this property only holds for on-axis momenta. For the F_4 and SI models anisotropies in the differential cross-section only occur at order $1/\Lambda^4$.

To evaluate $A(\hat{s})$ we need to know the pion interactions. For this we go back to the action (5.5) and introduce pion and Higgs fields via eq. (5.7). We then expand around the saddle but do not integrate over δH and $\delta \vec{\pi}$ yet. The part of the action giving the pion interaction is then

$$S_1^{int} = \frac{\eta}{2} \int_x \delta\lambda(x) \left[\int_y \delta\vec{\pi}(x) g_{x,y} \delta\vec{\pi}(y) \right] + \frac{1}{2} \int_x \delta\rho(x) (\delta\vec{\pi})^2(x) . \tag{6.3.2}$$

The $\pi\pi\rho$ and $\pi\pi\lambda$ vertices are now easily obtained, and one can see that the latter vanishes for on-shell pions, since then $g(p) = 0$. Thus, the on-shell amplitude with $q = p_1 + p_2$ is

given by

$$A(q) \propto \langle \delta\rho\delta\rho \rangle (q) \quad . \quad (6.3.3)$$

Following closely section (4.5) where the Pauli–Villars case was dealt with and using the same notation, we find the same leading order result for the invariant scattering amplitude, eq. (4.5.6). Including the subleading order we obtain on the lattice

$$\bar{\delta}_{|A|^2} = \left(c_2 - \frac{\gamma r_0^2 \eta^4 \beta_2^2}{(b\eta^2 \beta_2 - 2\epsilon r_0^2)^2} \right) \mu_0^2 \text{Re}[N A_0(R, g_0)] \left[4R \cos^2\left(\frac{\theta_0}{2}\right) - \cos(\theta_0) - \sin(\theta_0) \frac{(\pi + \theta_0)(1 + \cot(\theta_0) \tan(\frac{\theta_0}{2})) - \tan(\frac{\theta_0}{2})}{1 + (\pi + \theta_0)(\tan(\frac{\theta_0}{2}) - \cot(\theta_0))} \right] \quad . \quad (6.3.4)$$

This cutoff correction has again factorized into a cutoff dependent part and a function of g_0 which is the same as the one found for the Pauli–Villars models, eq. (4.5.7). The cutoff dependent part is identical to the cutoff dependent factor we have obtained for the width to mass ratio in equation (6.2.2).

7. FROM $N = \infty$ TO $N = 4$.

In this section we shall extract quantitative information about the Higgs mass bound from our large N results. To do that we need to first discuss how large the corrections to the $N = \infty$ limit are when $N = 4$. Our objective will be to argue that, in the region of interest for the bound, the $N = \infty$ numbers should be expected to be different from the $N = 4$ values by about 25 percent ($1/N$). The question of the difference between $N = \infty$ and $N = 4$ has been studied in some detail before by Lin, Kuti and Shen[20]. They arrived at the conclusion that the difference between $N = \infty$ and $N = 4$ is very large and that $N = \infty$ results are qualitatively wrong at $N = 4$. We disagree with this conclusion in the region where the bound is close to saturation, and this is the region of interest to us. Some of the approximations used in [20] for the lattice “bubble” diagram are unjustified and we suspect this to be the reason for the discrepancy between our views on the usefulness of the $1/N$ expansion for the Higgs mass bound problem.

Throughout this and the next section we undo the rescalings of F_π and f_π by \sqrt{N} so that, at $N = 4$ $F_\pi = 0.246 \text{ TeV}$.

7.1. Simple error estimates.

The quantity that we are extracting quantitative information from is the π – π scattering

invariant amplitude $A(q^2)$. From it we extracted the Higgs mass and width, m_H and γ_H , the quantity m_R and the cutoff correction $\bar{\delta}_{|A|^2}$. Moreover, from the behavior of the amplitude when $q^2 \rightarrow 0$ we can also extract f_π^2 . Therefore our basic question is how accurately is the “true”, $N = 4$, scattering amplitude $A(q^2)$ approximated by the $N = \infty$ expression for complex q^2 with $|q^2| \leq 4m_H^2$.

The best approach would be to compute the $1/N$ correction explicitly but this is a demanding calculation which we have not done. We are attempting to guess what the right order of magnitude of the result of such a calculation would be. The most naïve guess is that the leading correction will be suppressed by $1/N$, meaning that our results are good to 25% when applied to $N = 4$. Indeed, the most conspicuous omission in the $N = \infty$ limit is the fact that the number of pion types is $N - 1$ rather than N ; the naïve error estimate then follows from the observation that pairs of pions of identical type contribute more or less additively. There is one example where this sort of pion counting argument is believed to be exact: When one computes the finite volume leading correction to the $\langle \vec{\phi} \cdot \vec{\phi} \rangle$ correlation at zero momentum in the $1/N$ expansion, the leading and subleading terms are related by exactly a factor of N [21]. Moreover, it is believed that all higher order corrections in $1/N$ vanish if the pion wave function renormalization constant is extracted [22].

It is well known [23] that one cannot always expect the $1/N$ corrections to obey these naïve estimates; this point was also discussed in ref. [20]. Let us repeat the argument here, but rephrased for the amplitude $A(q^2)$: If the system is sufficiently close to criticality, the low q^2 behavior of A can be extracted from an appropriate RG equation and is dominated by the noninteracting fixed point. The function $\beta(g)$ appearing in this equation can be approximated by its leading term in g and that term is calculable because it comes from one loop diagrams. It is known that, to one loop, the beta function for the properly rescaled coupling is proportional to $1 + 8/N$ and, thus, the finite N answer is for $N = 4$ larger by a factor of 3 than the $N = \infty$ answer. This will affect the amplitude because the solution of the RG equation will simply say that $A(q^2)$ is well approximated by the tree level expression with an effective coupling that is dependent on q^2 with a dependence dictated by the β -function. If the coupling is also weak at cutoff scales, the effective coupling can be related to the bare coupling via the one loop β function; in this way one obtains $A(q^2)$ in terms of the bare coupling. If we are very close to the critical point the cutoff is very large (for example, when compared to the Higgs mass) and the effective coupling becomes almost entirely independent of the bare coupling; in that case the large error in the β function induces a large error in $A(q^2)$ and we can't trust the numbers obtained at $N = \infty$ when $N = 4$. Note that the difficulty arises due to the existence of two very disparate scales in the problem: One scale is the cutoff and the other is set by the pion decay constant. Two very different scales exist only when the system is very close to a critical point because f_π

vanishes there.

For the Higgs mass bound problem we are mostly interested in cases where $4\pi F_\pi \approx \Lambda$; in these cases the usefulness of the RG equations is very limited because we do not have to connect two very different scales. Therefore, for those actions that lead to the approximate saturation of the bound we do not need to worry about the $8/N$ error in the β -function and can hope for accuracies of order 25% at $N = 4$. In the next section we shall use available numerical data as evidence that this hope is realized in the broken phase of the models we are interested in.

In the symmetric phase more is known about the $1/N$ series. For the simplest nearest neighbor action on the hypercubic lattice one is able to get into the region where the triviality bound on the self-coupling is saturated (at a correlation length ξ of about 2 lattice spacings) with an accuracy on the coupling of the order of 2–3% if one keeps three orders in $1/N$ at $N = 4$ [24]. This is compatible with the assumption that the $1/N$ series for the coupling has a radius of convergence of order unity when $\xi \approx 2$.

Also, regarding the value of the bound on the coupling in the symmetric and broken phases, one can compare the results obtained for the single component model ($N = 1$) to those obtained for $N = 4$; in spite of the fact that there are no Goldstone bosons at $N = 1$ the upper bound on the coupling is relatively stable when expressed as a fraction of the tree level unitarity bound [25,26,19]. Again the $1/N$ series looks reasonably well behaved.

7.2. Numerical test of error estimates.

In Figures 7.1a to 7.1c we compare the large N predictions with $N = 4$ results for the simplest lattice models investigated to date by Monte Carlo and independent non-perturbative means. For the F_4 lattice (Fig. 7.1a) the numerical data follows the large N prediction quite consistently over the entire range of interest, $0.3 < m_H < 0.8$, with the large N numbers exceeding the $N = 4$ numbers by 20–30%. For the hypercubic lattice the excess is slightly smaller, 15–20% in the region of interest, and for the hypercubic improved less than 15%.

More importantly we see that the $N = \infty$ **difference** in M_H/F_π between the various lattices in the region of interest underestimates the $N = 4$ difference by up to a factor of two. Therefore, if we knew the $N = 4$ results for only one of the lattices we could predict the results for the others, using infinite N , to an overall relative accuracy of about 7–9%, which is of the same order of magnitude as the statistical error in a typical Monte-Carlo simulation. One of our objectives is to predict the results for the coupling at $N = 4$ for new lattice actions. Being interested in actions that are not fundamentally different from the ones that have already been investigated by other means, we can expect our predictions

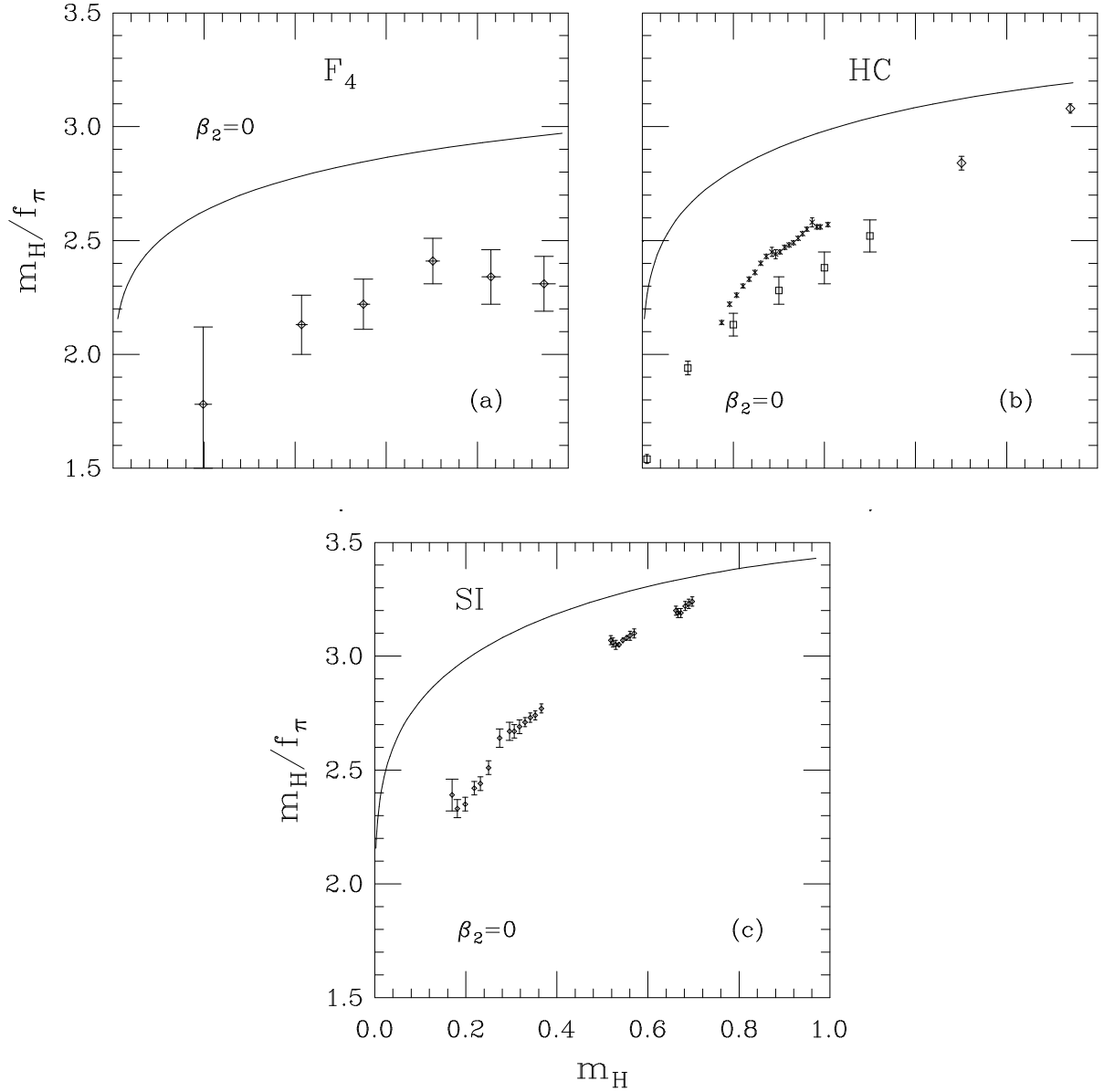


Figure 7.1 m_H/f_π vs. m_H for the naïve ($\beta_2 = 0$) lattice actions. The solid line is the large N result scaled to $N = 4$. The diamonds in fig. (a) are numerical results from [27]. In fig. (b) the boxes are results from [19], the diamonds are numerical results from [28], and the crosses from [29]. In fig (c) the diamonds are numerical results from [29].

based on large N to have an accuracy of the order of several percent. Preliminary results in the F_4 case provide further support to this claim [2]. This is very useful because one does not want to invest resources in simulating actions that end up not giving a higher

bound. We believe that quite reliable order of magnitude estimates (and definitely the right sign) for the effects of different terms in the action on the bound can be obtained from the $N = \infty$ results.

Until now we only tested the large N predictions against results that could be obtained at $N = 4$ by other non-perturbative means. But the estimates for the bound also need non-perturbative evaluations of the cutoff effects contributing to physical observables. There do not exist any tested, practical, non-perturbative methods yet that make it feasible to obtain numerical evaluations of physically observable cutoff effects at $N = 4$. It is possible that such methods will be developed but it is doubtful that one will be able to reach reasonable accuracies for estimating such small corrections by Monte Carlo methods. Therefore we are left with only two options for evaluating the cutoff effects: the loop expansion and the $1/N$ expansion. It is gratifying that the order of magnitude of the results at tree level order for nearest neighbor hypercubic and F_4 actions are in agreement with the large N estimates when the coupling constants are close to the upper bound. We could have worried about the tree level estimates because, as explained in Appendix B, higher loop effects are not negligible and a method for resumming the “leading log” terms contributing to order $1/\Lambda^2$ terms is not yet available. However, it seems that this does not have a major effect when the coupling is sufficiently large, probably for the same physical reasons that the β -function problem was relatively harmless for large couplings. We are further helped by the fact that the bound depends weakly on the magnitude of the cutoff effects: Changes of one order of magnitude in the latter have an effect on the bound of the order of only a few percent. If we assume that, when the coupling is sufficiently strong, the accuracy of the $N = \infty$ answer is of order 25% for the cutoff effects too, we can use the large N estimates for the leading cutoff effects to estimate the Higgs mass bound in a Monte Carlo calculation. We have not devised a method for computing the cutoff effects in the loop expansion for the more complicated actions that were the subject of this paper because we feel that the large N results are at least as reliable. Nevertheless, we think that it would be interesting to see the explicit N dependence emerging from a perturbative computation.

7.3. The large N numbers.

Let us now go over the quantitative results of our work. We start with the kind of results that are the typical outcome of a Monte Carlo simulation. In Figures 7.2a-d we show plots of the ratio m_H/f_π as a function of the quantity m_H . The latter is equal to M_H/Λ and contains an implicit understanding for what the cutoff is taken to be. For all the lattice results we take the cutoff as the inverse lattice spacing of the elementary hypercubic lattice on which the action is defined (the F_4 lattice is viewed here as a hypercubic lattice for which a choice of action was made so that no fields reside on sites who have an odd sum

of integer coordinates). In the Pauli–Villars case the cutoff was defined as the absolute magnitude of the distance, in the complex momentum square plane, to the ghost pole in the pion propagator closest to the origin.

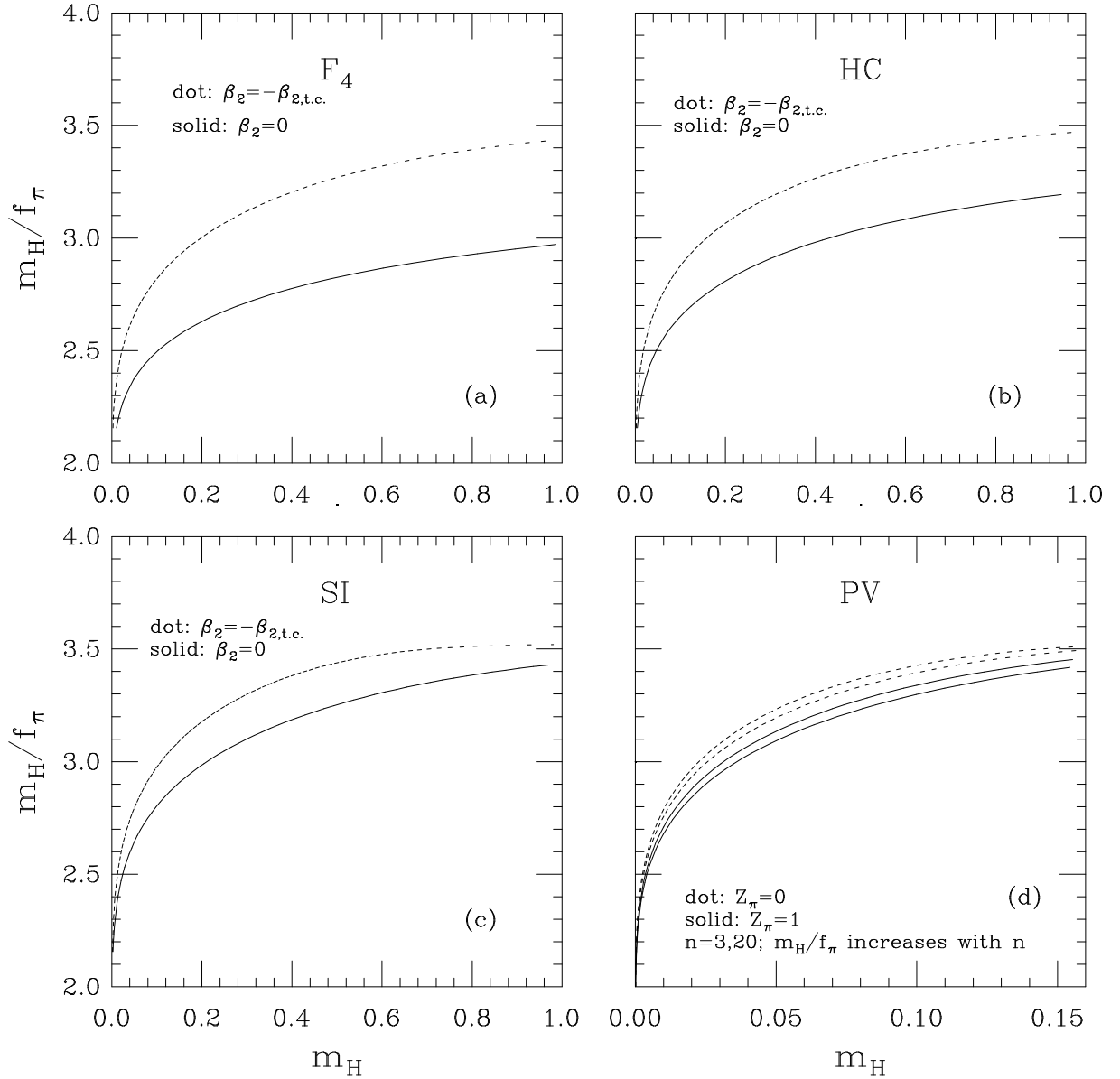


Figure 7.2 m_H/f_π vs. m_H : The solid lines represent the naïve actions ($\beta_2 = 0$ on the lattice and $Z_\pi = 1$ for PV) the dotted lines the actions with a four derivative term turned on to maximal allowed strength ($\beta_2 = -\beta_{2,t.c.}$ on the lattice and $Z_\pi = 0$ for PV). In figures (a)–(c) m_H is measured in lattice units and in fig. (d) it is measured in units of Λ_s .

For the three lattice cases we show two lines on each graph. The lower one gives m_H/f_π for the simplest action which is bilinear in the fields. From the higher line one can read off the increase in m_H/f_π that can be induced, at the same value of M_H/Λ , by turning on the four field terms to maximal acceptable strength in the direction of increasing repulsion between the pions. We see that the largest relative effect takes place in the F_4 case while the smallest relative effect takes place in the hypercubic “Symanzik tree level improved” case. Since the lines for the simple actions give higher values of m_H/f_π for exactly those cases for which the effect of the four field terms is smaller, we see a tendency towards “equalization” when the four–field terms are turned on. This fact supports some sort of approximate “universality” among the various bounds. Of course we cannot expect anything rigorous to hold in this respect, but it is impressive that the higher lines for all three lattice actions are closer to each other than the lower lines are.

In the Pauli–Villars case we can compare different values of n and see similar effects. While the overall “plateau” attained by the higher curves is quite similar to the lattice cases, a detailed comparison cannot be made because there is no “natural” relationship between the “cutoffs” in the two schemes.*

There is a simple explanation for the systematics we observed: Suppose each one of the actions is evaluated for slowly varying fields and a field rescaling is carried out in accordance with eq. (2.5.2) to remove the four derivative term from the term in the Lagrangian that is bilinear in the fields (this cannot be done for the simple hypercubic action and we shall discuss this presently). We see that the ordering of the lattices by m_H/f_π at fixed m_H and with naïve actions follows the magnitude of the four field coupling induced by the field redefinition of (2.5.2). For the hypercubic lattice there is no field redefinition that can eliminate the four derivative term but it is clear that this term is “weaker” than the corresponding term on the F_4 lattice, and obviously “stronger” than the absent term in the improved case. We obtain for the first time an explanation for why F_4 results for the bound have turned out to be smaller than the hypercubic ones [27] and preliminary numerical results with “Symanzik improvement” seem to give bounds [30] that are larger than the ones obtained on hypercubic lattices with the simplest action.†

Similar logic works when one tries to understand the effects of the four field terms.

* At $N = \infty$ one can define the ratio of the Pauli–Villars cutoff to a particular lattice cutoff by requiring exact matching of the coefficient c in equation (4.4.13). This is equivalent to an exact match of the cutoff effects at order $1/\Lambda^2$. However, this match cannot always be realized since some Pauli–Villars actions can make c vanish and this is impossible to achieve with the lattice actions that we investigated. In the text we meant by “natural” the sort of relationship one would guess by just looking at the bare action, not the more sophisticated relation described above in this footnote.

† Very recent work [29] reaffirms the trend; the newer data points have been included in Figures 7.1.

The bottom line is that one has full support for the “rule” that strengthening the repulsion between the pions in the low momentum approximation to the action, viewed as a chiral effective Lagrangian, increases the bound. Still, the answer is not entirely universal, and there are some finer differences, especially between the Pauli–Villars cases and the lattice cases.

We now turn to the cutoff effects. In order for the features observed above to really imply that higher Higgs masses are possible when the action is changed, we have to show that the above trends are also obeyed by the cutoff effects. This would free us from the somewhat arbitrary choice of comparing different lattice actions at the same m_H with a specific choice for the “cutoff” in each case. Because the mechanisms explaining the observed trends, even with this arbitrariness unresolved, are of a physical origin it is to be expected that the cutoff corrections will indeed follow these trends. Therefore just for the purpose of knowing which kind of action one should try to simulate at $N = 4$ the indications obtained up to this point should be taken seriously. However, to make well defined statements we shall need to know the magnitude of the cutoff effects in greater detail anyhow, even after Monte Carlo data replaces some of the large N graphs in Figures 7.2a-c. We therefore show in Figures 7.3a-d the cutoff effects on the width to mass ratio for the four cases under consideration. The numerical value of these effects is rather small, and this is in agreement with tree level perturbation theory in the simplest lattice action cases. We prefer to use the more stringent cutoff effects on the differential cross section for π – π scattering at ninety degrees in the center of mass frame. We chose this observable to be able to compare with existing perturbative results. The cutoff effects on the invariant amplitude square are shown in Figures 7.4a-d. Note that the trends are the same as in Fig 7.3a-d.

We see that the trends already seen in Figures 7.2a-d are respected. The amount of possible increase in the bound is smallest for the hypercubic improved case and largest for the F_4 case. We can immediately read off from the horizontal axis the mass in TeV that is permissible for the Higgs mass if one puts some restriction on the cutoff effects. Again one sees a tendency toward approximate “universality” with a bound on the Higgs mass at $N = \infty$ of about $0.820 TeV$.^{*} This is achieved with the smallest cutoff effects in a Pauli–Villars type of regularization. What seems to be special about our PV regularizations is that the pion propagator has no order p^4 term; this is also true of the SI action and can also be achieved on the F_4 lattice, but at the cost of introducing next nearest neighbor interactions.[†] The following is an “improved” action on an F_4 lattice with a tunable

^{*} The figure also shows that one does not need to set β_2 at exactly $-\beta_{2,t.c.}$ to obtain an effect of similar magnitude.

[†] While it is true that order p^4 terms in the bare action can be removed by field redefinitions, the nonlinear relationship between the bare parameters in the action and the cutoff effects implies that the elimination of the p^4 terms by field redefinition is not exact.

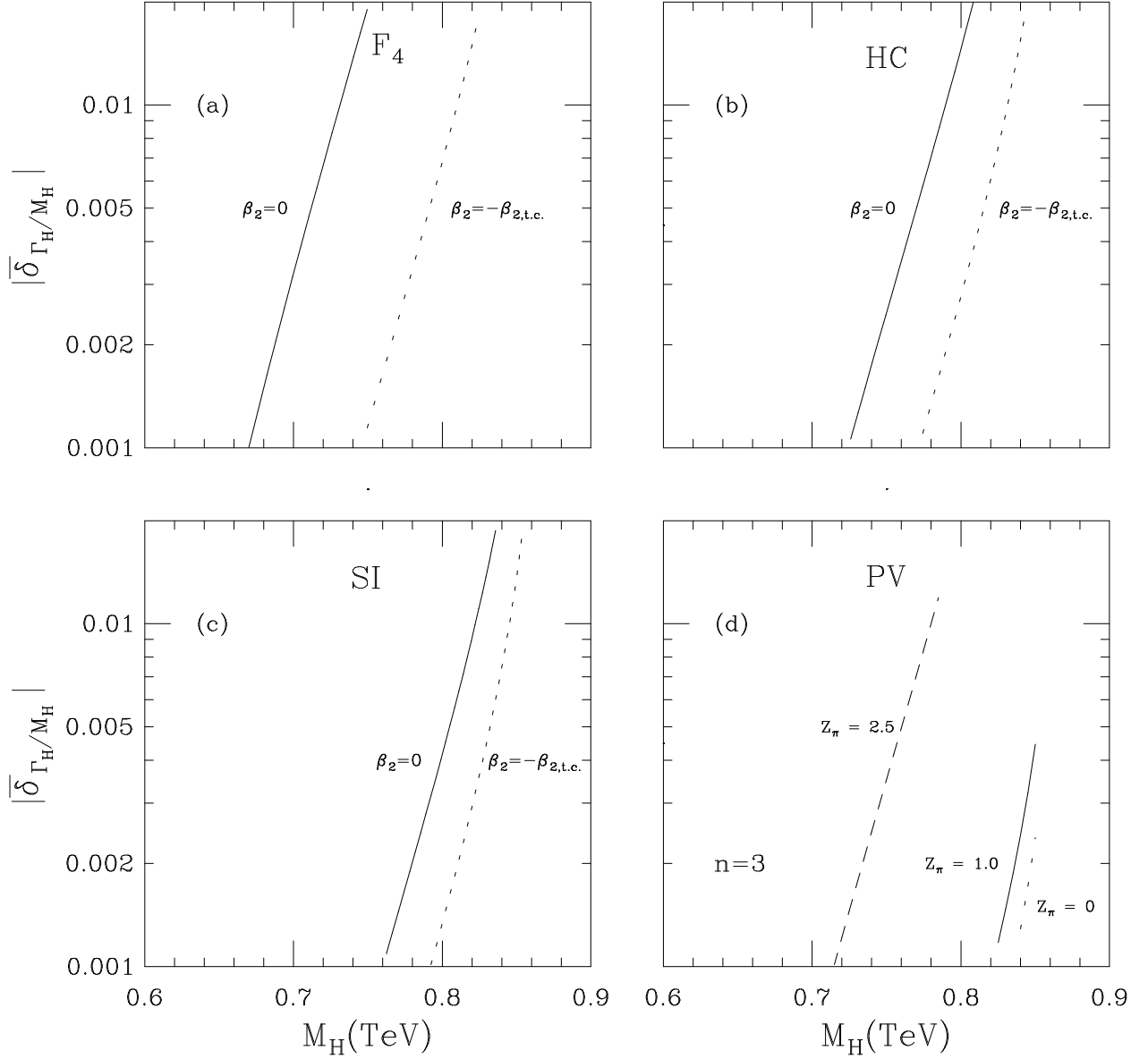


Figure 7.3 Leading order cutoff effects in the width to mass ratio: The solid line represents the naïve actions ($\beta_2 = 0$ on the lattice and $Z_\pi = 1$ for PV) and the dotted line the actions with a four derivative term turned on to maximal allowed strength ($\beta_2 = -\beta_{2,t.c.}$ on the lattice and $Z_\pi = 0$ for PV). The dashed line in the PV case shows an example with the “wrong” sign in front of the four derivative term, corresponding to $Z_\pi = 2.5$.

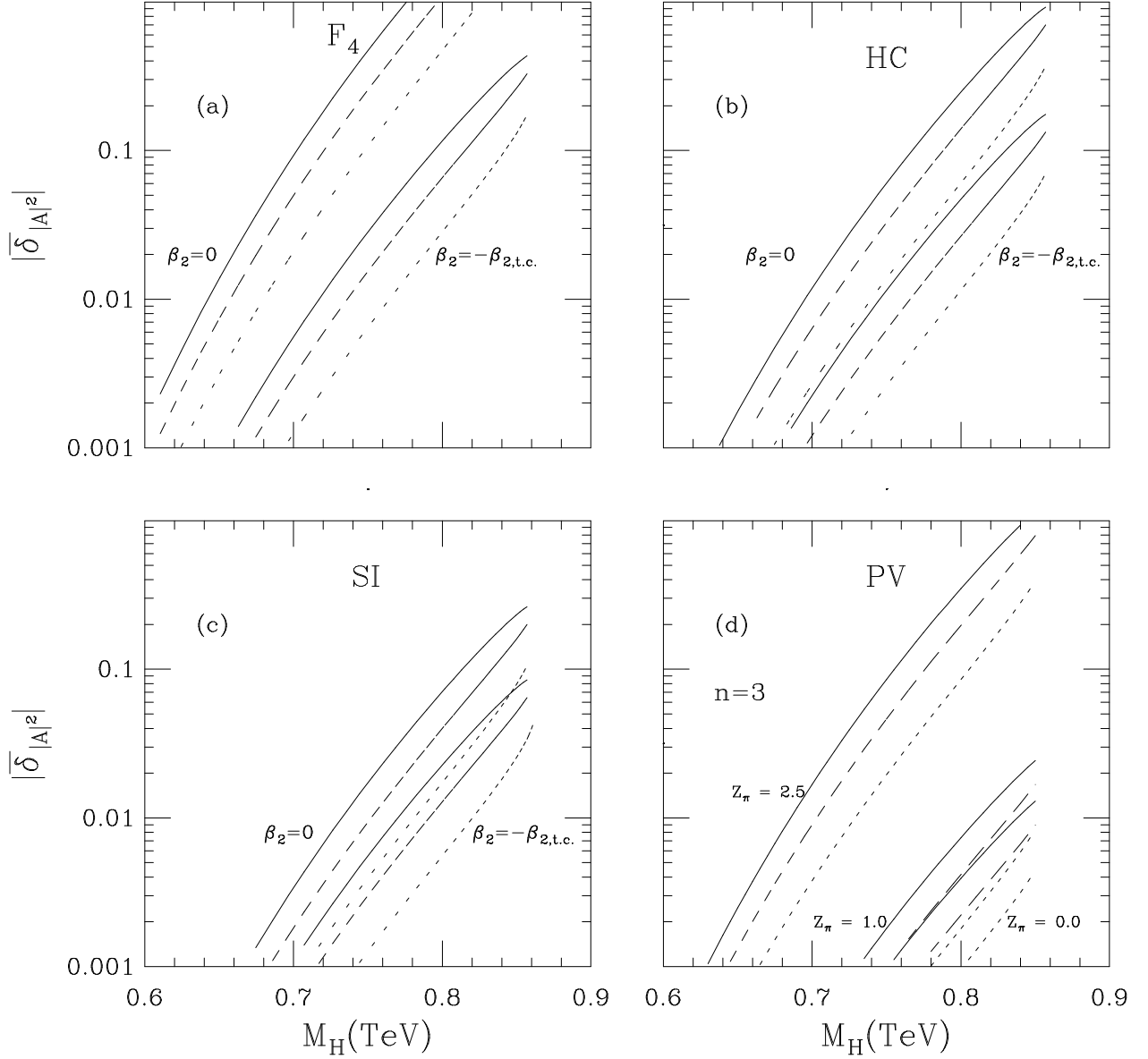


Figure 7.4 Leading order cutoff effects in the invariant $\pi - \pi$ scattering amplitude at 90° for the naïve actions ($\beta_2 = 0$ on the lattice and $Z_\pi = 1$ for PV) and for the actions with a four derivative term turned on to maximal allowed strength ($\beta_2 = -\beta_{2,t.c.}$ on the lattice and $Z_\pi = 0$ for PV). The dotted line represents center of mass energies $W = 2M_H$, the dashed line $W = 3M_H$ and the solid line $W = 4M_H$. In the PV case we again show an example with the “wrong” sign in front of the four derivative term corresponding to $Z_\pi = 2.5$.

“triangle term”

$$\begin{aligned}
S = & -2N(\beta_0 + \beta_1 + \beta_2) \left[2 \sum_{\langle x, x' \rangle} \vec{\Phi}(x) \cdot \vec{\Phi}(x') - \frac{1}{2} \sum_{\langle x, x'' \rangle} \vec{\Phi}(x) \cdot \vec{\Phi}(x'') \right] \\
& - N\beta_1 \sum_{\langle x, x' \rangle} [\vec{\Phi}(x) \cdot \vec{\Phi}(x') - 1]^2 \\
& - N \frac{\beta_2}{8} \sum_x \sum_{\langle ll' \rangle} \left[(\vec{\Phi}(x) \cdot \vec{\Phi}(x') - 1) (\vec{\Phi}(x) \cdot \vec{\Phi}(x'') - 1) \right]
\end{aligned}
\tag{7.3.1}$$

$l, l' \cap x \neq \emptyset, l \cap x' \neq \emptyset, l' \cap x'' \neq \emptyset, x, x', x''$ all n.n.

where x, x', x'', x''' denote sites, $\langle x, x' \rangle, l, l'$ links, and $\langle x, x'' \rangle$ next nearest neighboring pairs. The field is constrained by $\vec{\Phi}^2(x) = 1$. In (7.3.1) only sites separated at most a distance of two, in units of the embedding hypercubic lattice, are coupled.

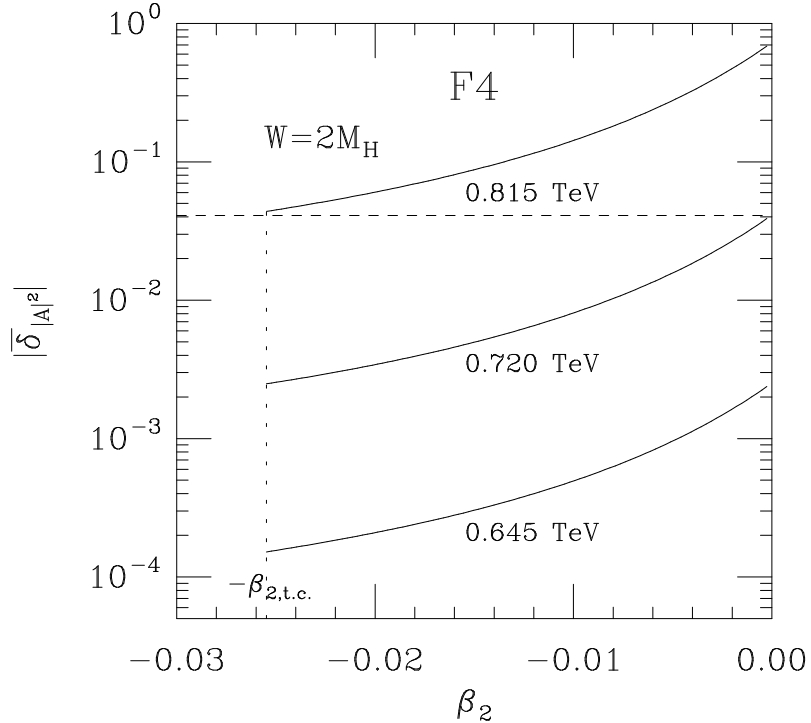


Figure 7.5 Leading order cutoff effects in the invariant $90^\circ \pi - \pi$ scattering amplitude vs. β_2 for three values of M_H on the F_4 lattice. The center of mass energy is set at $W = 2M_H$. The cutoff effects for a 0.815 TeV Higgs at $\beta_2 = -\beta_{2,t.c.}$ and for a 0.720 TeV Higgs at $\beta_2 = 0$ are equal in magnitude.

To see more clearly how the bound changes with the action we show an example in Figure 7.5 for the F_4 lattice: identical cutoff effects, of 4%, will be found at $N = \infty$ for a Higgs mass of 0.720 TeV with the simplest action, and for a Higgs mass of 0.815 TeV with an action that has the maximal amount of four field interaction we have allowed. It is important to understand that this difference is substantial when the width is considered. In Figure 7.6 we show the large N Higgs width as a function of the Higgs mass (note that the leading order weak coupling approximation severely underestimates the width when the Higgs becomes heavier). In our example the width went from 0.320 TeV to about 0.500 TeV and the heavier Higgs is definitely strongly interacting. There is no doubt therefore that, at least at infinite N , stopping the search for the Higgs mass bound at the study of the simplest possible actions would have been misleading.

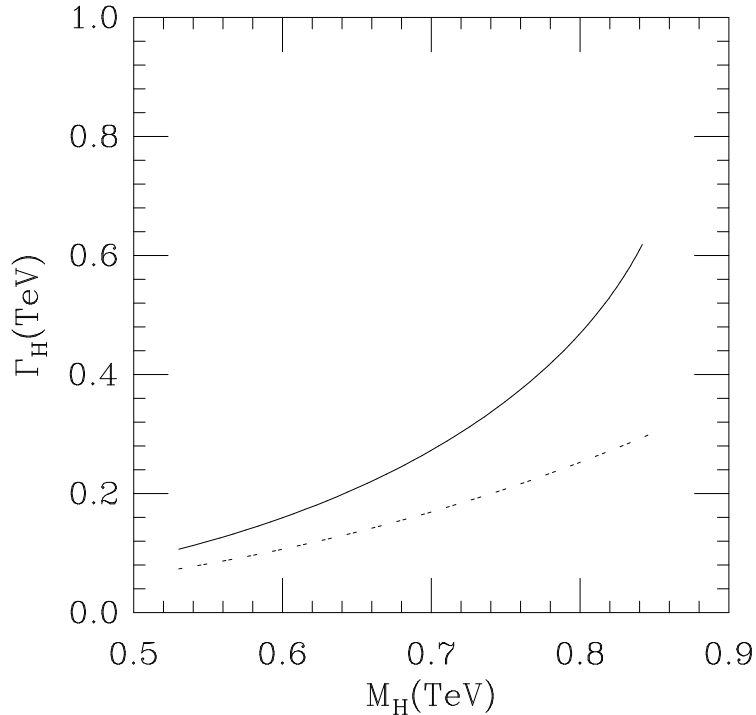


Figure 7.6 The regularization independent part of the width vs. M_H . The solid line displays the large N result scaled to $N = 4$ and the dotted line shows the leading order term in perturbation theory. For large M_H , the perturbative answer severely underestimates the width.

7.4. Predictions for $N = 4$.

We now turn to the most speculative, but quite important part of our work, namely numerical predictions for the physically relevant case at $N = 4$. Our approach is as follows: For the simplest actions (which are bilinear in the fields) numerical results at $N = 4$ are already available. We compare the M_H/F_π ratios we calculated at $N = \infty$, viewed as functions of m_H , to these numbers. We then use the difference between the $N = \infty$ and $N = 4$ numbers, at a given m_H , as an estimate for the same difference for each one of the new actions that have not yet been studied numerically. In this way we are able to make predictions for the new actions at $N = 4$ based on our $N = \infty$ results. We can test this method by assuming that we have numerical results for only one of the simple actions and “predict” the numerical results for another simple action. We find that our “predictions” are good to a few percent in the region where cutoff effects on the $\pi - \pi$ scattering cross section are of the order of a few percent. Comparisons between the $N = \infty$ and $N = 4$ results for the simplest lattice actions are given in figures 7.1a for F_4 , 7.1b for HC, and 7.1c for SI.*

For the F_4 lattice, we see from figure 7.1a that for the range of interest,[†] $m_H > 0.5$ (with m_H the Higgs mass in lattice units of the large N calculation at $N = 4$), the large N results are larger than the numerical ones by less than 0.150 TeV . For the HC lattice, figure 7.1b indicates that for $m_H > 0.4$ the large N results are larger by less than 0.100 TeV . Finally, for the SI case, figure 7.1c shows that for $m_H > 0.3$ the large N results are larger by less than 0.110 TeV . From these figures we also see that the large N results for M_H are consistently larger than the numerical ones. Therefore, given a large N estimate for M_H , we predict that the corresponding value, calculated in a numerical simulation at $N = 4$, will not exceed the large N estimate. We also predict that it will not be lower by more than the amounts given at the beginning of this paragraph, provided that m_H stays within the ranges of interest indicated there.

The largest Higgs mass is obtained when the four derivative term is turned on to maximal allowed strength. Using the guidelines of the previous paragraph and figures 7.3a – 7.3c or 7.4a – 7.4c we can estimate the Higgs mass bound for a given amount of allowed cutoff effects. We decide to allow up to 4% cutoff effects in the cross section at $W \leq 2M_H$ as computed in large N . For the F_4 case we find that the bound should be between 0.660 and 0.810 TeV ; this prediction is in agreement with our preliminary data [2]. For the HC it should be between 0.740 and 0.840 TeV , and for the SI between 0.750 and 0.860 TeV .

* Our plots include very recent data that appeared in [29]; this preprint became available during the final stages of preparing our paper for submittal. We have not yet had the time for a thorough study of [29].

† This is the range in which the bounds are obtained when $-\beta_{2,t.c.} \leq \beta_2 \leq 0$.

The second number in each case is the large N result ignoring the likely overestimates and hence is a very conservative estimate for the bound.

Although we do not have any large N results corresponding to the action (7.3.1), we expect the bound to increase by about 0.050 TeV from the value given for the F_4 lattice in the previous paragraph, to somewhere between 0.710 and 0.860 TeV . This is expected because the action (7.3.1) should be closer to the PV case, and from figures 7.4a and 7.4d we see that the Higgs mass bound given by the PV case is larger than the one given by the F_4 lattice by at least 0.050 TeV .

We see that if we allow up to 4% scaling violations in the cross section at $W \leq 2M_H$, we should expect, without being overly conservative, a Higgs mass bound of about 0.750 TeV . Renormalized perturbation theory suggests that such a heavy Higgs particle will have a width of at least 0.210 TeV . The large N results indicate an even larger width, around 0.290 TeV , already subtracting a possible overestimation by about 25%. It is unclear whether such a wide Higgs particle can still be seen on the lattice without applying more sophisticated techniques than mere direct measurement.

The approach of [29] is not based on direct measurement of the mass in the $I = 0, J = 0$ channel but relies quite heavily on the applicability of ordinary perturbation theory. We know from our large N computations that ordinary perturbation theory does not work that well for Γ_H/M_H when M_H/F_π gets close to the bound. However it is not ruled out that the particular quantities that are calculated in perturbation theory in [29] do have a “better” perturbative expansion. Using the expression for the variance of the magnetization squared in [4][#] (evaluated there also for the purpose of finding alternative definitions for the scalar self-coupling, definitions that lead to quantities that are more easily accessible numerically and don’t suffer from finite width contamination) one could test the validity of perturbation theory in the precise setting of [29], at least at infinite N .

It is important to stress that all our predictions in this subsection are relative to the presently generally accepted numerical values at $N = 4$. Thus, if there are systematic errors in the $N = 4$ results, for example due to ignoring finite width effects in the direct Monte Carlo measurements and/or due to the application of perturbation theory in [29], these errors will propagate into our predictions.

8. SUMMARY.

In this paper we have studied the regularization scheme dependence of the Higgs mass triviality bound in an $O(N)$ scalar field theory to leading order in $1/N$. All possible

[#] Equations (6) and (7a-b) there; see also the related discussion.

leading cutoff effects can be induced by adding only a few higher dimensional operators with adjustable coefficients to the standard $\lambda\Phi^4$ action. We have found that the highest Higgs masses are obtained in the non linear limit, at infinite λ . This has led us to consider non linear actions with the leading cutoff effects induced by four derivative terms with tunable couplings.

We used one class of continuum regularization schemes, of Pauli Villars type (PV), and three kinds of lattice regularizations: F_4 , Hypercubic (HC), and Symanzik Improved Hypercubic (SI). For these regularization schemes the action, when expanded for slowly varying fields to order momentum to the fourth power, is of the form

$$S_c = \int_x \left[\frac{1}{2} \vec{\phi} (-\partial^2 + 2b_0 \partial^4) \vec{\phi} - \frac{b_1}{2N} (\partial_\mu \vec{\phi} \cdot \partial_\mu \vec{\phi})^2 - \frac{b_2}{2N} (\partial_\mu \vec{\phi} \cdot \partial_\nu \vec{\phi} - \frac{1}{4} \delta_{\mu,\nu} \partial_\sigma \vec{\phi} \cdot \partial_\sigma \vec{\phi})^2 \right] \quad (2.5.1)$$

where $\vec{\phi}^2 = N\beta$. There are four control parameters in this action. One is redundant since to this order it can be absorbed into the other parameters by a field redefinition: The parameter b_0 can be absorbed in b_1 and b_2 by

$$\vec{\phi} \rightarrow \frac{\vec{\phi} - b_0 \partial^2 \vec{\phi}}{\sqrt{\vec{\phi}^2 + b_0^2 (\partial^2 \vec{\phi})^2 - 2b_0 \vec{\phi} \partial^2 \vec{\phi}}} \sqrt{N\beta} . \quad (2.5.2)$$

However, eliminating the dependence in b_0 to order momentum to the fourth power in the bare action does not necessarily imply that the dependence in b_0 has been eliminated to leading order in the inverse cutoff from physical observables. The vacuum fluctuations are “aware” of the full bare action and will carry that information to the non universal part of the physical observables. For example the parameter n of the PV case, although associated with an operator of dimension larger than four, does appear in the relation between bare and renormalized parameters and in the leading cutoff corrections to the width and cross section. Similarly for the lattice regularizations, some dependence on the full structure of the lattice propagators comes in through the constants r_0 , c_1 , c_2 , and γ . Because of this, the effects of b_0 , after the field redefinition, are not completely absent from the leading cutoff corrections to the physical observables. Still, the effect of b_0 is probably small and, as far as the value of the Higgs mass bound is concerned, one may be able to cover the whole range of leading cutoff effects by varying b_1 only. Our results indicate that this is realized to a good extend, leading to an approximate universality of the Higgs mass triviality bound.

For PV we simply set $b_0 = 0$, and for the lattice regularizations b_0 is set to the naïve value obtained in the expansion of the lattice kinetic energy term. We calculated the phase diagram for each regularization and found a second order line that ends at a tricritical point where a first order line begins. We studied the physically interesting region

close to the second order line in the broken phase. The parameter β corresponds to the relevant direction and is traded, as usual, for the pion decay constant f_π . The parameters b_1 and b_2 control the size of the leading order cutoff effects for a given value of f_π . Our analysis has shown that, to this order, the quantities we considered do not depend on the parameter b_2 . Therefore, a very simple situation emerged with the scale set by f_π and the leading cutoff effects parametrized by only one parameter b_1 . This simplification at infinite N makes it easy to relate very different regularization schemes, and leads to a reasonably “universal” bound on the renormalized charge g .

We calculated the leading cutoff effects on two physical quantities, namely the width of the Higgs particle and the 90 degrees $\pi - \pi$ scattering cross section. We found that they are given by the product of a “universal” factor (identical for all regularizations considered) which only depends on g and the dimensionless external momenta, and a non-universal factor that depends on the parameter b_1 but not on g or the momenta. The universal factor associated with the width is different from the one associated with the cross section, but the non-universal factors are identical for a fixed regularization scheme. These properties suggest that, to leading order in $1/N$, all cutoff effects in on-shell dimensionless physical quantities (viewed as functions of dimensionless momenta) are given by an effective renormalized action,

$$S_{eff} = S_R + c \exp\left[-\frac{96\pi^2}{g}\right] \mathcal{O} \quad , \quad (4.4.13)$$

where \mathcal{O} is a renormalized operator, c is a g independent free parameter containing all the non-universal information (i.e. a function of b_1 only), and S_R is describing the usual universal part of physical observables with the unit of energy set by $f_\pi = 1$. In the general RG framework this representation of S_{eff} is not unreasonable if one accepts that at $N = \infty$ the number of independent operators that contribute to observables at order $1/\Lambda^2$ decreases by one relatively to $N < \infty$. Because of the nonlinear relationship between c and the parameters in the bare action, the range in which c is allowed to vary depends on the type of action chosen. Different actions that realize the same c are indistinguishable to order $1/\Lambda^2$; all actions have large regions of total overlap but the triviality bounds are obtained from the area near the edges of the ranges in which c varies and therefore are somewhat dependent on the particular regularization scheme. Still, this dependence turns out to be weaker than what one would have been inclined to believe on the basis of the few simulations that had no continuous tuning ability for c built in. Thus, some of the stronger “universality” evident in (4.4.13) also makes its way into the triviality bound.

We developed an approximate physical picture associated with the models we studied. When the regularized model is nonlinear one has to think about the Higgs resonance as a loose bound state of two pions in an $I = 0, J = 0$ state. Pions in such a state attract because superposing the field configurations corresponding to individual pions makes the

state look more like the vacuum and hence lowers the energy. The four derivative term in the action can add or subtract to this attraction. We found that the smallest cutoff effects are obtained when the coupling b_1 of the four derivative term is set so that the term induces the maximal possible repulsion between the pions, postponing the appearance of the Higgs resonance to higher energies.

Our findings concerning the Higgs mass triviality bound are summarized by figures 7.3a – 7.3d and 7.4a – 7.4d for the four different regularization schemes considered. There the leading cutoff effects in the width and cross section are plotted versus the Higgs mass in TeV with the large N results presented for $N = 4$. We decided to extract the bound from figures 7.4a – 7.4d since the cross section cutoff effects provide a more stringent criterion. For all regularization schemes we extracted the bound by restricting the allowed cutoff effects in the cross section to 4%, at center of mass energies up to twice the Higgs mass.

To make predictions for the physically relevant case $N = 4$ we used the known differences between the $N = \infty$ and the $N = 4$ numerical results, for the simplest lattice actions, to extrapolate to the actions with four derivative terms that have not yet been studied numerically. We argued that the expansion in $1/N$ is expected to be “well behaved” in the region where the triviality bound is obtained, and because of that this extrapolation is sensible.

Based on what we have learned, it seems that a more realistic and not overly conservative estimate for the Higgs mass triviality bound is $0.750 TeV$, and not $0.650 TeV$ as it is sometimes stated. At $0.750 TeV$ the Higgs particle is expected to have a width of about $0.290 TeV$ and is therefore quite strongly interacting.

ACKNOWLEDGMENTS.

This research was supported in part by the DOE under grant # DE-FG05-85ER250000 (UMH and PV) and under grant # DE-FG05-90ER40559 (HN). UMH also acknowledges partial support by the NSF under grant # INT-8922411 and he would like to thank F. Karsch and the other members of the Fakultät für Physik at the University of Bielefeld for the kind hospitality while part of this work was done.

APPENDIX A.

In this appendix we show one example of the calculations needed to derive the asymptotic expansions of the “bubble” integrals in (4.1). We shall work out explicitly only the

simplest bubble, $I_{0,0}(p^2)$. The other bubbles are calculated by similar means. Our problem is to calculate the first two terms in the expansion in p^2 of

$$\begin{aligned}
I_{0,0}(p^2) &= \int_k \frac{1}{K(\frac{1}{2}p - k)K(\frac{1}{2}p + k)} \\
\frac{1}{K(q)} &= \frac{1}{q^2(1 + q^{2n})} = \frac{1}{q^2} - \frac{1}{n} \sum_{j=1}^n \frac{1}{q^2 + w_j} \\
w_j &= \exp[i\phi_j], \quad \phi_j = \frac{\pi}{n}(2j - 1 - n) \quad \text{for } j = 1, 2, \dots, n \ .
\end{aligned} \tag{A.1}$$

We rewrite the inverse propagator as

$$\frac{1}{K(q)} = \sum_{j=0}^n \frac{C_j}{q^2 + w_j} \quad \text{with } w_0 \equiv 0 \ . \tag{A.2}$$

The values of the constants C_j can be read off (A.1). We now analytically continue in all the w_j , $j = 1, \dots, n$, moving them to high positive imaginary parts. The bubble integral is now evaluated with this new propagator. We also analytically continue in the dimensionality d and first compute $I_{0,0}(p^2)$ with the new propagator in d dimensions and then take the limit $d \rightarrow 4$

$$B(p) = \lim_{d \rightarrow 4^-} \sum_{0 \leq i, j \leq n} C_i C_j \int \frac{d^d k}{(2\pi)^d} \frac{1}{[(\frac{1}{2}p - k)^2 + w_j][(\frac{1}{2}p + k)^2 + w_i]} \ . \tag{A.3}$$

At the end we intend to analytically continue the w_j 's back to their values on the unit circle.

We intend to use Feynman's formula

$$\frac{1}{AB} = \int_0^1 \frac{ds}{[sA + (1-s)B]^2} \ . \tag{A.4}$$

This is allowed as long as the straight line connecting the relevant points A and B never passes through the origin. This is ensured by all the w_j 's being in the upper half of the complex plane and thus making the segments connecting A and B also stay in the upper half plane for all real values of the momenta. We introduce (A.4) into (A.3) and do the angular part of the k integration. After a subsequent partial integration over the magnitude of k we obtain

$$B(p) = \lim_{d \rightarrow 4^-} \frac{d-2}{2^d \pi^{\frac{d}{2}} \Gamma(\frac{d}{2})} \sum_{0 \leq i, j \leq n} C_i C_j \int_0^1 ds \int_0^\infty \frac{dk k^{d-3}}{k^2 + s(1-s)p^2 + sw_i + (1-s)w_j} \ . \tag{A.5}$$

Let Φ_s be the phase of $z_s \equiv s(1-s)p^2 + sw_i + (1-s)w_j$. It is clear that $0 \leq \Phi_s < \pi$. We can deform the k integral from the positive axis to a ray starting from the origin at an angle $\Phi_s/2$. This ray will always be in the first quadrant of the complex plane. The contribution from the arc at infinity is seen to vanish. Along the ray we can easily do the integral over k and obtain

$$B(p) = \lim_{d \rightarrow 4^-} \frac{d-2}{2^d \pi^{\frac{d}{2}} \Gamma(\frac{d}{2})} \sum_{0 \leq i, j \leq n} C_i C_j \int_0^1 ds [s(1-s)p^2 + sw_i + (1-s)w_j]^{\frac{d-4}{2}} . \quad (\text{A.6})$$

The phase of the integrand is $\frac{d-4}{2}\Phi_s$ so that the associated sheet of the logarithm is the first sheet cut along the negative real axis in the usual way.

We now take the limit on the dimension and obtain, with an unambiguously defined logarithm,

$$\begin{aligned} B(p) &= \lim_{d \rightarrow 4^-} \left(\frac{2}{d-4} - \gamma_E \right) \left(\sum_{j=0}^n C_j \right)^2 \\ &\quad - \frac{1}{16\pi^2} \sum_{0 \leq i, j \leq n} C_i C_j \int_0^1 ds \int_0^\infty ds \log[s(1-s)p^2 + sw_i + (1-s)w_j] . \end{aligned} \quad (\text{A.7})$$

The first term vanishes because $\sum_{j=0}^n C_j = 0$. We separate out the terms containing w_0

$$\begin{aligned} B(p) &= J_1 + J_2 + J_3 \\ J_1 &= -\frac{1}{16\pi^2} \int_0^1 ds \log[s(1-s)p^2] \\ J_2 &= \frac{1}{8\pi^2 n} \sum_{j=1}^n \int_0^1 \log[s(1-s)p^2 + sw_j] \\ J_3 &= -\frac{1}{16\pi^2 n^2} \sum_{i, j=1}^n \int_0^1 ds \log[s(1-s)p^2 + sw_i + (1-s)w_j] . \end{aligned} \quad (\text{A.8})$$

Since none of the integrals goes through the cut along the negative real axis they can be

expanded in p^2 quite easily leading to

$$\begin{aligned}
J_1 &= -\frac{1}{16\pi^2} \log p^2 + \frac{1}{8\pi^2} \\
J_2 &= \frac{1}{8\pi^2 n} \sum_{j=1}^n \left[\frac{p^2}{2w_j} + \log w_j - 1 \right] + O((p^2)^2) \\
J_3 &= -\frac{1}{16\pi^2 n^2} \sum_{j=1}^n \left[\frac{p^2}{6w_j} + \log w_j \right] - \frac{1}{16\pi^2 n^2} \\
&\sum_{1 \leq i \neq j \leq n} \left[\frac{w_i \log w_i - w_j \log w_j}{w_i - w_j} - 1 + p^2 \left(\frac{1}{2} \frac{w_i + w_j}{(w_i - w_j)^2} - \frac{w_i w_j}{(w_i - w_j)^3} (\log w_i - \log w_j) \right) \right] \\
&+ O((p^2)^2) .
\end{aligned} \tag{A.9}$$

Finally we take the w_j 's back to their original values, always staying on the first sheet, and never crossing the cut. We know then that in the above equations $\log w_j = i\phi_j$ for $j \geq 1$ with the angles ϕ_j given by (A.1). The summations can now be performed by using

$$\sum_{j=1}^n \frac{1}{z + w_j} = \frac{nz^{n-1}}{1 + z^n} = \frac{d}{dz} \log[1 + z^n] \tag{A.10}$$

and derivatives of this identity.

The calculation of the other bubble integrals to the same order needs some additional manipulations but is essentially of the same type as the one outlined above.

APPENDIX B.

In this appendix we shall evaluate the scaling violations in β -functions defined along particular lines in the space of bare couplings of the simplest model

$$S = \int_x \left[\frac{1}{2} \vec{\phi} K \vec{\phi} + \frac{1}{2} m_0^2 \vec{\phi}^2 + \frac{g_0^2}{4N} (\vec{\phi}^2)^2 \right] . \tag{B.1}$$

We shall work in the symmetric phase for simplicity.

Introducing the auxiliary field $\sigma = \frac{g_0^2}{N} \vec{\phi}^2$ we get a new action

$$S_1 = \frac{N}{2} \text{Tr} \log[K + m_0^2 + \sigma] - \frac{N}{4g_0^2} \int_x \sigma^2 . \tag{B.2}$$

Defining the bubble integral

$$J(m^2) = \int_p \frac{1}{K(p^2) + m^2} \quad (\text{B.3})$$

one obtains for the renormalized coupling g^2

$$g^2 = \frac{g_0^2}{1 - g_0^2 J'(m^2)} \quad (\text{B.4})$$

where the prime denotes differentiation. The mass m^2 is given by the saddle point equation

$$m^2 = m_0^2 + g_0^2 J(m^2) \quad . \quad (\text{B.5})$$

Suppose now that $g_0^2(s)$, $m_0^2(s)$ are a parametric description of a path in parameter space and we calculate along this path the variation of g^2 with respect to m^2 . We obtain

$$\begin{aligned} \frac{d \log g^2}{dm^2} &= g^2 J''(m^2) + \frac{d \log g_0^2}{dm_0^2} X \\ X &= \frac{1 + g^2 J'(m^2)}{1 + g^2 J'(m^2) + J(m^2) g^2 \frac{d \log g_0^2}{dm_0^2}} \quad . \end{aligned} \quad (\text{B.6})$$

It must be true that $\frac{d \log g_0^2}{dm_0^2} \neq \infty$ because one cannot get to the critical surface without varying m_0^2 . Let us now consider the non-linear limit $g_0^2 \rightarrow \infty$ $m_0^2 \rightarrow -\infty$ with $g_0^2/m_0^2 \rightarrow \xi$. One can still have a path in parameter space ending at a critical point by varying ξ and it makes sense to compute $\frac{d \log g^2}{dm^2}$ along this path. At $g_0^2 = \infty$ one gets $g^2 J'(m^2) = -1$ (see (B.4)) and therefore $X = 0$ leading to

$$\frac{d \log g^2}{dm^2} = g^2 J''(m^2) \quad . \quad (\text{B.7})$$

This answer is independent of the sequence of s dependent paths we took the large g_0^2 , $-m_0^2$ limit on, as it should be.

Let us now compute in ordinary perturbation theory to one loop order. One gets

$$\frac{d \log g^2}{dm^2} = g^2 J''(m^2) + \frac{d \log g_0^2}{dm_0^2} \left[1 - g^2 J(m^2) \frac{d \log g_0^2}{dm_0^2} \right] \quad (\text{B.8})$$

with an explicit dependence on the sequence of paths, except if one happened to choose $\frac{d \log g_0^2}{dm_0^2} = 0$, but this is not necessary as the following example shows explicitly:

$$\begin{aligned} m_0^2 &= \frac{1 - 2\lambda}{s} - 8 \\ g_0^2 &= \frac{\lambda}{s^\alpha} \quad . \end{aligned} \quad (\text{B.9})$$

The nonlinear limit is attained when $\lambda \rightarrow \infty$. We see that, unless $\alpha = 0$, we shall have an answer that is different from the exact answer in (B.7) and that higher orders in g^2 that have been neglected depend on α in such a way as to conspire to add up to give an α independent answer. The problem can be easily traced now to the fact that the quantity X in (B.6), which vanishes in the nonlinear limit, does so only as a result of keeping all the powers in $g^2 J'(m^2)$ that come in from the denominator. Since $J'(m^2) \propto \log m^2$ we see that the culprit for finding a spurious α dependence in the leading order expansion of an α independent quantity is the truncation in the number of loops. As pointed out in section (4.3) graphs with an infinite number of loops contribute even at leading order in the physical coupling constant to the coefficient of the leading correction in inverse powers of the cutoff. All we are stressing here is that the unsolved problem of summing up the logarithms in the subleading corrections in the inverse cutoff is a serious problem. Maybe the $1/N$ expansion is the right place to tackle this issue.

APPENDIX C.

In section 2 the linear model was discussed for the Pauli–Villars regularization and it was shown that the largest Higgs mass is obtained in the nonlinear limit of the model, where the four-point coupling λ is taken to infinity. The action was restricted for simplicity to a three dimensional parameter space instead of the four dimensional one we really need to be concerned with (see introduction). In this appendix we will consider an action with four free parameters and again show that the largest Higgs mass is obtained in the nonlinear limit. However, our analysis is somewhat less general than the one in section 2 because it only covers a region close to the critical line. In section 2 we could do a better analysis because, with the particular Pauli–Villars regularization employed there, we had a simple closed formula for the “bubble” diagram, while here we work on the lattice and closed formulae for the “bubbles” are not available. We will use the F_4 lattice to regularize the model.

The action of the linear model with four bare parameters can be written as [6]

$$\begin{aligned}
S = & -2\kappa \sum_{\langle x, x' \rangle} \vec{\Phi}(x) \cdot \vec{\Phi}(x') + \sum_x \vec{\Phi}^2(x) + \frac{\lambda}{N} \sum_x [\vec{\Phi}^2(x) - N]^2 \\
& + \frac{\eta}{N^2} \sum_x [\vec{\Phi}^2(x)]^3 + \frac{\eta'}{N} \sum_{\langle x, x' \rangle} \vec{\Phi}^2(x) \cdot \vec{\Phi}^2(x') \quad .
\end{aligned}
\tag{C.1}$$

To make the action bilinear on the $\vec{\Phi}$ fields we introduce (as in section 2.1) two auxiliary

fields ω and σ by inserting

$$\prod_x \int_{-\infty}^{\infty} d\sigma(x) \frac{N}{2\pi} \int_{-i\infty}^{i\infty} d\omega(x) e^{N\omega(x)[\sigma(x) - \frac{\vec{\phi}^2(x)}{N}]} = 1 \quad (\text{C.2})$$

into the functional integral. The zero mode of the $\vec{\Phi}$ field is separated as in (2.1.7) and the $N = \infty$ pion propagator can be immediately read off. From the pion propagator and using standard conventions (see (3.3.5) and (3.3.6)) the pion wave function renormalization constant is found to be

$$Z_\pi = \frac{1}{6\kappa} . \quad (\text{C.3})$$

As in section 2.1, to get the saddle point equations we integrate the H and $\vec{\pi}$ fields and take the $N \rightarrow \infty$ limit. The saddle point equations are

$$\begin{aligned} \frac{1}{6\kappa} J_1(\omega_s') + v^2 &= \sigma_s \\ (1 - 2\lambda - 24\kappa) + 2(\lambda + 12\eta')\sigma_s + 3\eta\sigma_s^2 &= 6\kappa\omega_s' , \end{aligned} \quad (\text{C.4})$$

with

$$\omega_s' = \frac{\omega_s}{6\kappa} - 4 \quad (\text{C.5})$$

and with J_1 the F_4 lattice integral defined in (5.1.1). The symmetric phase is characterized by $v^2 = 0$, $\omega_s' > 0$ and the broken phase by $v^2 > 0$, $\omega_s' = 0$. The phase diagram is obtained with the method described in sections 3.1 and 5.1. It can be drawn on a two dimensional plane spanned by the parameters a and b , where

$$\begin{aligned} a &= \frac{\lambda + 12\eta'}{(6\kappa)^2} \\ b &= 2 - \frac{1 - 2\lambda}{12\kappa} - r_0 \frac{\lambda + 12\eta'}{(6\kappa)^2} \end{aligned} \quad (\text{C.6})$$

with $r_0 = J_1(0)$ (see (5.1.5)). There is a second order line described by

$$b = hr_0^2, \quad a > -2hr_0, \quad \text{with } h = \frac{3\eta}{2(6\kappa)^3} . \quad (\text{C.7})$$

This second order line turns into a first order line at the point $a = -2hr_0$, $b = hr_0^2$. This point is a tricritical point. We see that the generic phase structure we obtained for the non-linear actions can also be found in the linear case.

The physically relevant part of the phase diagram is the region near the second order line in the broken phase. In the broken phase the first of the saddle point equations (C.4) gives

$$\kappa = \frac{r_0 + f_\pi^2}{6\sigma_s} \quad (\text{C.8})$$

where we have used $v^2 = Z_\pi f_\pi^2$ (equation (4.1.3)). We use this equation to trade the parameter κ for f_π .

Following sections 2.2 and 2.3 we obtain the propagators in Fourier space in terms of a matrix M as in (2.3.6). M is given by

$$M = \begin{pmatrix} \frac{g(p)(r_0+f_\pi^2)}{\sigma_s} & \sqrt{N}v & 0 \\ \sqrt{N}v & -\frac{N\sigma_s^2 I(p)}{2(r_0+f_\pi^2)^2} & -\frac{N}{2} \\ 0 & -\frac{N}{2} & N[\lambda + 12\eta' + 3\eta\sigma_s - 3\eta'g(p)] \end{pmatrix} \quad (\text{C.9})$$

with $I(p) = -\frac{1}{16\pi^2} \log p^2 + c_1 - c_2 p^2 + O(p^4 \log p^2)$ (see (5.2.8)), the ‘‘bubble’’ integral defined in (5.2.7) and $g(p)$, the kinetic energy term on the F_4 lattice given in (2.5.5).

Close to the second order line and using an analysis similar to the one in section 4.1 we obtain equation (4.1.2) with the non-universal constant C depending on λ , η , and η'

$$m_R^2 \approx C^2(\lambda, \eta, \eta') \exp[-96\pi^2/g_R] \quad (\text{C.10})$$

where

$$C(\lambda, \eta, \eta') = \exp \left[8\pi^2 c_1 + \frac{4\pi^2 r_0^2}{\sigma_c^2 (\lambda + 12\eta' + 3\eta\sigma_c)} \right] . \quad (\text{C.11})$$

In (C.11) $\sigma_c = \sigma_c(\lambda, \eta, \eta')$, the critical value of σ_s , is determined from equations (C.6, C.7) with $\kappa_c = \frac{r_0}{6\sigma_c}$.

From (C.10, C.11) it is clear that for a given m_R the maximum $g_R = 3\frac{m_R^2}{f_\pi^2}$ is obtained when $C(\lambda, \eta, \eta')$ is the smallest. If the factor $\lambda + 12\eta' + 3\eta\sigma_c$, appearing in the exponent in (C.11), could take negative values then C would have been the smallest for those values. However, this factor cannot take negative values because of the second of eq. (C.7) which when written out is

$$\lambda + 12\eta' + 3\eta\sigma_c > 0 . \quad (\text{C.12})$$

This is a consequence of the fact that the physical region is the one close to the second order line and does not include the tricritical point or the region close to the ‘‘would be’’ second order line ($b = hr_0^2$, $a < -2hr_0$) which corresponds to an unstable saddle point. Therefore for given η, η' the minimum value of $C(\lambda, \eta, \eta')$ is obtained for $\lambda \rightarrow \infty$. We see, therefore, that the maximal Higgs mass is again obtained in the non-linear limit, at least as long as we restrict the observable cutoff effects sufficiently to justify the neglect of subleading cutoff effects in (C.10).

REFERENCES

- 1) U. M. Heller, H. Neuberger and P. Vranas *Phys. Lett.* **B283** (1992) 335.
- 2) U. M. Heller, M. Klomfass, H. Neuberger and P. Vranas, *Nucl. Phys. B (Proc. Suppl)* **26** (1992) 522; and work in progress.
- 3) H. Neuberger, talk given at the workshop “*Non-perturbative Aspects of Chiral Gauge Theories*”, Rome, 1992, to appear in the proceedings.
- 4) H. Neuberger, in “*Lattice Higgs Workshop*”, eds. Berg et. al., World Scientific, (1988).
- 5) H. Neuberger, *Nucl. Phys. B (Proc. Suppl)* **17** (1990) 17.
- 6) G. Bhanot, K. Bitar, U. M. Heller and H. Neuberger, *Nucl. Phys.* **B343** (1990) 467.
- 7) H. Neuberger, *Phys. Lett.* **B199** (1987) 536.
- 8) S. Weinberg, *Physica*, **96A** (1979) 327.
- 9) M. Einhorn, *Nucl. Phys.* **B246** (1984) 75.
- 10) M. Einhorn, in “*Lattice Higgs Workshop*”, eds. Berg et. al., World Scientific, (1988).
- 11) C. Whitmer, “*Monte Carlo Methods in Quantum Field Theory*”, unpublished Princeton University dissertation (1984).
- 12) M. M. Tsypin, in “*Lattice Higgs Workshop*”, eds. Berg et. al., World Scientific, (1988).
- 13) J. Kuti, L. Lin and Y. Shen, *Phys. Rev. Lett.* **61** (1988) 678.
- 14) S. Coleman, R. Jackiw, H. D. Politzer, *Phys. Rev.* **D10** (1974) 2491.
- 15) H. Georgi, “*Weak Interactions and Modern Particle Theory*”, Addison-Wesley, (1984).
- 16) R. S. Chivukula, M. J. Dugan, M. Golden, preprint HUTP-92/A025.
- 17) W. Bardeen, M. Moshe and M. Bander, *Phys. Rev. Lett.* **52** (1983) 1188.
- 18) M. C. Berger and F. David, *Phys. Lett.* **B135** (1984) 412.
- 19) M. Lüscher and P. Weisz, *Nucl. Phys.* **B318** (1989) 705.
- 20) L. Lin, J. Kuti, Y. Shen, in “*Lattice Higgs Workshop*”, eds. Berg et. al., World Scientific, (1988).
- 21) H. Neuberger, *Phys. Rev. Lett.* **60** (1988) 889.

- 22) A. Hasenfratz, K. Jansen, J. Jersak, C. B. Lang, H. Leutwyler and T. Neuhaus, *Z. Phys.C* **46** (1990) 257.
- 23) R. Dashen and H. Neuberger, *Phys. Rev. Lett.* **50** (1983) 1897.
- 24) H. Flyvbjerg, F. Larssen, C Kristjansen, *Nucl. Phys. B (Proc. Suppl)* **20** (1991) 44; C. Kristjansen, H. Flyvbjerg, preprint, NBI-HE-90-55.
- 25) M. Lüscher and P. Weisz, *Nucl. Phys.* **B290[FS20]** (1987) 25.
- 26) M. Lüscher and P. Weisz, *Nucl. Phys.* **B295[FS21]** (1988) 65.
- 27) G. Bhanot, K. Bitar, U. M. Heller and H. Neuberger, *Nucl. Phys.* **B353** (1991) 551.
- 28) M. Göckeler, K. Jansen, T. Neuhaus, *Phys. Lett.* **B273** (1991) 450.
- 29) M. Göckeler, H. A. Kastrup, T. Neuhaus and F. Zimmermann, preprint HLRZ 92–35/PITHA 92-21.
- 30) M. Göckeler, H. A. Kastrup, T. Neuhaus and F. Zimmermann, *Nucl. Phys. B (Proc. Suppl)* **26** (1992) 516.